DOSSIER D'HABILITATION A DIRIGER DES RECHERCHES

Alejandra Recio-Blanco

Université de Nice Sophia Antipolis
Laboratoire Lagrange, CNRS
Observatoire de la Côte d'Azur

ARCHEOLOGIE GALACTIQUE A L'ERE DE GAIA

Curriculum Vitae 3
Publications 5
Foreword 15
Chapter 1. Introduction 17
1.1 The formation and evolution of the Milky Way as a disc galaxy 18
1.2 Milky Way Stellar population surveys 19
Chapter 2. Searching for the archaeological remains through stellar spectra parametrization 23
2.1 Stellar spectra parametrization and data mining methodologies 23
2.2 Summary of automated stellar spectra parametrization methods 25
2.3 The MATISSE, DEGAS and GAUGUIN methods 26
2.4 General conclusions on automated stellar spectra parameterisation 29
Chapter 3. Archaeology of the Galactic disc 31
3.1 State of the art about the thick/thin disc dichotomy 31
3.2 Disc characterisation through low resolution spectroscopy 32
3.3 Chemical characterisation of the thin and thick discs 34
3.4 Spatial distributions of disc stellar populations 37
3.5 Chemo-kinematical and chemo-dynamical correlations 38
3.6 General conclusions about the Galactic disc 41
Chapter 4. Archaeology of the Galactic bulge 43
4.1 Observational framework and formation scenarios 43
4.2 The Gaia-ESO Survey bulge observations 45
4.3 Metallicity distribution functions 46
4.4 Double red clump characterisation 48
4.5 Kinematical features 48
4.6 General conclusions about the bulge 49
Chapter 5. Stellar parametrisation of Gaia spectroscopic data 51
5.1 Stellar parameters from Gaia RVS: GSP-Spec 51
5.2 Comparison of different algorithm performances for GSPspec 52
5.3 Expected parametrization performances for end-of-mission data 53
5.4 Comparison with BP/RP parametrization performances 57
5.5 Expected scientific impact of Gaia GSPspec results 58
Chapter 6. Conclusions and perspectives 59
6.1 The ARCHEOGAL project 60
6.2 Gaia activities 62
6.3 Long term perspectives 63
Bibliography 65

Alejandra Recio-Blanco

Curriculum Vitae

Passport: Spanish
Born on 20th October 1975 – A Coruña, Spain
1 child

Current address: Laboratoire Lagrange UMR 7293
Observatoire de la Côte d'Azur
Boulevard de l'Observatoire CS 34229
Nice Cedex 04 (France)
Tel.: 00 33 (0) 4 92 30 14
email: arecio@oca.eu
Webpage: https://gandc.oca.eu/spip.php?article417

Position

2007- Present, Assistant Astronomer, Observatoire de la Côte d'Azur, France
2007 Henri Poincaré Fellowship, Observatoire de la Côte d'Azur, France
2004-2006 European Space Agency external Fellowship, Observatoire de la Côte d'Azur, France
2003-2004 Post-doctoral research contract, Università degli Studi di Padova, Italy
2003 PhD, Instituto de Astrofísica de Canarias (Spain) and Università degli Studi di Padova (Italy)

Education

1999-2003 **PhD in Astrophysics, Instituto de Astrofísica de Canarias (Spain) and Università degli studi di Padova (Italy)**
Thesis: *On the nature of hot horizontal branch stars in Galactic Globular Clusters*.
Advisors: A. Aparicio (IAC) and G. Piotto (Univ. Padova)

1997-1998 **Master in Astrophysics**
La Laguna University (Tenerife, Spain)

Research Interests

- Galactic archaeology - Globular clusters - Disc formation
- Stellar evolution of low and intermediate mass stars - Chemical anomalies
- Automated spectral analysis methods and chemical analysis
- Galactic spectroscopic surveys

International Responsibilities

- **Responsible of the Development Unit 823 ”Generalized Stellar Parametrizer -Spectroscopy”** (2005-) within the Coordination Unit 8 “Astrophysical Parameters” of the **Gaia Data Processing and Analysis Consortium**: automated determination of the atmospheric parameters and the chemical abundances of stars observed by the RVS.
- **Project builder** of the **Gaia-ESO Large Public Survey (2011-2016)** and **responsible of the “WP10 GIRAFFE FGK Spectral Analysis”**.
- **Co-responsible of the AMBRE project** (2009-2014): OCA-ESO agreement for the automated parametrisation of all the high and intermediate resolution stellar spectra in the ESO archive (FEROS, UVES, HARPS, FLAMES).
- **Responsible within the PLATO-2 Consortium** of the **Work Package-131130 “Analysis of Gaia Spectroscopic performance”:** constraints for the targets selection from the Gaia/RVS spectroscopy.
- Member of the WEAVE spectrograph science team.
- Member of the Maunakea Spectroscopic Explorer (MSE) science team.

- Member of the **Observing Programmes Committee** - Stellar Panel of the **European Southern Observatory** (ESO) (2006-2007)

National Responsibilities (French community)

- Nominated member of the National Committee of the **Conseil National des Astronomes et Physiciens (CNAP)** (2011-2015).
- Nominated member of the Scientific Committee of the **Programme National de Physique Stellaire** (2010-2014).
- Member of the **Observing Programmes Stellar Committee** for the 2m Telescopes (2010-2014)
- Expert for the French **Agence d'Evaluation de la Recherche et l'Enseignement Supérieur** (2013).

Responsible of the ANR project *ARCHEOGAL* (2015-2018)

Teaching Experience

- 2003-2004, Università degli Studi di Padova (Italy): 80h *Stellar Spectroscopy*
- 2007-Present, Université de Nice Sophia Antipolis (France): 70h/year on the following topics

  - Introduction to Astrophysics – *Licence* level
  - Statistics and scientific methodology – *Licence* level
  - Stellar spectroscopy and Galactic stellar populations. – *Master* level

Student advising

- PhD

- G. Guiglion, *Chemical abundances and the history of the Galactic Disc*, will defend in October 2015.
- A. Rojas, *Galactic Bulge formation with the Gaia-ESO survey*, will defend December 2016.

- **Master's** : C. Moni Bidin (2003, Padova), D. Fabbian (2003, Padova), C. Paladini (2006, Padova), G. Kordopatis (2006, 2007, Nice), J.C. Gazzano (2007, Nice), G. Guiglion (2011, Nice), J. Lannier (2012), C. Clastres (2013, Nice)

Scientific Organization (SOC) of International meetings

- *Gaia-ESO Survey second science meeting*, Porto, 11/2014
- *Gaia-ESO Survey First Science*, Nice, 04/2013
- *Gaia : perspectives for stellar physics*, Journées de la Societé Francaise d'Astronomie et Astrophysique, Montpellier, France, 2013
- *Stellar Physics*, Journées de la Societé Francaise d'Astronomie et Astrophysique, Nice, France, 2012
- *Stellar and Interstellar physics for the modelling of the Galaxy*, Journées de la Societé Francaise d'Astronomie et Astrophysique, Paris, June 2011.

Professional service

Reviewer : Astronomy and Astrophysics, Astrophysical Journal
Thesis referee: V. Sommariva (Univ. Padova, Italy, 2008), O. Zamora (Univ. Granada, Spain, 2009), A. Rajpurohit (Univ. Besançon, France, 2013), S. Blanco Cuaresma (Obs. Bordeaux, France, 2014).

Spoken languages : Spanish, French, English, Italian, Portuguese, Galician

Publication list

15^{th} October 2014

Refereed Publications

1. "*Rotation of Hot Horizontal-Branch Stars in the GCs NGC 1904, NGC 2808, NGC 6093 and NGC 7078*"
Recio-Blanco A., Piotto G., Aparicio A. & Renzini A. 2002, ApJL , 572, 71

2. "*A New Feature along the Extended Blue Horizontal Branch of NGC 6752.*"
Momany Y., Piotto G., Recio-Blanco A., Bedin L. R., Cassisi S. & Bono G., 2002, ApJL, 576, 65.

3. "*HST color-magnitude diagrams of 74 galactic globular clusters in the HST F439W and F555W bands.*"
Piotto G., King I. R., Djorgovski S. G., Sosin C., Zoccali M., Saviane I., De Angeli F., Riello M., Recio Blanco A., Rich R. M., Meylan G. & Renzini A., 2002, A&A, 391, 945.

4. "*Why Hot Horizontal Branch Stars Can Appear Redder Than Red Giants?*"
Momany Y., Cassisi S., Piotto G., Bedin L., Ortolani S., Castelli F. & Recio-Blanco A. 2003, A&A, 407, 303

5. "*The red giant branch luminosity function bump.*"
Riello M., Cassisi S., Piotto G., Recio-Blanco A., De Angeli F., Salaris M., Pietrinferni A. Bono G. & Zoccali M., 2003, A&A, 410, 553

6. "*Rotation velocities of hot horizontal branch stars in the globular clusters NGC 1904, NGC 2808, NGC 6093, and NGC 7078: the database*"
Recio-Blanco A., Piotto G., Aparicio A. & Renzini A. 2004, A&A, 417, 597

7. "*Blue hook stars in the massive globular cluster M54*"
Rosenberg A., Recio-Blanco A., Garcia M., 2004, ApJ, 603, 135

8. "*The ubiquitous nature of the Horizontal Branch second U-jump. A link with the Blue Hook scenario?*"
Momany Y., Bedin L.R., Piotto G., Cassisi S., Recio-Blanco A., Ortolani S., De Angeli F. & Castelli F. 2004, A&A, 420, 605

9. "*Relative Frequencies of Blue Stragglers in Galactic GCs: Constraints for the Formation Mechanisms*"
Piotto G., De Angeli F., King I. R., Djorgovski S. G., Bono G., Cassisi S., Meylan G., Recio-Blanco A., Rich M.R., Davies M. B., 2004, ApJL, 604, 109

10. "*A homogenous set of globular cluster relative distances and reddenings*"
Recio-Blanco A., Piotto G., De Angeli F., Riello M., Bono G., Cassisi S., Zoccali M.& Aparicio A., 2005, A&A, 432, 851

11. "*Metallicities on the double main sequence of Omega Centauri imply large helium enhancement*"
Piotto G., Villanova S., Bedin L.R., Gratton R.G., Cassisi S., Momany Y., Recio-Blanco A., Lucatello S., Anderson J., King I.R., Pietringerni A., Carraro G., 2004, ApJ, 621, 777

12. "*Abundance Anomalies in Hot Horizontal Branch Stars of the Galactic Globular Cluster NGC1904*"
Fabbian D., Recio-Blanco A., Gratton R.G., Piotto G., 2005, A&A, 434, 235

13. "*Galactic globular cluster relative ages. II* "
De Angeli, F., Piotto, G., Cassisi, S., Busso, G., Recio-Blanco, A., Salaris, M., Aparicio, A., Rosenberg, A., 2005, AJ, 130, 116

14. "*Spectroscopic survey of the Galaxy with Gaia II. The expected science yield from the Radial Velocity Spectrometer*"
Wilkinson, M.I.,...., Recio-Blanco, A. et al., 2005, MNRAS, 359, 1306

15. "*Multivariate analysis of globular cluster horizontal branch morphology: searching for the second parameter problem*"
Recio-Blanco, A., Aparicio, A., Piotto, G. and De Angeli, F., Djorgovski, G., 2006, A&A, 452, 875

16. "*Precise Reddening and Metallicity of NGC6752 from FLAMES spectra*"
Gratton,R., Bragaglia,A., Carretta,E., Lucatello,S., Momany,Y., Piotto,G., Recio-Blanco, A., 2005, A&A, 442, 947

17. "*A lack of close binaries among hot horizontal branch stars in NGC6752*"
Moni-Bidin., C., Moehler, S., Piotto, G., Recio-Blanco, A., Momany, Y., Méndez, R.A., 2006, A&A, 451, 499

18. "*Na-O Anticorrelation and HB I. The Na-O anticorrelation in NGC 2808*"
Carretta, E., Bragaglia, A., Gratton, R.G., Leone, F., Recio-Blanco A., Lucatello, S., 2006, A&A, 450, 523.

19. "*Lithium abundances for early F stars: New observational constraints for the Li dilution.*"
Jasniewicz, G., Recio-Blanco A., de Laverny, P., Parthasarathy, M., De Medeiros, J.R., 2006, A&A, 453, 717.

20. "*Abundance anomalies in hot horizontal branch stars of the Galactic globular cluster NGC 2808.*"
Pace, G., Recio-Blanco A., Piotto, G., Momany, Y., 2006, A&A, 452, 493

21. "*Automated derivation of stellar atmospheric parameters and chemical abundances: the MATISSE algorithm*"
Recio-Blanco A., Bijaoui A. & de Laverny P., 2006, MNRAS, 370, 141

22. "*On the extra-mixing efficiency in low metallicity RGB stars*"
Recio-Blanco, A. and de Laverny, P., 2007, A&A 461, L 13

23. "*Na-O Anticorrelation and HB. VI. The chemical composition of the peculiar bulge globular cluster NGC 6388*"
Carretta, E., Bragaglia, A., Gratton, R.G., Momany, Y., Recio-Blanco, A., 2007, A&A, 464, 967

24. "*Na-O Anticorrelation and HB. V. The Na-O anticorrelation in NGC 6441 form Giraffe spectra*"
Gratton, R.G., ..., Recio-Blanco, A. et al., 2007, A&A, 464, 953

25. "*The multiplicity of the subgiant branch of ω Centauri: Evidence for prolonged star formation* "
Villanova, S., Piotto, G., King, I.R., Anderson, J., Bedin L.R., Gratton R.G., Cassisi, S., Momany, Y., Bellini, A., Cool, A.M., Recio-Blanco, A., Renzini, A., 2007, ApJ, 663, 296

26. "*Radial velocities of open stellar clusters: A new solid constraint favoring Tsallis maximum entropy theory*"
Carvalho, J.C., Soares, B.B., Canto Martins, B.L., do Nascimento, J.D., Recio-Blanco, A., De Medeiros, J.R., 2007, Physica A: Statistical Mechanics and its Applications, Vol. 384, Issue 2, pag. 507

27. "*A new spin for understanding the peculiar horizontal branch morphology of the Galactic GCs NGC6388 and NGC6441*"
Busso, G.,..., Recio-Blanco, A. et al., 2007, A&A, 474, 105

28. "*Spectroscopy of horizontal branch stars in NGC6752 - Anomalous results on atmospheric parameters and masses* "
C. Moni Bidin, S. Moehler, G. Piotto, Y. Momany, A. Recio-Blanco, 2007, A&A, 474, 505

29. "*The Link between Chemical Anomalies along the RGB and the Horizontal Branch Extension in Globular Clusters* "
Carretta, E.; Recio-Blanco, A; Gratton, R. G.; Piotto, G.; Bragaglia, A., 2007, ApJL, 671, 125

30. "*Doppler search for exoplanet candidates and binaries in the CoRoT fields using a multifiber spectrograph I: global analysis and first results*"
Loeillet, B., ..., Recio-Blanco, A. et al., 2008, A&A 479, 865

31. "*Fluorine in AGB Carbon Stars Revisited*"
Abia, C., Recio-Blanco, A., de Laverny, P.,Cristallo, S., Dominguez, I., Straniero, O., 2009, ApJ 694, 971

32. "*The Lack of Binaries Among Hot Horizontal Branch Stars: M80 and NGC5986*"
Moni Bidin, C.; Moehler, S.; Piotto, G.; Momany, Y.; Recio-Blanco, A., 2009, A&A, 498, 737

33. "*Na-O Anticorrelation and HB. VII. The chemical composition of first and second generation stars in 15 globular clusters from GIRAFFE spectra*"
Carretta, E., Bragaglia, A., Gratton, R.G.,..Recio-Blanco, A., et al., 2009, A&A, 505, 117

34. "*An overview of the rotational behavior of metal-poor stars along the Hertzprung-Russel diagram.*"
Cortes, C.; da Silva,J.; Recio-Blanco, A.; Catelan, M.; do Nascimento, J.D., de Medeiros, J.R., 2009 ApJ, 704, 750

35. "*BVRIJHK photometry and proper motion analysis of NGC 6253 and of the surrounding field*"
Montalto, M.; Piotto, G.; Desidera, S.; Platais, I.; Carraro, G.; Momany, Y.; De Marchi, F.; Anderson, J.; Recio-Blanco, A., 2009, A&A, 505, 1129

36. "*Fluorine Abundances in AGB Carbon Stars: New Results?*"
Abia, C.; de Laverny, P.; Recio-Blanco, A.; P.,Cristallo, S.; Dominguez, I.; Straniero, O., 2009, PASA, 26, 351

37. "*Properties of stellar generations in globular clusters and relations with global parameters*
Carretta, E.; Bragaglia, A.; Gratton, R.G.; Recio-Blanco, A.; Lucatello, S.; D'Orazi,V.; Cassisi, S., 2010, A&A, 516, 55

38. "*Stellar characterization of the CoRoT/Exoplanet fields with MATISSE*"
Gazzano, J.C.; de Laverny, P.; Deleuil, M.; Recio-Blanco, A.; et al., 2010, A&A, 523, 91

39. "*Fluorine abundances in Galactic AGB stars*"
Abia, C.; K. Cunha; S. Cristallo; P. de Laverny; I. Domínguez; K. Eriksson; L. Gialanella; K. Hinkle; G. Imbriani; Recio-Blanco, A.; V. Smith, 2010, ApJL, 715, 94

40. "*The First Fluorine Abundance Determinations in Extragalactic Asymptotic Giant Branch Carbon Stars*"
Abia, C.; Cunha, K.; Cristallo, S.; de Laverny, P.; Domínguez, I.; Recio-Blanco, A.; Smith, V. V.; Straniero, O., 2011, ApJL, 737, 8

41. "*Automatic stellar parametrisation in the IR CaII triplet region*"
Kordopatis, G., Recio-Blanco A., de Laverny, P., Bijaoui, A., Hill, V., Gilmore, G., Wyse, R.M., Ordenovic, C., 2011, A&A, 535, 106

42. "*A spectroscopic survey of Thick Disc stars outside the solar neighbourhood*"
Kordopatis, G., Recio-Blanco A., de Laverny, P., Gilmore, G., Hill, V., Wyse, R.M., Helmi, A., Bijaoui, A., Zoccali, M., Bienaymé, O., 2011, A&A, 535, 107

43. "*An overview of parameter estimation methods from a model grid in astrophysics*"
Bijaoui, A., Recio-Blanco A., de Laverny, P., Ordenovic, C., 2012, Statistical Methodology, vol. 9, p. 55

44. "*Fluorine abundances in dwarf stars of the solar neighbourhood*"
Recio-Blanco A., de Laverny, P., C. Worley, N. Santos, C. Melo, 2012, A&A, 538, 117

45. "*The AMBRE Project: Stellar parameterisation of the ESO:FEROS archived spectra*"
C. Worley, P. de Laverny, A. Recio-Blanco, V. Hill, A. Bijaoui, C. Ordenovic, 2012, A&A, 542, 48

46. "*The AMBRE project: A new synthetic grid of high-resolution FGKM stellar spectra*
P. de Laverny, Recio-Blanco A., C.C. Worley, B. Plez, 2012, A&A, 544, 126

47. "*Comparative modelling of the spectra of cool giants*
T. Lebzelter, U. Heiter,...,Recio-Blanco A., et al., 2012, A&A, 547, 108

48. "*Characterisation of the Galactic Thin Disc with CoRoT targets*"
Gazzano, J.-C., Kordopatis, G., Deleuil, M., de Laverny, P., Hill, V., Recio-Blanco, A., 2013, A&A, 550, 125

49. "*Fluorine abundances and the puzzle of globular cluster chemical history*"
P. de Laverny & Recio-Blanco A., 2013, A&A, 555, 121

50. "*The Gaia astrophysical parameters inference system (Apsis). Pre-launch description*"
C. Bailer-Jones, ..., Recio-Blanco A., et al., 2013, A&A, 559, 74

51. "*The Radial Velocity Experiment (RAVE): Fourth Data Release*"
G. Kordopatis, ..., Recio-Blanco A., et al., 2013, A&A, 146, 134

52. "*Revisited fluorine abundances in the globular cluster M 22*"
de Laverny, P. & Recio-Blanco A., 2013, A&A, 560, 74

53. "*The Gaia-ESO Survey: Reevaluation of the parameters of the open cluster Trumpler 20 using photometry and spectroscopy*"
Donati, P.; ..., Recio-Blanco A., et al., 2014, A&A, 561, 94

54. "*The Gaia-ESO Survey: Abundance ratios in the inner-disk open clusters Trumpler 20, NGC 4815, NGC 6705*"
Magrini, L.;Randich, S.; Romano, D.; ...,Recio-Blanco A., et al., 2014, A&A, 563, 44

55. "*The Gaia-ESO Survey: Kinematic structure in the Gamma Velorum cluster*"
Jeffries, R. D.;Jackson, R. J.; Cottaar, M.; ...,Recio-Blanco A., et al., 2014, A&A,563, 94

56. "*Gaia-ESO Survey: Properties of the intermediate age open cluster NGC 4815*"
Friel, E. D.; Donati, P.; Bragaglia, A.; ...,Recio-Blanco A., et al., 2014, A&A,563, 117

57. "*Gaia FGK benchmark stars: Metallicity*"
Jofr, P.; Heiter, U.; Soubiran, C.; Blanco-Cuaresma, S.;...,Recio-Blanco A., et al., 2014, A&A,564, 133

58. "*Global and Nonglobal Parameters of Horizontal-branch Morphology of Globular Clusters*"
Milone, A. P.; Marino, A. F.; Dotter, A.; ...,Recio-Blanco A., et al., 2014, ApJ, 785, 21

59. "*The Gaia-ESO Survey: radial metallicity gradients and age-metallicity relation of stars in the Milky Way disk*"
Bergemann, M.; Ruchti, G. R.; Serenelli, A.; ...,Recio-Blanco A., et al., 2014, A&A, 565, 89

60. "*The Gaia-ESO Survey: processing FLAMES-UVES spectra*"
Sacco, G. G.; Morbidelli, L.; Franciosini, E.; ...,Recio-Blanco A., et al., 2014, A&A,565, 113

61. "*Gaia-ESO Survey: Empirical classification of VLT/Giraffe stellar spectra in the wavelength range 6440-6810 in the Velorum cluster, and calibration of spectral indices*"
Damiani, F.; Prisinzano, L.; Micela, G.;... ,Recio-Blanco A., et al., 2014, A&A, 566, A50

62. "*The Gaia-ESO Survey: the Galactic Thick to Thin Disc transition* "
Recio-Blanco A.; de Laverny, P.; Kordopatis, G., et al. 2014, A&A, 567, A5

63. "*The Gaia-ESO Survey: the first abundance determination of the pre-main-sequence cluster Gamma Velorum*"
Spina, L.; Randich, S.; Palla, F.; ...,Recio-Blanco A., et al., 2014, A&A, 567, A55

64. "*The Gaia-ESO Survey: Metallicity of the Chamaeleon I star-forming region*"
Spina, L.; Randich, S.; Palla, F.; ...,Recio-Blanco A., et al., 2014, A&A, 568, 2

65. "*The Gaia-ESO Survey: Metallicity of the Chamaeleon I star-forming region*"
Cantat-Gaudin, T.; Vallenari, A.; Zaggia, S.; ...,Recio-Blanco A., et al., 2014, A&A, 569, 17

66. "*The Gaia-ESO Survey: metallicity and kinematic trends in the Milky Way bulge* "
Rojas-Arriagada, A.; Recio-Blanco A.; Hill, V. et al., 2014, A&A, 569, 103

67. "*The Gaia-ESO Survey: the chemical structure of the Galactic discs from first internal data release* "
Mikolaitis, S.; Hill, V.; Recio-Blanco A. et al., 2014, A&A, accepted, astro-ph 1408.6687

68. "*The AMBRE Project: Parameterisation of FGK-type stars from the ESO:HARPS archived spectra* "
De Pascale, M.; Worley, C.; de Laverny, P.; Recio-Blanco A.; Hill, V. & Bijaoui, B., 2014, A&A, accepted, astro-ph 1409.2258

69. "*The Gaia-ESO Survey: The analysis of high-resolution UVES spectra of FGK-type stars*"
Smiljanic, R.; Korn, A.; Bergemann, M.; ...,Recio-Blanco A., et al., 2014, A&A, accepted, astro-ph 1409.0568

70. "*The Gaia-ESO Survey: the most metal-poor stars in the Galactic bulge*"
Howes, L.; Asplund, M.; Casey, A.M.; ...,Recio-Blanco A., et al., 2014, A&A, accepted, astro-ph 1409.7952

71. "*The Gaia-ESO Survey: Extracting diffuse interstellar bands from cool star spectra, DIB-based interstellar medium line-of-sight structures at the kpc scale*"
Puspitarini, L.; Lallement, R.; Babusiaux, C.;...,Recio-Blanco A., et al., 2014, A&A, accepted, astro-ph 1409.0842

—

72. "*Stellar parametrization from Gaia RVS spectra*"
Recio-Blanco A.; de Laverny, P.; Allende Prieto, C.; Fustes, D.; Manteiga, M., Arcay, B.; Bijaoui, A.; Dafonte, C.; Ordenovic, C. and Ordoñez Blanco, D., 2014, A&A, submitted

Invited talks

1. "*Gaia stellar chemical abundances and Galactic archeology*"
Recio-Blanco, A. & Thévenin, F., 2004, in "The three dimensional universe with Gaia", European Space Agency, SP-576.

2. "*Inferred properties of globular clusters from their colour-magnitude diagrams*"
Recio-Blanco, A., 2005, in "Resolved Stellar Populations", eds. D. Valls-Gabaud and M. Chavez, The Astronomical Society of the Pacific.

3. "*Anomalies in horizontal branch of globular clusters and in SDB stars*"
Recio-Blanco, A., 2005, in "Element Stratification in stars: 40 years of atomic diffusion", eds. G. Alecian, O. Richard and S. Vauclair, EAS Publication Series, vol. 17, EDPsciences.

4. "*Parameter Estimation from Model Grids. Application to Gaia RVS spectra*"
Bijaoui, A., Recio-Blanco, A., de Laverny, P. and Ordenovic, C., 2010 Astronomical Data Analysis VI, eds. Strack and Murtagh, Monastir (Tunisie) 3-7 Mai 2010

5. "*Analysing spectroscopic data: current methods and performances, needs for new developments*"
Recio-Blanco, A., de Laverny, P., Bijaoui, A., 2010, GCDS Survey Science meeting, November 2010, Nice (France)

6. "*Galactic spectroscopic surveys: Gaia scientific exploitation*"
Recio-Blanco, A., SF2A Annual meeting, June 2012, Nice (France)

7. "*The analysis of FGK stars from GIRAFFE spectra of the Gaia-ESO Survey*"
Recio-Blanco, A., Gaia-ESO Survey First Science meeting, March 2013, Nice (France)

8. "*Automated abundance analysis*"
Recio-Blanco, A., IAU Symposium 298, May 2013, Lijang (Chine)

9. "*Stellar parameters from Gaia and Gaia-ESO Survey data*"
Recio-Blanco, A., SF2A Annual meeting, June 2013, Montpellier (France)

10. "*Stellar Rotation and abundances in large surveys*"
Recio-Blanco, A., 400yrs of stellar rotation, November 2013, Natal (Brazil)

11. "*The Milky Way stellar populations seen by the Gaia ESO Survey* "
Recio-Blanco, A., SF2A Annual meeting, June 2014, Paris (France)

12. "*Scientific synergies of Gaia with ground based spectroscopic surveys*"
Recio-Blanco, A., The Milky Way unraveled by Gaia: GREAT Science from the Gaia Data Releases, December 2014, Barcelona (Spain)

Non refeered publications

1. "*Stellar rotation along the horizontal branches of globular clusters*"
Piotto, G.; Recio-Blanco, A., 2000. Proceedings of the workshop "SARG at TNG", Ed. by R. G. Gratton and R. U. Claudi. Published by Osservatorio Astronomico Padova, p. 101.

2. "*The anomalous horizontal branch of NGC 2808: Is it the result of environmental effects?* "
Bedin, L. R.; Piotto, G.; Zoccali, M.; Saviane, I.; Stetson, P. B.; Bono, G.; Cassisi, S.; Recio-Blanco, A., Proceedings of "Dynamics of Star Clusters and the Milky Way", Astronomische Rechen-Institut (Heidelberg, Germania), 2002, ASP Conference Series, Vol. 228. Ed. by S. Deiters, B. Fuchs, R. Spurzem, A. Just, e R. Wielen.

3. "*Rotation of hot horizontal branch stars in Galactic globular clusters: the case of NGC 2808.*"
Recio-Blanco, A.; Piotto G., Aparicio Juan, A.; Bedin L.R., Lucatello S. Proceedings of " Observed HR diagrams and stellar evolution: the interplay between observational constraints and theory", A.S.P. Conference Series, vol 274, 2001

4. "*Unveiling the stellar Initial Mass Function of Galactic Globular Clusters.*"
G. Piotto, L. R. Bedin, Recio-Blanco A., J. Montalbán, F. D'Antona, S. Cassisi, D. Heggie. Proceedings of " Observed HR diagrams and stellar evolution: the interplay between observational constraints and theory", A.S.P. Conference Series, vol 274, 2001

5. "*The HST snapshot project on Galactic Globular Clusters*"
Piotto G., de Angeli F., Recio-Blanco A., Riello M., King I. R., Djorgovski S., Zoccali M., Saviane I., Renzini A., Bono G., Cassisi S., Meylan G., Rich, M. Proceedings of " Observed HR diagrams and stellar evolution: the interplay between observational constraints and theory", A.S.P. Conference Series, vol 274, 2001.

6. "*Rotation of hot horizontal branch stars in Galactic globular clusters.*"
Recio-Blanco, A.; Piotto, G.; Aparicio, A.; Renzini A. Proceedings of "New horizons in globular cluster astronomy", A.S.P. Conf. Ser., Vol. 296, 2003. Ed. by G. Piotto, G. Meylan, G. Djorgovski & M. Riello.

7. "*The Red Giant Branch Bump.*"
M. Riello, G. Piotto, Recio-Blanco A., S. Cassisi, M. Salaris. Proceedings of "New horizons in globular cluster astronomy", A.S.P. Conf. Ser., Vol. 296, 2003. Ed. by G. Piotto, G. Meylan, G. Djorgovski & M. Riello.

8. "*HST Color-Magnitude Diagrams of 74 Galactic Globular Clusters: the Snapshot Database*"
Piotto G., de Angeli F., Riello M., Recio-Blanco A., King I. R., Djorgovski S. G., Zoccali M., Renzini A., Saviane I., Sosin C., Rich R. M., Meylan, G. A.S.P. Conf. Ser., Vol. 296, 2003. Ed. by G. Piotto, G. Meylan, G. Djorgovski & M. Riello.

9. "*Rotation of hot horizontal branch stars in Galactic globular clusters.*"
Recio-Blanco A., G. Piotto, A. Aparicio. Oral contribution to the "IAU Symposium No. 215: Stellar Rotation", 11/15 November 2002.

10. "*Chemical and Rotational Properties of Cluster Hot HB Stars.*"
Recio-Blanco A., G. Piotto, R. Gratton, D. Fabbian, A. Aparicio. Poster at the " 25th meeting of the IAU, Joint Discussion 4", 16/17 July 2002.

11. "*Improving synthetic model & spectra for the RVS.*"
de Laverny P., Recio-Blanco A., Thévenin, et al. Oral contribution to the 7th RVS workshop, Nice, December 2003.

12. "*Atmospheric parameters from RVS spectra & test fields.*"
Recio-Blanco A., de Laverny P., Thévenin F., Bijaoui A., et al., Oral contribution to the 7th RVS workshop, Nice, December 2003.

13. "*The Milky Way Formation Timescale*"
Aparicio A., Rosenberg A., Piotto G., Saviane I., Recio-Blanco A., Memorie della Societa Astronomica Italiana, v.75, p.13, 2004.

14. "*Atmospheric parameters and test fields*"
Recio-Blanco A., de Laverny P., Thévenin F., Bijaoui A. Oral contribution to the 8th RVS workshop, Padova, May 2004.

15. "*Improving synthetic models and spectra*"
Thévenin F., Bigot L., Recio-Blanco A., de Laverny P. Oral contribution to the 8th RVS workshop, Padova, May 2004.

16. "*Automatic derivation of stellar atmospheric parameters and chemical abundances*"
Recio-Blanco, A., Bijaoui, A., de Laverny, P., Katz, D. and Thévenin, F., The three dimensional universe with Gaia, European Space Agency, SP-576, 2004.

17. "*Abundance anomalies in hot horizontal branch stars of the Galactic globular cluster NGC 1904.*"
Recio-Blanco, A., Fabbian, D. and Gratton, R.G., Chemical abundance and mixing in stars in the Milky Way and its satellites., Springer-Verlag Series "ESO Astrophysics Symposia", 2004.

18. "*Photometry and spectroscopy of bright stars in the Carina dSph galaxy.*"
Monelli, M., Bono, G., Nonino, M., James, J.G., François, P., Buonanno, R., Nevils, G., Recio-Blanco, A., Smith, H.A., Stetson, P.B., Thévenin F., Walker, A., Chemical abundance and mixing in stars in the Milky Way and its satellites., Springer-Verlag Series "ESO Astrophysics Symposia", 2004.

19. "*Giraffe observations of 47 Tuc: Lithium abundances along the RGB*"
Lèbre, A., Jasniewicz, G., de Laverny, P., Thévenin, F., Charbonnel, C., Recio-Blanco, A., Chemical abundance and mixing in stars in the Milky Way and its satellites., Springer-Verlag Series "ESO Astrophysics Symposia", 2004.

20. "*Stellar chemical abundances and atmospheric parameters from the Gaia/RVS spectra.*"
Recio-Blanco A., de Laverny P., Bijaoui A. et al. Oral contribution to the 9th RVS workshop, Barcelona, May 2005.

21. "*The globular cluster system as a tracer of the Galactic Halo formation and evolution*"
Recio-Blanco A., 2005, Semaine de l'Astrophysique Francaise, Journées de la SF2A, EDPsciences, Edited by F. Casoli, T. Contini, J.M. Hameury and L. Pagani,Conference Series, 2005, p. 561.

22. "*Chemical properties of field Halo and Thick Disk blue straggler stars: first results*"
Bragaglia, A., Carretta, E., Recio-Blanco A., Cacciari, C. and Kinman, T. D., From Lithium to Uranium: Elemental Tracers of Early Cosmic Evolution, Proceedings IAU Symposium No. 228, eds. V. Hill, P. Francois and F. Primas, IAU, 2005, pp.279

23. "*Li abundance evolution as probe of extra-mixing in 47 Tuc RGB stars*"
Lèbre, A., Palacios, A., Jasniewicz, G., de Laverny, P., Charbonnel, C., Recio-Blanco A., Thévenin, F., From Lithium to Uranium: Elemental Tracers of Early Cosmic Evolution, Proceedings IAU Symposium No. 228, eds. V. Hill, P. Francois and F. Primas, IAU, 2005, pp.399-400

24. "*Spectroscopic search for binaries among EHB stars in globular clusters*"
Moni-Bidin., C., Moehler, S., Piotto, G., Recio-Blanco, A., Momany, Y., Méndez, R.A., 2005, Oral presentation in Hot Subdwarf Stars and Related Objects, Baltic Astronomy, Vol. 15, p. 53-60

25. "*Automated determination of stellar atmospheric parameters and chemical abundances with MATISSE*"
Recio-Blanco, A., de Laverny, P., Bijaoui, A., 9th Corot Week, 5-9 Décembre 2005, ESA/ESTEC, Noordwijk.

26. "*The lack of binaries among hot horizontal branch stars: M80 and NGC5986*"
Moni-Bidin., C., Moehler, S., Piotto, G., Momany, Y., Recio-Blanco, A., Méndez, R.A., 2006, Proceedings of the "Globular Clusters: Guides to Galaxies" conference, Mars 2006, Concepcion, Chile, astro-ph/0606035

27. "*Status of the Generalized Stellar Parametrizer - spectroscopy*"
Recio-Blanco, A., Contribution orale au premier meeting de l'Unité de Coordination 8 "Astrophysical Parameters" du DPAC de Gaia, Nice, Mars 2006

28. "*Model fitting through the MATISSE method*"
Bijaoui, A., Recio-Blanco, A., de Laverny, P., Proceedings of the "Astronomical Data Analysis IV", Marseille, 18-20 September (2006).

29. "*Détermination automatique des paramètres atmosphériques et des abondances chimiques avec MATISSE*"
Recio-Blanco, A., Contribution orale au "Second Workshop on Databases in Stellar Spectroscopy", Paris, 18-19 Octobre 2006

30. *Automatic parametrization of CoRoT stellar targets with MATISSE*
Recio-Blanco, A., de Laverny, P., 2007, Third Corot-Brazil workshop, Natal, Ed. de Medeiros.

31. *From stars to planets : Understanding the properties of the planetary systems detected by Corot*"
Gazzano J.C., Deleuil M., de Laverny P., Recio-Blanco A., 2007, ELSA school on the Science with Gaia

32. *Automatic classification of unresolved galaxies using the Matisse algorithm*
Kordopatis G., Recio-Blanco A., de Laverny P., Bijaoui A., 2007, , ELSA school on the Science with Gaia

33. *Stellar populations as a test for the stellar evolution*" Aparicio,A.; Gallart,C.; Zoccali,M.; Cassisi,S.; Hidalgo,S.L.; Recio-Blanco,A., MmSAI, 2008, 79, 301

34. *How did a typical galaxy form? - Clues from the old stellar populations of the Milky Way Thick Disc*"
Recio-Blanco, A., P. Laverny, G. Gilmore, R. Wyse, O. Bienaym, A. Vallenari, A. Bijaoui, M. Zoccali, G. Bono, J. Norris, M. Wilkinson, 2008, ; IAU symposium 254.

35. *Froms stars to planets : Understanding the properties of the planetary systems detected by Corot*
Gazzano J.C., Deleuil M., de Laverny P., Recio-Blanco A., de Laverny, 2008, Exoplanet forum, Pasadena (USA)

36. *Parameter Estimation from an Optimal Projection in a Local Environment*"
A. Bijaoui, Recio-Blanco, A., P. de Laverny, 2008, AIP Conference Proceedings, Editor C. Bailer-Jones, 1082,54

37. "*Multiobject spectrography as a complement for Gaia*"
A. Recio-Blanco, 2009, Contribution orale au ESO Spectroscopic workshop 9-10 Mars 2009, Garching, Munich

38. "*Multiobject spectrography as a complement for Gaia*"
A. Recio-Blanco & V. Hill, 2009, Contribution orale aux Journées de l'Sf2a, Besancon, 29 Juin 2009

39. "*Estimation de parametres par projection optimale dans un environnement local*"
Bijaoui, A., Recio-Blanco, A. and de Laverny, P., 2009, colloque du GRETSI, Edition lectronique

40. "*From stars to planets*"
Gazzano, J.-C., Deleuil, M., de Laverny, P., Recio-Blanco, A., Bouchy, F., Gandolfi, D. and Loeillet, B.,2009, IAU Symposium, 253, pp. 404-405

41. "*Automated stellar parametrization with MATISSE : application to Galactic populations*"
de Laverny, P., Recio-Blanco, A., Bijaoui, A., Gazzano, J.C., Kordopatis, G., Ordenovic, C. and Worley, C., 2010 Astronomical Data Analysis VI, eds. Strack and Murtagh, Monastir (Tunisie) 3-7 Mai 2010

42. "*Massive spectroscopic analysis: the stellar population in three CoRoT/Exoplanet fields*"
Gazzano, J.C., de Laverny, P., Deleuil, M., Recio-Blanco, A. and Kordopatis, G., 2010 Semaine de l'Astrophysique Franaise Journes de la SF2A 2010 , Marseille-France 21-24/06/2010

43. "*Spectroscopic survey of Thick Disc stars outside the Solar neighborhood*"
Kordopatis, G., Recio-Blanco, A., de Laverny, P., Bijaoui, A., Hill, V., Gilmore, G., Helmi, A., Bienaym, O., Ordenovic, C. and Wyse, R.FG., 2010, LSA conference 2010 - Gaia: at the frontiers of astrometry, ed. C. Turon, Svres (france) sous presse

44. "*Properties of the thick disc far from the Solar neighbourhood*"
Kordopatis, G., Recio-Blanco, A., de Laverny, P., Bijaoui, A., Hill, V., Gilmore, G., Helmi, A., Bienaym, O., Ordenovic, C. and Wyse, R.FG., 2010, Semaine de l'Astrophysique Franaise Journes de la SF2A 2010 , Marseille-France 21-24/06/2010

45. "*The AMBRE Project: Looking for Stellar Clusters in FEROS Archived Spectra*"
Worley, C. C.; de Laverny, P.; Recio-Blanco, A.; Hill, V.; Kordopatis, G., 2010, Stellar Clusters & Associations: A RIA Workshop on Gaia. Proceedings. Granada, Spain, May 23 - 27, 2011. Edited by: Alfaro Navarro, E. J.; Gallego Calvente, A. T.; Zapatero Osorio, M. R., pp.371-372

46. "*Tests of MATISSE on large spectral datasets from the ESO archive*"
Worley, C. C.; de Laverny, P.; Recio-Blanco, A.; Hill, V.; Bijaoui, A.; Ordenovic, C.; Vernisse, Y., 2011, EAS, 45, 209

47. "*GYES, A Multifibre Spectrograph for the CFHT*"
Bonifacio, P.; Mignot, S.;...,Recio-Blanco, A., et al., 2011, EAS, 45, 219

48. "*A spectroscopic survey of the Thick Disc outside the Solar neighbourhood: A comparison with the Besanon model*"
Kordopatis, G.; Recio-Blanco, A.; de Laverny, P.; Gilmore, G.; Hill, V.; Wyse, R. F. G.; Helmi, A.; Bijaoui, A.; Ordenovic, C.; Zoccali, M.; Bienaym, O., 2011, EAS, 45, 405

49. "*Probing the thick disc formation scenarios outside the solar neighbourhood*"
Kordopatis, G.; Recio-Blanco, A.; de Laverny, P.; Gilmore, G.; Hill, V.; Wyse, R. F. G.; Helmi, A.; Bijaoui, A.; Ordenovic, C.; Zoccali, M.; Bienaym, O., 2011, Proceedings of the Annual meeting of the French Society of Astronomy and Astrophysics Eds.: G. Alecian, K. Belkacem, R. Samadi and D. Valls-Gabaud, pp.311-314

50. "*The AMBRE project: Results from the MATISSE analysis of the ESO-FEROS archived spectra*"
Worley, C. C.; de Laverny, P.; Recio-Blanco, A.; Hill, V.; Kordopatis, G., 2012, Assembling the Puzzle of the Milky Way, Le Grand-Bornand, France, Edited by C. Reyl; A. Robin; M. Schultheis; EPJ Web of Conferences, Volume 19, id.09008

51. "*Automated stellar spectra parameterisation for Gaia-RVS*"
Kordopatis, G.; Recio-Blanco, A.; de Laverny, P.; Bijaoui, A.; Hill, V.; Gilmore, G.; Wyse, R. F. G.; Ordenovic, C., 2012, Assembling the Puzzle of the Milky Way, Le Grand-Bornand, France, Edited by C. Reyl; A. Robin; M. Schultheis; EPJ Web of Conferences, Volume 19, id.09010

52. "*The Gaia-ESO Public Spectroscopic Survey*"
Gilmore, G.; Randich, S.;...,Recio-Blanco, A., et al., 2012, The ESO Messenger, vol. 147, p. 25-31

53. "*The AMBRE Project: Exploring Stellar Populations in the Milky Way Disk with FEROS Archived Spectra*"
Worley, C. C.; de Laverny, P.; Recio-Blanco, A.; Hill, V.; Kordopatis, G., 2012, ASPC 458, 143

54. "Metallicity and Kinematics of Thick Disc Stars at Intermediate Galactic Latitudes"
Kordopatis, G.; Recio-Blanco, A.; de Laverny, P.; Gilmore, G.; Hill, V.; Wyse, R. F. G.; Helmi, A.; Bijaoui, A.; Zoccali, M.; Bienaym, O., 2012, ASPC, 458, 175

55. "The AMBRE Project: Stellar Parameterisation of ESO Archived Spectra"
de Laverny, P.; Recio-Blanco, A.; Worley, C. C.; De Pascale, M.; Hill, V.; Bijaoui, A., 2013, The ESO Messenger, 153, 18

56. "A Community Science Case for E-ELT HIRES"
Maiolino, R.; Haehnelt, M.; Murphy, M. T.; ... Recio-Blanco, A. et al. 2013, White Paper for E-ELT HIRES, astro-ph 1310.3163

57. "The Mixed Origin of the Galactic Thick Disk"
Cui, W. Y.; Liu, C.; de Laverny, P.; Recio-Blanco, A.; Van de Ven, G., 2014, "Setting the scene for Gaia and LAMOST", Proceedings of the International Astronomical Union, IAU Symposium, Volume 298, pp. 402

58. "Chemical tagging with Gaia-ESO Survey and Gaia-RVS data"
Guiglion, G.; Recio-Blanco, A.; de Laverny, P., 2014, "Setting the scene for Gaia and LAMOST", Proceedings of the International Astronomical Union, IAU Symposium, Volume 298, pp. 408

European Space Agency Technical Notes (Gaia mission)

1. "*A library of synthetic spectra over the Gaia/RVS spectral range*"
A. Recio-Blanco, P. de Laverny & B. Plez, 2005, ESA technical note RVS-ARB-001

2. "*Estimates of Data Processing Requirements for the Gaia GSP-spec*"
A. Recio-Blanco, 2005, ESA technical note GAIA-C8-TN-OCA-ARB-001

3. "*Estimates of Data Processing Requirements for the Specific Source Unit Cool Stars*"
A. Recio-Blanco, 2005, ESA technical GAIA-C8-TN-OCA-ARB-002

4. "*Gaia Data Processing & Analysis Consortium: Response to the ESA's announcement of Opportunity. Proposal for the Gaia Data Processing*"
De Angeli, F., ..., A. Recio-Blanco et al., soumis à l'ESA le 6 Décembre 2006 par le DPAC, ESA tecnical note GAIA-CD-SP-DPAC-FM-030-1, Ed. F. Mignard & R. Drimmel

5. "*A new grid of synthetic spectra*"
B. Edvardsson, K. Eriksson, A. Recio-Blanco, P. de Laverny, 2007, DPAC/CU8 internal report

6. "*GSPspec Software Release Note for Cycle 2.*"
A. Recio-Blanco, P. de Laverny, A. Miniussi, Avril 2007, GAIA-C8-SP-OCA-ARB-001-1

7. "*GSPspec Software Requirements Specification, Software Design and Software User Manual for Cycle 2.*"
A. Recio-Blanco, P. de Laverny, A. Miniussi, Avril 2007, GAIA-C8-SP-OCA-ARB-002-1

8. "*GSPspec Software Test Plan and Verification Report for Cycle 3.*"
A. Recio-Blanco, P. de Laverny, A. Miniussi, Juillet 2007, GAIA-C8-SP-OCA-ARB-003-2

9. "*GSPspec Software Requirements Specification, Software Design and Software User Manual for Cycle 3.*"
A. Recio-Blanco, P. de Laverny, A. Miniussi, October 2007, GAIA-C8-SP-OCA-ARB-002-2

10. "*GSPspec Software Release Note for Cycle 3.*"
A. Recio-Blanco, P. de Laverny, A. Miniussi, October 2007, GAIA-C8-SP-OCA-ARB-001-2

11. "*GSPspec Software Test Plan and Verification Report for Cycle 4.*"
A. Recio-Blanco, C. Ordenovic, P. de Laverny, April 2008, GAIA-C8-SP-OCA-ARB-003-4

12. "*GSPspec Software Requirements Specification, Software Design and Software User Manual for Cycle 4.*"
A. Recio-Blanco, C. Ordenovic, P. de Laverny, April 2008, GAIA-C8-SP-OCA-ARB-002-4

13. "*GSPspec Software Release Note for Cycle 4.*"
A. Recio-Blanco, C. Ordenovic, P. de Laverny, April 2008, GAIA-C8-SP-OCA-ARB-001-4

14. "*GSPspec Software Release Note for Cycle 6.*"
A. Recio-Blanco, C. Ordenovic, P. de Laverny, Juillet 2009, GAIA-C8-SP-OCA-ARB-001-6

15. "*GSPspec Software Test Plan and Verification Report for Cycle 6.*"
A. Recio-Blanco, C. Ordenovic, P. de Laverny, April 2008, GAIA-C8-SP-OCA-ARB-003-6

16. "*GSPspec Software Release Note for Cycle 9.*"
C. Ordenovic,A. Recio-Blanco, January 2010, GAIA-C8-SP-OCA-ARB-001-5

17. "*GSPspec Software Test Plan and Verification Report for Cycle 9.*"
C. Ordenovic,A. Recio-Blanco, January 2010, GAIA-C8-SP-OCA-ARB-001-6

18. "*GSPspec Software Requirements Specification, Software Design and Software User Manual for Cycle 9.*"
C. Ordenovic,A. Recio-Blanco, January 2010, GAIA-C8-SP-OCA-ARB-001-7

19. "*GSPspec Software Requirements Specification, Software Design and Software User Manual for Cycle 10.*"
C. Ordenovic,A. Recio-Blanco, July 2011, GAIA-C8-SP-OCA-ARB-002-6

20. "*GSPspec Software Release Note for Cycle 10.*"
C. Ordenovic,A. Recio-Blanco, July 2011, GAIA-C8-SP-OCA-CO-001-10

21. "*GSPspec Software Test Report for Cycle 10.*"
C. Ordenovic,A. Recio-Blanco, July 2011, GAIA-C8-SP-OCA-CO-002-10

22. "*GSPspec Software Release Note for Cycle 12.*"
C. Ordenovic,A. Recio-Blanco, March 2012, GAIA-C8-SP-OCA-CO-003-10

23. "*GSPspec Software Test Report for Cycle 12.*"
C. Ordenovic,A. Recio-Blanco, March 2012, GAIA-C8-SP-OCA-CO-004-10

24. "*CU8 Software Design Description: Scientific Algorithms*"
A. Lanzafame, C. Liu,...,A. Recio-Blanco, et al., August 2012, GAIA-C8-SP-OACT-AL-006

25. "*Validation of the GSPspec parameters*"
G. Kordopatis, A. Recio-Blanco & C. Ordenovic, September 2014, GAIA-CU8-TN-IOA-GK-001

GALACTIC ARCHAEOLOGY IN THE GAIA ERA

Foreword

This HDR report includes part of the work I developed since my arrival at the Observatoire de la Côte d'Azur in August 2004. It mainly describes the implementation, evolution and main science results of an extensive project, started ten years ago, and devoted to the study of the Milky Way history through the spectroscopic analysis of its stellar populations.

Since its beginning, this project was in synergy with the perspectives of the Galactic populations research field. On one hand, the Gaia mission was accepted by the ESA Science Programme Committee in 2000, although it was still in its definition phase in 2004. On the other hand, multi-object spectrographs with medium to high resolution capabilities, like 6dF at the Anglo Australian Observatory (commissioned in 2001) and FLAMES at the European Southern Observatory (commissioned in 2002) were opening new horizons for the chemo-kinematical study of statistically relevant samples of stars.

Nevertheless, several challenges needed to be tackled. First, the spectroscopic data analysis had to evolve from the classical manual procedures to automated methods able to produce, for huge quantities of spectra, reliable enough physical parameters and individual chemical element abundances to disentangle the stellar populations puzzle of the Milky Way. Second, the Galactic populations research had not to forget its interaction with the stellar physics, crucial for the correct interpretation of the stars physical characteristics, taking properly into account stellar evolution processes, internal mixing mechanisms, stellar atmospheres physics, nucleosynthesis, etc... Finally, the progress of observational studies, had to be in synergy with new models of disc galaxy formation and evolution, having high enough resolution to produce predictions for stellar populations.

During my PhD thesis and a first post-doc, I had focused on the Galactic globular clusters population, combining stellar physics and halo formation studies. This experience and my arrival at the Gaia team of the Observatoire de la Côte d'Azur offered me the opportunity to take up the challenge of the above mentioned project. The development of MATISSE (Recio-Blanco et al. 2006) and other automated stellar parametrization methods was the first step (see *Chapter 2*). They were implemented in a pioneer context, where only other few attempts were being performed, as the Sloan Digital Sky Survey SEGUE pipeline methods (ex. Allende-Prieto et al. 2006, Re Fiorentin et al. 2007) and the first RAVE survey procedures (Zwitter et al. 2008). In addition, the MATISSE algorithm developed an innovative mathematical approach trying to combine the efficient data analysis, in terms of computational time, with an easy physical interpretation of it.

Then came the first successful applications of the implemented procedures to real data, as the CoRot exoplanet fields follow up (Gazzano et al. 2010) and Giraffe CaII triplet spectra (Kordopatis, Recio-Blanco et al. 2011a). The agreement with the European Southern Observatory to parametrize the high and medium resolution archive stellar spectra with MATISSE (AMBRE project, de Laverny, Recio-Blanco et al. 2013) was also very important to prove the capabilities of our methods at a large scale. AMBRE started at the end of 2009 and its results (Worley et al. 2012; de Laverny et al. 2012; De Pascale et al. 2014 and Worley et al. 2014) are not included in this HDR report.

A crucial step has of course been the derivation of Galactic science results from the automatedly determined stellar parameters. To this purpose, as shown in this report, I mainly focused on Galactic disc science (Kordopatis, Recio-Blanco et al. 2011b; Recio-Blanco et al. 2014; Mikolaitis et al. 2014, Guiglion, Recio-Blanco et al. 2014, see *Chapter 3*) and more recently on the bulge characterization (Rojas-Arriagada, Recio-Blanco et al. 2014, see *Chapter 4*). In addition, I also participated as a close collaborator to other thin and thick disc studies (ex. Gazzano et al. 2013; Kordopatis et al. 2013a) that are not included in this HDR report.

Moreover, the involvement in Galactic Archeology surveys has been essential. First of all, my activities in the Gaia Data Processing and Analysis Consortium, as responsible for the stellar parameters derivation from RVS spectra, motivated my work since the beginning. Our recent evaluation of the Gaia RVS parametrization performances (Recio-Blanco et al. 2014, see *Chapter 5*) shows that the contribution of the RVS based stellar parameters will be unique in the brighter part of the Gaia survey, allowing crucial age estimations and accurate chemical abundances. My Gaia activities also include many ESA technical notes, from 2005 to today, that are not described here.

Furthermore, since 2009, I supported the scientific and technical definition of a European Galactic chemo-dynamical survey from the ground (Recio-Blanco et al. 2009), to reinforce the science exploitation of the Gaia mission. In 2011, ESO accepted the Gaia-ESO large public survey (GES, P.Is G. Gilmore and S. Randich), and I was proposed to be co-responsible of the Working Group in charge of the FGK type stars parametrization from Giraffe data. This group treats around 70% of the GES stellar spectra, furnishing their atmospheric parameters and individual element abundances. The analyzed targets belong to all the main stellar Galactic populations. In addition, I produce, thanks to the MATISSE application, one of the three sets of results that are combined to derive the final GES recommended parameters for those stars. Moreover, I contribute to the analysis of the GES high resolution UVES spectra, through the work of the Nice node. My GES activities, both in stellar parametrization and Galactic population studies are today a central part of my work and they prepare the way for my involvement in the Gaia science analysis. Lastly, regarding spectroscopic surveys and thanks to a collaboration with the RAVE project, the MATISSE and DEGAS methods are now at the core of the RAVE analysis pipeline. This offered me the opportunity to be co-author of the more recent RAVE data release (Kordopatis et al. 2013b), already used by the RAVE consortium for many science results. This RAVE application is not included in this report.

Finally, in parallel with the above described activities, I continued to work on Galactic globular clusters (ex. Carretta, Recio-Blanco et al. 2007, Carretta et al. 2010; de Laverny & Recio-Blanco 2013a,b) and stellar physics, in particular on internal mixing processes (ex. Pace, Recio-Blanco et al. 2006; Recio-Blanco & de Laverny 2007) and fluorine nucleosynthesis (ex. Abia, Recio-Blanco et al. 2009; Recio-Blanco et al. 2012). None of these results are included in this HDR report, with the exception of the Recio-Blanco et al. 2012 work, that additionally helps to the chemical characterization of thin disc stars.

In summary, the above detailed context describes the framework and boundaries of the present HDR report. It is also the starting point of the projects detailed in the perspectives chapter. Both the past and the future of this project are indeed deeply anchored in the Galactic archaeology research of the Gaia era.

Chapter 1

INTRODUCTION

How did our galaxy form? What is its place, and ours, in the cosmic evolution? Modern astronomy has revealed that the origins of our planet, our Sun and the Milky Way are intricately tied to the nature of the early Universe and the laws of physics.

Galactic Archaeology aims at unveiling the history of the Milky Way by analysing stars, just as the history of life was deduced from examining rocks. Stars record the past in their ages, compositions and kinematics and can provide unprecedented detailed constraints on the early phases of galaxy formation, back to redshifts greater than two (a look-back time of ~10 billion years). In particular, the chemical abundance patterns imprinted on stellar atmospheres reflect the gas conditions at the time of the stars' formation. The 'chemical tagging' approach (Freeman & Bland-Hawthorn, 2002) opens the way to the temporal sequencing of a large fraction of stars.

In addition, the detailed examination of our Galaxy offers a near-field small-scale cosmological approach. The current cosmogony paradigm, described by a ΛCDM cosmology, has been extremely successful in explaining the large-scale matter and galaxy distribution. Yet, on smaller scales, reproducing the physical properties of galaxies like the Milky Way, remains challenging (e.g. Scannapieco et al. 2012). In particular, the extremely complex physics of baryons is still unreliably simulated. Baryon physics implies highly non-linear processes that are presently introduced in the galaxy evolution models via parameterized heuristic algorithms. Models require calibration with well-studied, nearby, test cases and the Galactic Archaeology approach offers a unique opportunity to provide such constraints.

From the observational side, we are hampered today by i) the small size of stellar samples observed outside the solar neighbourhood with precise enough chemical information, ii) the lack of 3D velocities for complete dynamical studies, iii) the very important errors in the stellar distances that blur our knowledge of the Galaxy structure, and as a consequence, iv) by the absence of stellar age estimations for most of the observed stars. Gaia (launched on Dec. 2013) and the new ground-based spectroscopic surveys, as the Gaia-ESO Survey (GES) are quickly changing this situation and opening a new era of Galactic research. They will reveal a moving, 3D Milky Way map of unprecedented scope and precision, as well as provide the physical properties of each star, including luminosity, surface gravity, temperature and chemical composition.

The goal of my research work is to study the Galactic stellar populations to reconstruct the time evolving chemo-dynamical picture of the Milky Way, in which we live. This picture can then be used as a basis to produce observational diagnostics about the Milky Way populations, that can be compared to theoretical models predictions of Galaxy formation. In addition, this approach can shed new light on the detailed processes that led the Milky Way to form and evolve as a disc-type (barred) galaxy, in the more general context of galaxy evolution. The different galaxy formation and evolution processes have left their fingerprints on stars, that are the fossil targets of Galactic archaeology research. These remaining signatures have to be searched in a high-dimensional parameter space constituted by i) chemical, ii) spatial and iii) kinematical distributions, plus iv) their temporal gradients. To unveil them, appropriate analysis tools have to be developed. For this reason, part of my work has been dedicated to the implementation of new automated data analysis procedures that efficiently and rigorously treat the archaeological remains at our disposal. Moreover, I am deeply involved in Milky Way observational projects, from P.I. spectroscopic programs, to large public surveys like GES and the European Space Agency Gaia mission. This work has allowed me to shed new light on the properties of some of the main Galactic components: the thick disc, the thin disc and the bulge.

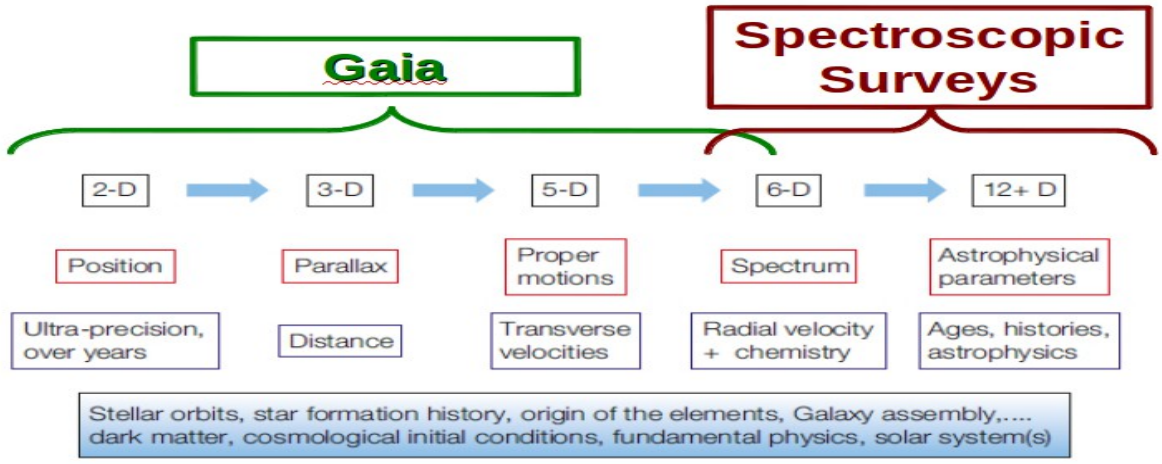


***Figure 1**: Dimensionality of data and parameter spaces for Galactic Archaeology with the contribution of Gaia and ground-based spectroscopic surveys (adapted by Recio-Blanco, 2012 from Gilmore et al. 2012).*

1.1 The formation and evolution of the Milky Way as a disc galaxy

Our Galaxy is a late-type spiral, as is evident from the high concentration of stars, gas and dust into a narrow strip strung across the night sky. The Galaxy is conventionally decomposed into: (i) a central bar/bulge that extends out to ~3 kpc; (ii) a nearly spherical halo that extends out to about 100 kpc and is studded with globular clusters; and (iii) a disc that defines the Galactic plane and is probably confined to R<~15 kpc. The disc is often decomposed into a metal-rich thin disc and a more metal-poor thick disc.

In the current cosmogony paradigm, Λ-Cold Dark Matter (ΛCDM) cosmology, dark matter and dark energy shape the large-scale expansion of the Universe, while on smaller scales, tiny initial fluctuations grow into large dark matter halos, where galaxies like ours form. Galaxies grow through a sequence of mergers and accretion events and, inside galaxies, baryonic matter aggregates to form stars. However, the interplay between gas, stars, black holes, dark matter and dark energy has only started to be understood.

Eggen, Lynden-Bell and Sandage (1962) were the first to show that it is possible to study Galactic archaeology using stellar abundances and dynamics. They inferred that the Galactic metal-poor stars reside in a halo that was created during the rapid free-fall collapse of an isolated protogalactic cloud, shortly after it decoupled from the universal expansion. This picture was challenged by Searle & Zinn (1978), who, studying globular clusters, suggested a halo built up over an extended period from independent fragments. The ideas of galaxy formation via hierarchical aggregation of smaller elements from the early Universe fit in easily with the view of a Galaxy formed from small fragments.

Although the hierarchical model may be fundamentally different from the collapse model, they may have a few features in common. It is not unlikely that, early on in the history of the Galaxy, there was a phase which could be described as a fast dissipative collapse, but which was triggered by gas-rich mergers (Brook et al. 2004), rather than by the collapse of a giant gas cloud. Collisionless minor mergers are also proposed today to play a role in the formation of our Galaxy (Toomre, 1977a) as well as external gas accretion from filaments of the cosmic web (Combes 2009; Putman et al. 2012) and internal secular processes (e.g. Kormendy & Kennicutt 2004).

Producing a galaxy through *ab initio* calculations, that in its properties resembles the Milky Way, has remained challenging (Rix & Bovy, 2013). Nevertheless, several approaches are producing fruitful predictions about the Milky Way chemo-dynamical properties. Among them, one can cite semy-analytic models (e.g. Somerville et al. 2008), hydrodynamical simulations in a cosmological context (e.g. Martig et al. 2012, Guedes et al. 2011, Brook et al. 2012, Stinson et al. 2013, Scannapieco et al. 2012, Semelin & Combes 2005, etc...) and dynamical models (e.g. Binney & McMillan, 2011; Rix & Bovy 2013). In addition, a large body of work has investigated processes relevant to disc evolution from an analytic or numerical perspective (not cosmological *ab initio* simulations), with an emphasis on chemical evolution (e.g. Matteucci & Francois 1989, Chiappini et al. 2001, Fraternali & Binney 2008,...), thick disc formation (e.g. Roskar et al. 2013, Villalobos & Helmi 2008, Brook et al. 2004, Bournaud et al. 2007,2009; Di Matteo et al. 2011, 2013) and bulge formation (e.g. Di Matteo et al. 2014; Martínez-Valpuesta & Gerhard 2013), etc.... Finally, Minchev et al. (2013a) have introduced a new approach, combining detailed chemical evolution models with cosmological N-body simulations.

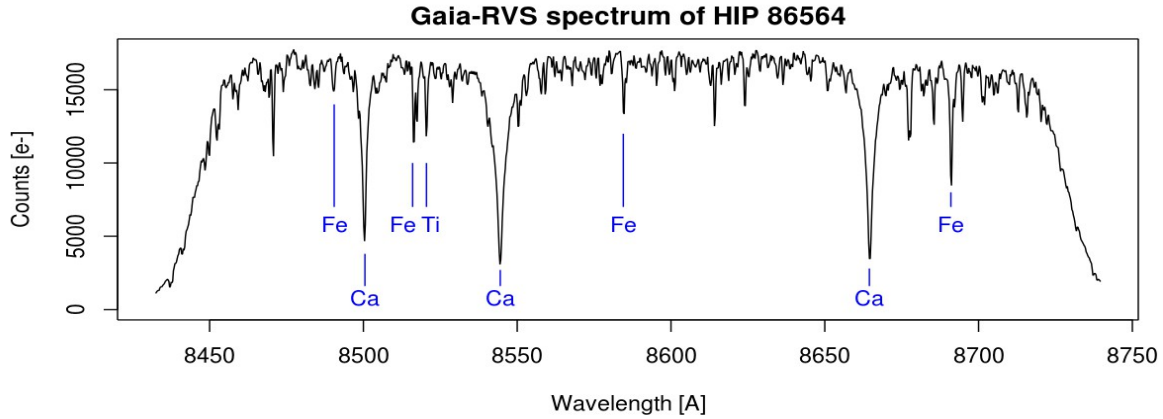


Figure 2: *Gaia RVS spectrum taken during commissioning (D. Katz & Gaia Project team)*

1.2 Milky Way stellar population surveys

A suite of ground-based vast stellar surveys mapping the Milky Way, culminating in the Gaia mission, is revolutionizing the observational information about Galactic stellar populations.

Dimensionality of data and parameter spaces for Galactic Archaeology studies

The Galactic history has been imprinted in the stars spatial, kinematical and chemical distributions, plus their temporal evolution. Therefore, our understanding of the Milky Way history will always be ill-defined if only a few dimensions of that parameter space are probed.

As explained in Gilmore et al. (2012), there are four basic observational thresholds that we need to pass to have a complete view of the fossil record of our Galaxy formation and evolution. Fig. 1 shows the dimensionality of the data and parameter spaces, illustrating those observational challenges. The first step is source identification (or discovery) trough its position and photometric data. This is provided today by photometric surveys of the Galaxy as VISTA and VST. Secondly, the temporal domain is added, allowing us to explore a 5-D space formed by parallaxes (and therefore distances) and proper motions (or transverse velocities). The Gaia mission will be revolutionary here by providing this 5-D view of the Galaxy for about 10^9 stars down to a magnitude of G=20. The third step is the line-of-sight (radial) velocity, that allows to determine stellar orbits. In addition, if the spectral domain and resolution and the data quality are high enough, the stellar atmospheric parameters and chemical abundances can be derived. Finally, the fourth threshold is passed when stellar ages can be derived, allowing the access to the temporal dimension. The Gaia mission, thanks to its Radial Velocity Spectrograph (RVS) will provide medium resolution spectra for most stars brighter than ~16th magnitude. This will allow the determination of the radial velocity, the global metallicity and whenever possible, the α-element (in particular Ca, Mg, Si and Ti) abundance for several tens of millions of stars. Unfortunately, the Gaia RVS magnitude limit is about three magnitudes brighter than that of astrometry and photometry. For this reason, the contribution of ground-based spectroscopic surveys is crucial in the two last observational thresholds mentioned above (radial velocity and detailed stellar chemistry).

The European Space Agency Gaia mission

The Gaia space mission, successfully launched on the 19th December 2013, has already started to provide (see Fig. 2) a stereoscopic census of our Galaxy through the measurement of high accurate astrometry, radial velocities and multi-colour photometry. Due of its huge expected impact in our knowledge of the Milky Way, the Gaia advent and preparation has opened the path to a new era of Galactic investigation, well before the launch.

Over the course of its baseline 5 year mission, Gaia will measure parallaxes and proper motions for each object in the sky brighter than (G) magnitude 20 — amounting to over 10^9 stars, galaxies, quasars and solar system objects. It will achieve an astrometric accuracy of 12–25 mas, depending on colour, at G=15 and 100–300 mas at G=20. Multi-colour photometry will be obtained for all objects by means of low-resolution spectrophotometry which is realized through prisms dispersing the light entering the field of view. One disperser — called BP for Blue Photometer — operates in the wavelength range 330–680 nm; the other — called RP for Red Photometer - covers the wavelength range 640–1050 nm. BPRP data will provide estimations of stellar atmospheric parameters and interstellar extinction (Bailer-Jones et al. 2013).

In addition to the spectrophotometric instrument, Gaia features the so-called Radial Velocity Spectrometer

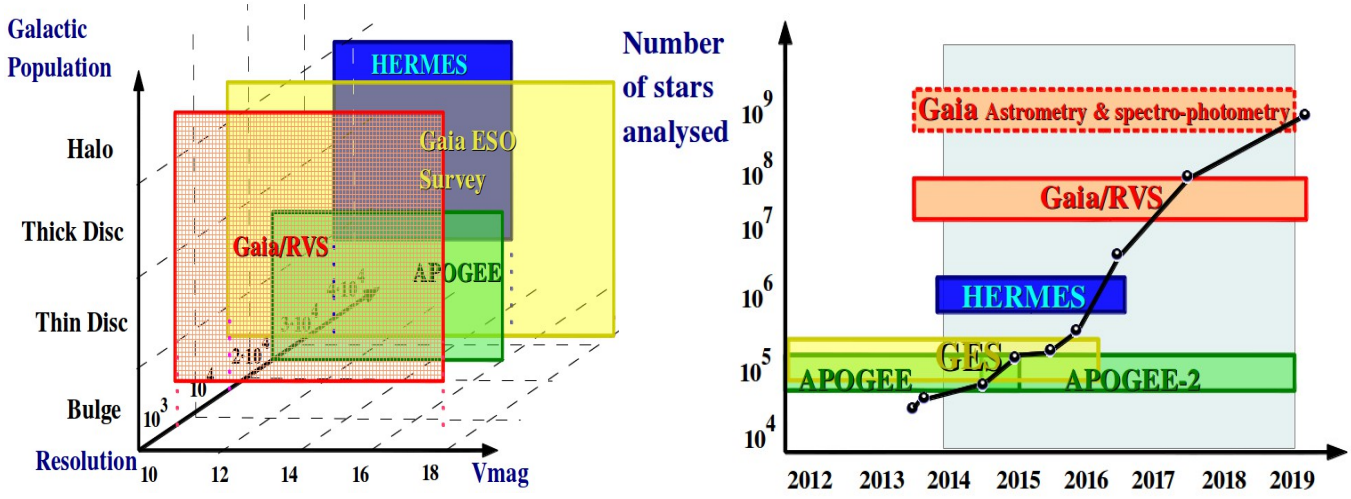


Figure 3: Left: on-going and planned spectroscopic surveys. Right:time-line of the surveys. The black line shows the increase in the number of available stars following the surveys data releases.

(RVS, Fig. 2) that provides the third component of the space velocity of each star down to about G=16 (V-band for K stars). The RVS is a medium-resolution (R=11000), integral-field spectrograph dispersing all the light entering the field of view. With this instrument, radial velocities with a precision of 1–15 km/s will be measured for all objects to V ~ 16-17, complementing the astrometry to provide full 6-D space information for the brighter sources. In addition, spectroscopic atmospheric parameters (Teff, logg and metallicy) will be provided for ~ 50x10^6 of stars, together with the individual abundances of several elements (mainly Fe, Ca, Ti, Mg, Si) for about 2x10^6 stars. Our team has the responsibility of this last mentioned aspect.

A large pan-European team of expert scientists and software developers known as DPAC (Data Processing and Analysis Consortium, Chair A. Brown) is responsible for the processing of Gaia's data with the final objective of producing the Gaia Catalogue. DPAC has been in place since 2006 and has the task to develop the data processing algorithms, the corresponding software, and the IT infrastructure for Gaia. It also executes the algorithms during the mission in order to turn the raw telemetry from Gaia into the final scientific data products that will be released to the scientific community. The Gaia DPAC is also in charge of the design, development and operation of the Gaia catalogue and archive, which will contain the intermediate and final mission products of interest to the scientific community at large.

DPAC is structured around specialised Coordination Units (CUs). Each CU is responsible for developing the scientific algorithms and software corresponding to a particular sub-system of the overall Gaia data processing system. The software developed by the CUs is run by one of the data processing centres. These centres host the computing hardware and provide software engineering expertise to support the CUs.

I have personally been involved in Gaia preparation activities well before the creation of the Gaia DPAC, within the OCA Gaia team led by F. Mignard (Gaia DPAC manager from its beginning until 12/2012). In particular, my activities concern the CU8, in charge of the astrophysical parameters determination (Bailer-Jones et al. 2013). I am the manager of the Gaia DPAC top level Work Package in charge of the automated stellar parameterisation of Gaia/RVS spectra (Generalised Stellar parametrizer – spectroscopy, GSPspec). Together with A. Bijaoui and P. de Laverny, we have implemented automated physical and chemical parameterisation procedures for the Gaia RVS data. We are now in charge, with the help of C. Ordenovic (computer engineer) of the RVS stellar parameters estimation and scientific validation, prior to the ingestion of the final products into the Gaia archive (see also Chapter 5).

The Gaia data releases are currently foreseen for mid-2016 (DR1), early-2017 (DR2), 2017-18 (DR3), 2018-19 (DR4) and 2022 (final release and publication of the Gaia catalogue).

On going and planned ground-based surveys for Galactic Archaeology

Until the end of 2003, most of the information was confined to small samples, for which high-resolution spectroscopic data was obtained (for instance, Edvardson et al. 1993, Furmann et al. 1998, Reddy et al. 2003). Then, the Geneva Copenhagen Survey (Nordström et al. 2004) obtained the first large photometric sample of around 16 000 stars together with radial velocities, as part of a Hipparcos follow-up campaign (hence, confined to 100 pc from the Sun). Later on, very wide (or all-sky) **multi-band photometric surveys** have flourished, like the Sloan Digital Sky Survey (SDSS, Eisenstein et al. 2011) and the Two-micron All

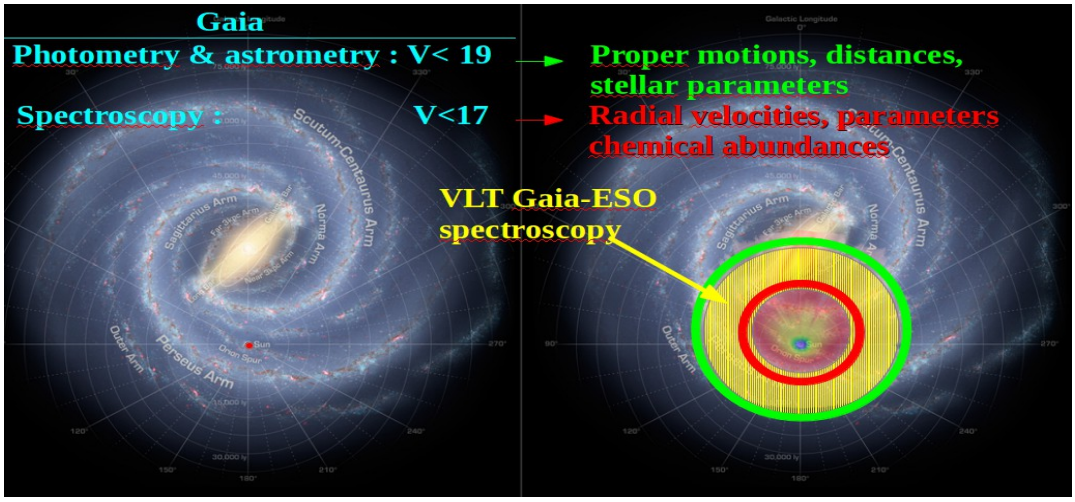


Figure 4: *Coverage of the Gaia spectro-photometry and astrometry (green circle), the Gaia spectroscopy (red circle) and the Gaia ESO Survey complementary high resolution spectroscopy.*

Sky Survey (2MASS, Skrutskie et al. 2006). They allowed to probe the Milky Way populations (especially the halo) to a depth and homogeneity that had never been reached before. One striking example concerns the tomography of the Milky Way halo from SDSS down to magnitudes of g~22 by Juric et al. (2008) or Ivezic et al. (2008).

This triggered the era of optical **low-resolution spectroscopic surveys**. They have increased the number of stars with chemo-kinematical information by more than an order of magnitude and extended the studied volume to distances of a few kpc from the Sun. The SDSS project, in its series of operations (SDSS I, II and III) has publised about 250 000 spectra (R=1800) from the Sloan Extension for Galactic Understanding and Exploration (SEGUE, Yanny and Rockosi 2009). SDSS spectra have provided only limited information on the structures revealed in the SDSS photometry, but they produced radial velocity measurements to 10-20 km/s and [Fe/H] abundances to 0.25 dex for stars with $14 < r < 19$ mag (Schlesinger et al. 2011). SDSS3 stellar spectroscopy continues, at ~5 stars/sq deg, as this project does not observe the Galactic thin disc and the Bulge. A striking, albeit debated result from SEGUE is the dual nature of the Halo (Carollo et al. 2008).

The RAdial Velocity Experiment (RAVE, Steinmetz et al. 2006) is obtaining accurate radial velocities (< 5 km/s) and global metallicities for 5×10^5 stars with I<13 from spectra with R=7500. RAVE is also estimating the individual abundances of some elements for several thousand stars. This project, due to its rather bright magnitude limit is probing essentially the galactic discs populations. Among the many RAVE papers already published up to date, our team has importantly contributed to the fourth data release (Kordopatis,..., Recio-Blanco, et al. 2013) that has been possible thanks to parameterisation algorithms developed in Nice by our group. RAVE DR4 has already been used for a number of science applications as, for instance, constraints on the Galactic bar (Antoja et al. 2014), disc chemical gradients (Boeche et al. 2013) and the study of the disc velocity dispersions (Minchev et al. 2014).

The results of the first low-resolution surveys revealed the key role of the stars chemical information to disentangle the Milky Way stellar population puzzle. Therefore, in order to obtain precise chemical constraints, complementary to kinematics, **high-resolution spectroscopic surveys** have aroused. Three vast high-resolution spectroscopic surveys will be active from the ground during the period 2014-2019. Two of them are not European (APOGEE, part of the Sloan Digital Sky Survey III and After-SDSSIII and the Australian HERMES/GALAH survey), while the third one is the Gaia-ESO Survey (c.f. Fig. 3).

The SDSS Apache Point Observatory Galactic Evolution Experiment (APOGEE, Eisenstein et al. 2011) is obtaining high-resolution (R=30 000) high signal-to-noise, H-band spectra of 10^5 stars. APOGEE provides abundances for about 15 elements per star. Thanks to its IR observations, the APOGEE survey probes mainly Bulge and Thin Disc regions that are unaccesible to optical surveys, including the majority of the Gaia sampled volume. The spectrum analysis of the first APOGEE data have already produced several papers about the disc chemical signatures and structure (e.g. Schlesinger et al. 2014, Nidever et al. 2014, Hayden et al. 2014,...). An extension of this survey is also included as part of the After-SDSSIII project.

The Galactic Archaeology with AAO HERMES (GALAH) survey, started in April 2014, aims to obtain precision multi-element abundances for a million stars with V< 14, from high signal-to-noise, R=30000 spectra. The HERMES-GALAH project will explore an abundance chemical space of about 25 elements.

Finally, **the Gaia-ESO Survey (300 nights with the VLT)** is today the core of the European ground-based efforts complementing Gaia.

The Gaia-ESO Survey

Since 2009, the European stellar populations community was highly involved in the scientific and technical definition of a Galactic chemo-dynamical survey from the ground, to support the scientific exploitation of the Gaia mission. I had an active role from the beginning, by (i) preparing the French scientific support to the project (Recio-Blanco et al. 2009), (ii) participating in a dedicated ESO workshop (Melnick et al. 2009, see Fig. 5) and (iii) defining the necessary technical characteristics (resolution, wavelength domain, limiting magnitude, analysis pipelines...).

In 2011, ESO accepted the **Gaia-ESO large public survey** (GES, Gilmore et al. 2012, P.Is: G. Gilmore & S. Randich). GES begun on the 31th December 2011 and it is obtaining high quality spectroscopy of some 10^5 Milky Way stars, in the field and open clusters, down to magnitude V=19. GES employs the VLT FLAMES instrument to observe well-defined samples, based on current VISTA photometry for field stars.

The survey has already started to quantify the kinematic-multi-element abundance distribution functions of the Bulge, the Thick and the Thin discs and the Halo stellar components, as well as a significant sample of 100 open clusters, covering all accessible cluster ages and stellar masses. GIRAFFE spectra (R~20 000), with two settings (HR10 and HR21), are obtained for statistically significant samples of stars in all major stellar populations. These are supplemented by UVES spectra (R=40 000) of an unbiased sample of G-stars within 2 kpc of the Sun, providing the abundance distribution function for the local Thin and Thick discs. This alone will revolutionise our knowledge of Galactic stellar populations. In addition, when combined with precision astrometry from Gaia, delivering accurate distances and proper motions, GES will allow the derivation of precise 3D spatial distributions, 3D space motions, chemical patterns and ages that will quantify the formation history and evolution of young, mature and ancient populations far from the solar neighbourhood. Moreover, as illustrated in Fig. 4, the spatial volume covered by the GES spectroscopy is a perfect complement to the Gaia spectroscopic observations (c.f. above), that have a magnitude limit of V~16, while the Gaia photometry and astrometric data go down to V~20. This extends the magnitude volume and the number of stars (by 100 000 more objects) for which we will have the third velocity component of the stars (radial velocity), as well as precise chemical abundance measurements and atmospheric parameters.

Since the beginning of the project, I was proposed to be **co-responsible of one of the GES Working Groups in charge of the spectrum analysis of the most abundant targets of the survey** (FGK-type stars observed with VLT/Giraffe). This WG is composed of people from all across Europe, involved in the analysis with different methodologies. In addition, I am member of the WG in charge of the final parameters calibration and, in collaboration with other OCA members (P. de Laverny, V. Hill, M. Schultheis) I contribute to the WG in charge of the UVES FGK-type spectral analysis.

GES has now finished its third internal data release and I have already strongly contributed to five papers (of which one as first author and two as a second one, after the PhD students). The main results of those articles, concerning the Galactic disc and the bulge, are presented in Chapters 3 and 4. In addition, I am co-author of another 17 already published papers, based on GES data, that are not included in this report.

Chapter 2

SEARCHING FOR THE ARCHAEOLOGICAL REMAINS THROUGH STELLAR SPECTRA PARAMETRIZATION

The physical parametrisation of stars is a crucial step in our comprehension of stellar and Galactic astrophysics. By way of illustration, we could cite the impact of the Hertzsprung–Russell (HR) diagram on our understanding of stellar evolution, or the identification and characterization of the different components and stellar populations of the Milky Way and its satellites. The classification of stars, from rich collections of stellar properties and vast catalogues of objects, is now opening new horizons in, for instance, the disentangling of the detailed sequence of events which led to the MilkyWay galaxy. In this sense, the chemical parametrization of stars is mandatory for a fruitful classification attempt, reinforcing the traditional approach. For instance, the chemical abundance ratios of some species to anothers (e.g. the [α/Fe] ratio) provide an indication of the star formation history time-scale and details of the chemical enrichment for one specific population.

In recent years, the use of spectrographs with multi-object capabilities (FLAMES, 2dF, etc.) and the implementation of extensive surveys (Sloan, RAVE, etc.) have enormously increased the quantity of available data and, as a result, the efforts needed for their analysis (see Fig. 3, right panel). The European Space Agency Gaia mission has already started to collect millions of stellar spectra ($3 \cdot 10^9$ RVS spectra collected up to the 15th October 2014). In this context, automated techniques of spectral analysis and classification are mandatory, in order to perform a rapid and homogeneous processing of the data and to allow an efficient scientific return.

The intrinsic physical properties of stars can be indirectly derived from stellar spectra. Effective temperature (T*eff*), surface gravity (*log* g) and chemical composition are the main parameters governing the stellar atmosphere and non-linear combinations of them characterize the features on a stellar spectrum. The knowledge of these quantities, together with stellar structure and evolution models, can help to determine a star's history and future evolution. Traditionally and for historical reasons, the more empirical variables of luminosity and colour index have been used to indirectly describe spectroscopic parameters. The MK system (Morgan, Keenan & Kellman 1943) avoids the complexities of spectral line formation by the use of standard spectra. Spectral class and luminosity type are assigned from medium–low resolution spectra in, essentially, a two-parameter classification effort, representative of Teff and log g. Nevertheless, this approach suffers from a series of disadvantages, mainly arising from the lack of a metallicity quantification. On the other hand, a classification directly based on the physical parameters, although model dependent, takes more naturally into account the scientific quantities of interest and offers a continuous parametrization instead of a discrete spectral/luminosity-type assignment.

2.1 Stellar parametrization and data mining methodologies.

The parameter estimation problem consists in deriving the stellar atmospheric parameters (mainly effective temperature, surface gravity, global metallicity and individual chemical abundances) that define a model estimation (usually synthetic spectra, or equivalent widths) that is an optimal fit to an observed spectrum.

This estimation cannot be made analytically, because of the complexity of the stellar spectra, which involves the very complex physics included in stellar atmosphere model and spectral line formation theory. As a consequence, the stellar spectra parameterisation has to be performed, for instance, by using synthetic spectra grids which span the whole parameter space. For an example of this kind of grids, see de Laverny, Recio-Blanco et al. (2012).

The main problems encountered by the different automated estimation methods are caused by the possible non-linearity of the model spectra and the non-convexity of the distance function, which quantifies the difference between a model and the data. On one hand, a change in the atmospheric parameters can induce

Reference spectra		Main applications	Mathematical approach
Computation time ↑	**- On the fly computations:**		
	Spectral Synthesis	**GES, GALAH**	Optimization
	Equivalent widths	**GES**	Optimization
	- Pre-computed grid:		
	Without training	**GES, RAVE, SEGUE, LEGUE**	Optimization
	With training	**GES, RAVE, AMBRE, SEGUE, Gaia**	Projection & Classification

***Figure 5**: Different types of automated stellar spectra parameterisation methods currently used by Milky Way spectroscopic surveys and Galactic archaeology projects.*

non-linear variations of the spectral flux: two sets of parameters, distant in parameter space, can result in very similar spectra. On the other hand, the flux changes caused by the variation of a given parameter, as the. effective temperature, can be very similar to those induced by another parameter, usually the surface gravity or the metallicity. Therefore, secondary minima and multiple solutions to the stellar spectra fitting problem may exist. Parameter degeneracy is usually more severe when the available information about the parameters decreases: e.g. with a narrower spectral range, lower spectral resolution, lack of spectral signatures, and so on. In addition, secondary minima can also be artificially generated by noise disturbing the distance function.

As presented in Recio-Blanco et al. (2013) and Bijaoui, Recio-Blanco et al. (2012), several methods exist in the literature for the automatic parameter estimation from stellar spectra. There are three main mathematical parametrization approaches: optimization methods, projection methods and classification. All of them try to find the absolute minimum of the distance function, with different techniques.

Optimization methods : The exhaustive exploration of the grid of reference models in order to find the nearest neighbour is the simplest optimization method. It consists in calculating the distance between the observed spectrum and each of the spectra of the reference grid. This technique can be very time consuming, but it ensures the finding of the absolute minimum. Nevertheless, the precision of the result is limited by the parameter step of the reference grid. To tackle this problem, different methods of interpolation in the parameter space can be used. The nearest neighbour method can also be affected by the noise, as noise features can be confused with spectral signatures of a given physical parameter. For instance, the strength of a magnesium line can be modified by the noise in a way that mimics a higher or lower magnesium abundance than the real value. In those cases, the reference model to which the calculated distance is smaller, will not be the one with the nearest parameters (e.g. magnesium abundance) to the target one. Gradient descent methods, as the Gauss-Newton algorithm GAUGUIN, have been developed in order to reduce the computing time of the minimum distance method (see, for instance, Bijaoui et al., 2012). Their goal is to find the direction in the parameter space that has the highest negative gradient as a function of the distance. Once this direction is found, the methods proceed in an iterative way, by modifying the initial guess of the studied parameter and re-calculating the gradient again, until convergence of the parameter solution. This kind of algorithms does not guarantee the convergence to the absolute minimum, as they can be trapped in secondary minima when the application conditions are those of bad quality data. Other methods, as the Nelder & Mead (1965) algorithm have been developed to avoid the local minima traps, although the computation time can significantly increase.

Projection methods: Contrary to optimization methods, projection algorithms need a training phase during which a set of projection vectors is calculated. Those vectors contain the most important signatures of the flux that allow the derivation of a given physical parameter. Then, during the application phase, this parameter value (for instance, the abundance of alpha-elements with respect to iron) is determined by the projection of the target spectrum into the calculated vectors. The MATISSE method (Recio-Blanco et al.,

2006) and the penalized chi-square algorithm are examples of this kind of approach. When the distance function is convex and linear, projection methods allow to project the target spectra close to their nearest neighbours. This considerably reduces the application time. In addition, the projection vectors can be adjusted in order to take into account the noise effects, given less weight to high order variations of the stellar flux. Nevertheless, this kind of methods can also be trapped in secondary minima, usually not very far from the absolute one, as they have a local application that avoids a global view of the parameter space.

Classification methods: In the limit of the sampling precision, the parameter estimation is a recognition problem. The grid of synthetic spectra can be treated as a known set of patterns among which we aim to identify the observed spectra. In the learning phase, the recognition rules are established using the grid of theoretical spectra. Decision trees (as DEGAS developed by our group, Kordopatis, Recio-Blanco et al., 2011), neural networks and support vector machines are examples of classification algorithms used for stellar parametrization.

2.2 Summary of automated stellar spectra parametrization methods

Figure 5 shows the main different types of automated abundance analysis methods found in the literature, currently used by Milky Way spectroscopic surveys and Galactic archaeology projects. The algorithms can be divided depending on the way in which the reference models are computed and used. This has an important influence on the computation time and, ultimately, it depends on the implemented mathematical approach. In addition, Figure 5 shows what approaches are used by the main spectroscopic surveys and projects, including the European Space Agency Gaia mission.

In the next subsections, the main algorithms in the literature are reviewed, following the scheme of Figure 5. The list of methods does not intend to be complete, but it will guide the reader through the general picture of approaches developed up to date. The main procedures I contributed to develop (MATISSE, DEGAS and GAUGUIN) will be only mentioned here and further described in Sect. 2.3.

2.2.1 Methods using on-the-fly computations of the reference synthetic spectra

These are the simplest parametrization algorithms. They implement the automatization of the classical procedures through optimization approaches. The methods in the literature can be divided between those using spectral synthesis and those using the equivalent widths of spectral lines.

Algorithms using spectral synthesis :

Spectroscopy Made Easy (SME) was developped by Valenti & Piskunov (1996). The SME algorithm is a Chi-square optimization method. It is used for the determination of atmospheric parameters and individual element abundances. SME is part of the methods used in the Gaia-ESO Survey spectrum analysis of FGK-type stars. Other minimum of distances methods recently implemented are the one developed by Van der Swaelmen et al. (2013) and Mikolaitis et al. (2014). The last one is used for the derivation of individual abundances from the GIRAFFE data of FGK-type stars observed by GES. More recently, the iSpec method (Blanco-Cuaresma et al. 2014b) was implemented and applied to the Gaia benchmark stars library (Blanco-Cuaresma et al. 2014a).

Finally, the Australian GALAH survey project is implementing an AUTOMOOG based method for its abundance determination pipeline.

Algorithms using equivalent widths :

Automatized classical manual procedures are implemented in this kind of approaches. The automatic measurement of the spectral lines equivalent widths is coupled with on the fly fits of the observed equivalent widths with theoretical ones.

The algorithm of the Porto group of Sousa et al., uses the automated equivalent width measurements with the code ARES (Sousa et al. 2007) and it is part of the GES methods used for the analysis of UVES data. It is also currently used for other studies of the solar neighbourhood like Adibekyan et al. (2012), and the characterization of stars hosting exoplanets. More recently, Mucciarelli et al. (2013) presented the GALA method, that uses an automated equivalent width measurement with DAOSPEC.

2.2.2 Methods using a pre-computed grid of reference synthetic spectra

The use of a pre-computed grid of synthetic spectra reduces the computing time of the algorithms application. The methods using this kind of approach are divided into those without and with a phase of

algorithm training.

Without training :

This category of methods is based on optimization approaches. It includes the Nelder-Mead method implemented by Allende-Prieto et al. (2006). This non-linear downhill simplex method was already used for the SDSS-SEGUE SSPP pipeline for the derivation of both the iron abundance and the [α/Fe] (Lee et al. 2011) from low resolution stellar spectra. It is also part of the methods used by the Gaia-ESO Survey and it is the core of the APOGEE ASPCAP pipeline.

The penalized chi-square method of Zwitter et al. (2008) is also in this category of algorithms. It has been used for the RAVE survey first and second data releases for the derivation of the iron abundance. The RAVE survey also developed the Boeche et al. (2011) method for the individual abundance analysis of the high signal-to-noise data (third data release). It is a minimum of distances method using of a grid of pre-computed equivalent widths. The UlySS method of Koleva et al. (2009) implements a full spectrum fitting and a parametric minimisation using chi-square maps. It was part of the SEGUE SSPP pipeline and it is actually integrated in the LASP LAMOST pipeline for the analysis of the LEGUE survey data.

The GAUGUIN method (Bijaoui, Recio-Blanco et al. 2012) uses the Gauss-Newton algorithm for the determination of the stellar atmospheric parameters and individual chemical abundances (c.f. Sect. 2.3).

Finally, the Abbo and MyGIsFOS approach (Bonifacio & Caau, 2003) and the SPADES method (Posbic et al. 2012) are also part of this type of algorithms.

With training :

The methods with a faster application are those relying on a training phase. They are based on projection and classication approaches. The neural network algorithms of Re Fiorentin et al. (2007) is an example of this kind of methods. It is part of the SEGUE SSPP pipeline for the derivation of the iron abundance, simultaneously with the effective temperature and the surface gravity. It implements a global and non-linear regression mapping.

The MATISSE (projection method, Recio-Blanco et al. 2006) and DEGAS (decision tree, Kordopatis et al. 2011a) algorithms are also part of this category. They will be further described in the following section.

2.3 The MATISSE, DEGAS and GAUGUIN methods

In the last ten years, I contributed to develop, in collaboration with A. Bijaoui and P. de Laverny, a series of innovative methods of stellar spectra parametrization: MATISSE (Recio-Blanco et al. 2006), DEGAS (Kordopatis, Recio-Blanco et al. 2011a) and GAUGUIN (Bijaoui, Recio-Blanco et al. 2012). They belong to the three main families of mathematical parametrization approaches described in Sect. 2.1 and they are now currently used to analyse the data of recent and ongoing spectroscopic surveys of the Milky Way, including the Gaia mission. Figure 6 shows the JAVA user-friendly interface of both MATISSE, DEGAS and GAUGUIN.

2.3.1 The MATrix Inversion for Spectral Synthesis (MATISSE) method

The MATISSE algorithm (MATrix Inversion for Spectral SynthEsis) is a local multi-linear regression method. MATISSE estimates a stellar atmospheric parameter ($T_{\rm eff}$, log g, [M/H]) and the [α/Fe] ratio by projecting the observed spectrum $O(\lambda)$ on a particular vector $B_\theta(\lambda)$ associated to a theoretical θ_i parameter, as follows:

$$\hat{\theta}_i = \sum_{\lambda} B_{\theta_i}(\lambda) O(\lambda). \qquad \text{Eq. (1)}$$

These vectors, called $B_\theta(\lambda)$ functions hereafter, are computed during a learning phase from a library of synthetic spectra that cover the same wavelength range and have the same spectral resolution and wavelength sampling as the observed spectra. They relate in a quantitative way the pixel-pixel flux variations in a spectrum to a given variation of the θ_i parameter. If the $B_\theta(\lambda)$ are orthogonal, the effects from each parameter affect the spectrum in a different way (as in most applications), and therefore the atmospheric parameters are derived accurately. When this is not the case, possible degeneracies in parameter space can occur, which cause a correlation of the parameter errors. The $B_\theta(\lambda)$ functions are computed from an optimum multi-linear

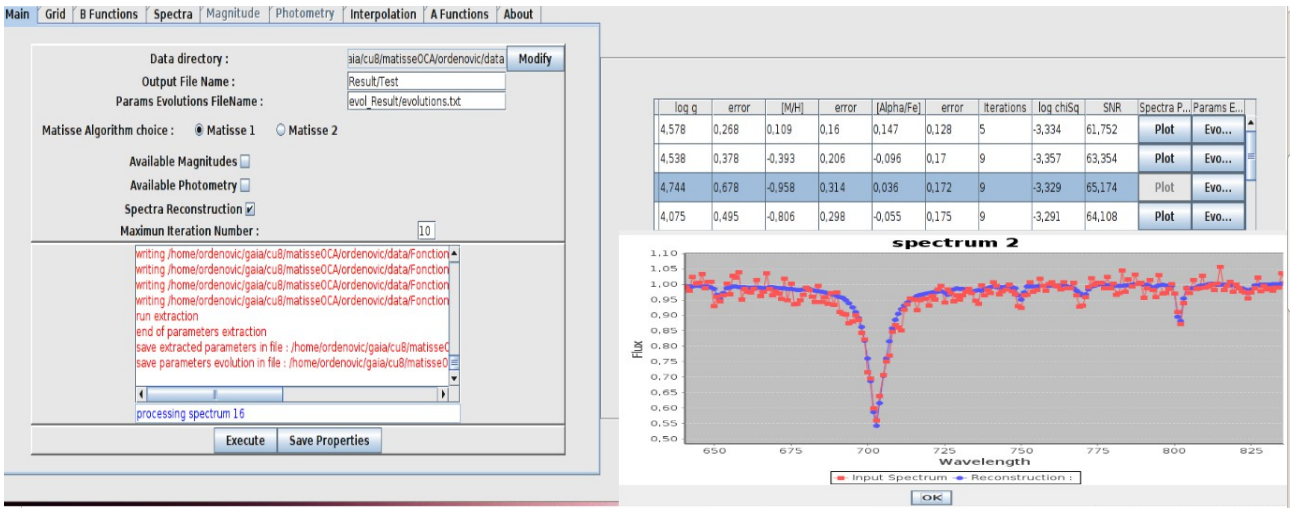


Figure 6: *User java interface of the MATISSE, DEGAS and GAUGUIN parameterisation methods.*

combination of theoretical, synthetic spectra $S(\lambda)$, as follows:

$$B_{\theta_i}(\lambda) = \sum_j \alpha_{ij} S_j(\lambda) \qquad \text{Eq. (2)}$$

where the α_{ij} factor is the weight associated with each synthetic spectrum $S_j(\lambda)$ to retrieve the parameter θ_i. To compute these weights during the learning phase, Eq. 1 is applied to a subset of synthetic spectra. Accordingly, we obtain by combining Eq.1 and 2:

$$\Theta_i = C\alpha_i \qquad \text{Eq. (3)}$$

where $C = [c_{jj'}]$ is the correlation matrix between S_j and $S_{j'}$. In addition, Θ_i and α_i are, respectively, the vector of the parameters θ_i and that of the weights α_{ij} for all considered spectra. The weights α_{ij} are then computed by inverting the correlation matrix C.

We have as many $B_\theta(\lambda)$ functions as there are spectra in the library of synthetic spectra. Each of them is computed using a small parameter range, for which we assumed the parameter variations to have a linear effect on the spectral flux variations. In practice, to converge to a parameter sub-space, one can use either generic $B_\theta(\lambda)$ functions, or impose *a priori* the $B_\theta(\lambda)$, if a first estimation of the parameters is available. When applying Eq. 1 to an observed spectrum, the method iterates for as long as the derived parameters are not included in the considered parameter sub-space for which the $B_\theta(\lambda)$ functions were computed. Usually, the final convergence is attained after a few iterations.

The MATISSE method deals with normalised spectra and consequently all the necessary information for deriving the atmospheric parameters is provided by the spectral lines, i.e. their relative strengths. This strength changes according to the spectral type, the luminosity class and the metal content of the stars. In noiseless spectra and when the synthetic spectra perfectly match real stellar spectra, all astrophysical information (i.e. spectral lines) can be taken into account during the training phase of MATISSE. Nevertheless, for noisier spectra or if there is a mismatch between the observed and the synthetic stellar spectra, it is better to consider only the most relevant features, and give less weight to second-order variations.

The possibility of identifying a specific subset of the spectral signatures that are to be used for an atmospheric parameter derivation, which is a particular feature of MATISSE, allows us to adopt an optimised strategy according to the SNR and the type of the star. Therefore, this permits to optimise the analysis according to the quality of each spectrum. This optimisation is achieved when computing the $B_\theta(\lambda)$ functions, and more precisely while inverting the correlation matrix C of Eq. (3). A direct inversion would take into account all the n-order variations caused by the parameters. If one only considers the first order variations of the spectral flux though, one has to approximate the inverse of C. The degree of approximation can be

controlled by using an iterative algorithm, such as that of Landweber (Landweber 1951). In that case, one can impose a correlation coefficient between the input and the output parameters to be equal to the desired degree of approximation. The higher the factor of correlation, the lower the degree of approximation. A correlation coefficient of one would be similar to a direct inversion.

In practice, the correlation matrix can sometimes be ill-conditioned, and can therefore imply many near-zero eigenvalues. The Landweber algorithm adapts the inversion to the matrix conditioning, in the sense that the first eigenvectors are inversed during the first iterations, and the inversion of the smallest ones need more iterations to be accomplished. The iteration number is linked with the correlation coefficient cited above.

2.3.2 The DEcision tree alGorithm for Astrophysics (DEGAS) algorithm

In the limit of the sampling precision, the parameter estimation is a recognition problem. The grid of synthetic spectra can be treated as a known set of patterns among which we aim to identify the observed spectra. In the learning phase, the recognition rules are established using the grid of theoretical spectra.

Decision trees are commonly used for data mining (Quinlan 1993). At each tree node, a decision is taken to split the data subset into two or more subsets. The leaf level corresponds to the identified classes. A $k-d$ tree is a basic space-partitioning structure in a k-dimensional space (in general, $k = 4$, $T_{\rm eff}$, log g, [M/H] and [α/Fe]). The decisions result from the projection of the observations on a node vector. Classical, or axis-parallel decision trees, check only one variable at each node. In the particular case of oblique decision trees, the node vectors (called D_n hereafter) are obtained from a linear combination of the structural features (i.e. the atmospheric parameters), resulting in a simpler and more accurate tree.

The DEGAS algorithm is an oblique k-d decision tree. The recognition rules at each node are built during the learning phase as follows:

1. The mean vector $\boldsymbol{M}$ of the flux values per pixel is computed.
2. For each spectrum $\boldsymbol{S}_j$ associated to the node, we calculate the scalar product $c_j = \boldsymbol{S}_j \cdot \boldsymbol{M}$.
3. The data are bisected into two subsets, T_1 and T_2, that correspond to those spectra with c_j higher and lower than the median value of c_j, respectively.
4. The mean vectors $\boldsymbol{M}_1$ and $\boldsymbol{M}_2$ of each subset are then computed, and the difference vector $\boldsymbol{D} = \boldsymbol{M}_1 - \boldsymbol{M}_2$ is determined.
5. According to the Huygens theorem, the best separation between T_1 and T_2 corresponds to the case for which the dispersions around M_1 and M_2 are minimal, which is obtained when $\boldsymbol{M}$ and $\boldsymbol{D}$ are parallel. Indeed, we examined the variation V of the dispersions that resulted from spectra exchange between the two sets T_1 and T_2. Because the V expression introduced the vector $\boldsymbol{D}$, we chose to get $\boldsymbol{M}$ and $\boldsymbol{D}$ parallel in order to maximise V. This dramatically improved the separation compared to the use of $\boldsymbol{M}$. Hence, in practice, if the angle between $\boldsymbol{M}$ and $\boldsymbol{D}$ is too wide (correlation coefficient smaller than 0.999), we iterate until convergence, re-separating the data by the hyperplane defined by $\boldsymbol{D}$ (going back to step 2, replacing $\boldsymbol{M}$ by $\boldsymbol{D}$).

Once this procedure has converged for a particular node n, we determine the final projection node vector $\boldsymbol{D}_n$, which will display the features that allow one to separate the data at that node, and the final median value of $c_j = \boldsymbol{S}_j \cdot \boldsymbol{D}_n$.

In this way, the recognition tree with $\log_2(N)$ levels is built, where N is the number of spectra of the training grid. At the lowest level nodes of the tree, the leaves, only one training spectrum remains associated with each node. During the application phase, the target data $\boldsymbol{O}_i$ passes through all levels of the recognition tree, and a template is associated to it.

Nevertheless, noise can induce possible misclassifications. At each node one has to take into account that the projection coefficient $c_i = \boldsymbol{O}_i \cdot \boldsymbol{D}_n$ is distributed according to a Gaussian law, defined for the entire real axis. So, theoretically both branches can be chosen, and the algorithm should fully explore the decision tree. This would lead to an inefficient method. To allow the assignation of a probability to each of the directions, we

chose to replace the Gaussian distribution by an Epanechnikov kernel, which corresponds to a truncated parabola.

After scanning all nodes, a subset of synthetic templates is selected, and the distances of the templates from the observed spectrum are computed. Then, either a weighted mean is evaluated on the parameters taking into account these distances, or the parameters of the minimum distance synthetic spectrum are chosen (this is enabled as an option of the algorithm).

2.3.3 The GAUGUIN algorithm

The GAUGUIN method (Bijaoui, Recio-Blanco et al. 2012) is a Gauss-Newton algorithm based on a linearization around a given parameter set $\Theta(0)$ associated with a theoretical spectrum S_0. The corrections $\delta\Theta$ are obtained with the relation:

$$\delta\boldsymbol{\Theta} = \left(\mathbf{J}^T\mathbf{J}\right)^{-1}\mathbf{J}^T\left(\mathbf{O} - \mathbf{S}_0\right) \quad \text{Eq. (4)}$$

J being the Jacobian matrix $[\partial S(l, \Theta(0))/\partial\theta i]$. In the case of large corrections, some iterations need to be carried out through linearization around the new values. The derivatives are computed using a cubic-Bézier interpolation. Generally, GAUGUIN converges but there is no guarantee that the resulting values correspond to the global minimum distance. The reference spectrum S_0, that is the starting point of the GAUGUIN method in terms of stellar parameters, can be provided by an initial photometric parameters estimation or by another algorithm exploring the parameter space at large, like DEGAS or MATISSE. The parameter space explored by GAUGUIN can therefore be limited to a local application that refines the first parameters solution.

Moreover, GAUGUIN can also be used for the derivation of individual abundances in a second step of the spectrum analysis (Guiglion et al. 2013).

2.3.4 Applications of MATISSE, DEGAS and GAUGUIN

The MATISSE and DEGAS methods have been used in Kordopatis, Recio-Blanco et al. (2011a) for a study of the thick Disc outside the solar neighbourhood (700 stars analysed) and for the last data release (DR4) of the RAVE Galactic Survey (Kordopatis et al. 2013b, 228 060 spectra). These two applications share the same wavelength domain and resolution of the RVS one.

Moreover, MATISSE is the core method of the AMBRE project (P.I. P. de Laverny). AMBRE (see de Laverny, Recio-Blanco et al. 2012), under agreement between the European Southern Observatory (ESO) and the Observatoire de la Côte d'Azur, aims at determining the stellar parameters (Teff , log g, [M/H] and [α/Fe]) of the high resolution stellar spectra contained in the ESO archive. This concerns the FEROS, HARPS, UVES and FLAMES spectrographs. The results of the AMBRE project are presented in Worley et al. 2012 (FEROS data analysis), De Pascale et al. (2014; HARPS data analysis) and Worley et al. (2014, UVES data analysis).

MATISSE has also been used for the characterization of several disc fields observed by the CoRoT mission (Gazzano et al. 2010 and Gazzano et al. 2013). In addition, the MATISSE and GAUGUIN algorithms are part of the methods used for the stellar parametrization of FGK type targets of the Gaia-ESO Large Public Survey. In particular, MATISSE is one of the three methods used to analyse the data of the FGK-type stars observed with the GIRAFFE spectrograph and it is also one of the algorithms in charge of the FGK-type UVES spectra (Smiljanic et al. 2014). In addition, GAUGUIN is one of the three methods used to derive the individual abundances of those stars.

Finally, the spectrum analysis of the Gaia mission is also based on this type of algorithms with a training phase. The computational time is a crucial constraint for the Gaia pipeline, as several tenths of millions of RVS spectra will be analysed in cycles of 6 months. The MATISSE, DEGAS and GAUGUIN algorithms are already included in the Gaia Apsis parametrization pipeline (Bailer-Jones et al. 2013). They are the core of the Generalized Stellar Parametrizer-spectroscopy (GSPspec) module (Recio-Blanco et al. 2014, and Chapter 5).

2.4 General conclusions on automated stellar spectra parametrization

Automated stellar parameters are the bedrock of Galactic spectroscopic surveys science. If they are wrong, with hidden anomalous behaviours, the surveys scientific conclusions can be wrong. In the literature, several

types of automated methods exists for the derivation of stellar atmospheric parameters and individual abundances. Each of them has its optimal application conditions that depend on the computation time constraints, the spectral resolution and wavelength domain, the data signal-to-noise ratio, the parameter degeneracy problems, etc...

Present Galactic surveys, including the Gaia mission, have motivated the development of a blossom of mathematical approaches for stellar parameterisation. In this new era of Milky Way exploration, data analysis has already a crucial position that we can not ignore. Our group in Nice and myself have contributed, since the first pioneering attempts, to the implementation of innovative methods of automated spectrum analysis like MATISSE, DEGAS and GAUGUIN. Our developed algorithms are very fast, with an easy physical interpretation and providing high quality results. They are our tools to dig in the Milky Way archaeological excavations. They are already providing us interesting Galactic history remains, and some of them are presented in the following two chapters.

Chapter 3

ARCHAEOLOGY OF THE GALACTIC DISC

What is the best place for hunting chemo-dynamical fossil remnants of the early galaxy evolution? The metal-poor Galactic halo is a natural candidate, as most of its stars are older than 12 Gyrs and it is a repository of merger debris. However, most of the on-going high-resolution spectroscopic surveys are not optimized for Halo exploration, as they face the obstacle of the low stellar density (e.g. Recio-Blanco, 2012). On the other hand, most spirals, including our Galaxy, have a second thicker disc component surrounding the thin disc (van der Kruit & Freeman 2011). It appears that thick discs are very common and mostly very old. The Milky Way thick disc (Gilmore & Reid, 1983) is therefore one of the most significant components for studying signatures of galaxy formation, although its origin and its detailed nature are still uncertain. It is believed to be formed during or shortly after the last major epoch of dissipation, early in the life of our Galaxy. Moreover, at least in its properties, the thick Disc seems to have complex relations with all the other Galactic components (the halo, the thin disc, the bulge), being a sort of key element of the Milky Way history puzzle. Therefore, an important part of my work in the last years has been dedicated to the study of the Galactic disc stellar populations with: i) dedicated P.I. VLT programmes and ii) with Gaia-ESO Survey data. In the future, the Gaia data and their combination with ground-based surveys as GES will be crucial to pursuit the disc formation studies (c.f. Chapters 5 and 6).

3.1 State of the art about the thick/thin disc dichotomy.

Since the first works highlighting the existence of the Milky Way's thin/thick disc dichotomy (Yoshii, 1982; Gilmore & Reid, 1983), the study of the structural and chemo-dynamical transition between the two disc populations has opened new pathways to constrain Galactic evolution models. External mechanisms, supported by the hierarchical formation of galaxies in the ΛCDM paradigm, have been invoked to explain the chemodynamical characteristics of thick disc stars. Among them, the accretion of dwarf galaxies (e.g. Statler, 1988; Abadi et al., 2003) and minor mergers of satellites (e.g. Quinn et al., 1993; Villalobos & Helmi, 2008) heating dynamically the disc, have been proposed. Similarly, Jones & Wyse (1983) and Brook et al. (2004, 2007) have proposed the accretion of a gas-rich merger from the collapse of which the thick disc would have formed. On the other hand, purely internal formation mechanisms have also been proposed, like the early turbulent phase of the primordial disc (e.g. Bournaud et al., 2009) and the stars radial migration due to resonances with the spiral structure or the bar of the Milky Way (e.g. Schönrich & Binney, 2009c; Minchev & Famaey, 2010; Loebman et al., 2011).

The relative importance of the different proposed physical processes of evolution can now be tested with increasing robustness, thanks to the Galactic spectroscopic surveys targeting the disc stars. Spectroscopic studies of the disc populations were initially based on kinematically selected samples of solar neighbourhood stars (e.g. Prochaska et al., 2000; Fuhrmann, 2004; Bensby et al., 2005; Reddy et al., 2006), with some exceptions like Edvardsson et al. (1993) or Fuhrmann (1998). In the classical picture that emerged from those studies, the thick disc population is characterized, compared to the thin disc one, as kinematically hotter (Casetti-Dinescu et al., 2011), and therefore, composed by stars moving in Galactic orbits with a higher scale height (~900 pc vs. ~300 pc, e.g. Juric et al., 2008). In addition, the thick disc metallicity distribution peaks at lower values (~-0.5 dex compared to ~-0.2 dex for the thin disc, e.g Wyse & Gilmore, 1995; Lee et al., 2011b, Recio-Blanco et al. 2014a). With respect to the thin disc, the thick disc stars are older and have an enhanced ratio of α-element abundances over iron ([α/Fe], e.g. Bensby et al., 2005, 2007; Fuhrmann, 2008). Nevertheless, it progressively appeared that the distributions in the above mentioned physical parameters displayed significant overlaps between the thin and the thick disc populations (e.g. Bensby & Feltzing, 2010). This blurred our comprehension of the interplay between the discs and questionned the classical kinematically-based definitions (Bovy et al., 2012c).

In the recent years, the number of stars analysed with high enough spectroscopic resolution to provide detailed chemical diagnostics has increased from a few hundreds to several tens of thousands. The advent of Milky Way spectroscopic surveys and of automatised chemical analysis techniques have improved both the statistical robustness and the homogeneity of the data. From the theoretical side, new approaches based, at least partially, on the chemical identification of disc sub-populations, as the chemical-tagging (Freeman & Bland-Hawthorn, 2002) or the mono-abundance populations (Rix & Bovy, 2013) methods, are opening promising pathways for constraining the Milky Way's evolutionary processes. This is also challenging our previous conception of the Milky Way disc and the way in which stellar populations can be defined.

In this context, the low resolution SEGUE survey addressed the question of the thin to thick disc transition with a robust statistical approach, inside and outside the solar neighbourhood. Lee et al. (2011b) analysed ~ 17 300 G-type dwarfs with errors of about 0.23 dex in [Fe/H] (Smolinski et al., 2011) and 0.1 dex for [α/Fe] (Lee et al., 2011a). This was complemented by Schlesinger et al. (2012) who analysed 24 270 G and 16 847 K dwarfs at distances up to 2.3 kpc from the Galactic plane. The Lee et al. (2011b) [α/Fe] versus [Fe/H] distribution of number densities allowed to chemically separate the thin and the thick disc populations, although no clear gap is observed between the two. The SEGUE data interpretations differ from authors proposing no thin-thick disc distinction (Bovy et al., 2012b) to those allowing the existence of a distinct thick-disc component formed through an external mechanism (Liu & van de Ven, 2012). Nevertheless, selection effects have been invoked to explain some of the distinctions between the Lee et al. (2011a) and the Bovy et al. (2012b) chemical distributions. On the other hand, the data interpretation in the sense of no thin-thick disc distinction agrees with the results of the Schönrich & Binney (2009a) theoretical study.

More recently, Boeche et al. (2013) analysed the chemo-kinematical characteristics of 9 131 giants included in the last RAVE survey data release, with available [M/H] and [α/Fe]. The Boeche et al. (2013) analysis, based on the eccentricity-Zmax plane combined with additional orbital parameters, allowed them to identify three stellar populations that could be associated with the Galactic thin disc, a dissipative component composed mostly of thick-disc stars, and the halo. Nevertheless, their thin and thick disc populations, defined with the above mentioned dynamical criteria, do not clearly separate in their [α/Fe] v.s. [M/H] plane.

On the other hand, recent studies of solar neighbourhood samples, analysed with high resolution spectroscopic data, have revealed the existence of a gap in the [α/Fe] versus [Fe/H] plane (e.g Fuhrmann, 2004; Reddy et al., 2006; Bensby et al., 2007). Recently, Adibekyan et al. (2013) used the stellar sample of 1111 long-lived FGK dwarf stars from Adibekyan et al. (2012) to separate and characterise the different Galactic stellar subsystems, taking into account the existence of the above mentioned gap. Their [α/Fe] measurements are based on Mg, Si and Ti averaged abundances and the typical relative uncertainties in the metallicity and [α/Fe] are of about 0.03 dex. Haywood et al. (2013) derived ages of the Adibekyan et al. (2012) sample, concluding that two regimes appear in the age-[α/Fe] plane, that they identify as the epochs of the thick and thin disc formation. In the Haywood et al. (2013) scenario, the thick disc "formed from a well mixed interstellar medium, probably first in starburst, then in a more quiescent mode, over a time scale of 4-5 Gyr". They also suggest that "the youngest thick disk set the initial conditions from which the inner thin disk started to form 8 Gyr ago, at [Fe/H] in the range of (-0.1,+0.1) dex and [α/Fe]=0.1 dex". Finally, they interpret the low-metallicity tail of the thin disc as having an outer disc origin, somewhat disconnected from the inner disc evolution. In addition, similar separations in the [α/Fe] versus [Fe/H] plane, for the Solar vicinity, are distinguishable in the Ramírez et al. (2013) oxygen-abundance versus [Fe/H] measurements. These authors also report similar age-[α/Fe] regimes as in Haywood et al. (2013).

The following sections describe the main results of my work about the disc characterisation and their implications for the different proposed formation scenarios. After the presentation of the first work based on a P.I. VLT/FLAMES project with low resolution data (sect. 3.2), the results concerning different types of observational constraints are described: chemical characterisation (sect. 3.3), spatial distributions (sect. 3.4), chemo-kinematical and chemo-dynamical correlations (sect. 3.5).

3.2 Disc characterisation through low resolution spectroscopy

Most spectroscopic surveys of the thick disc up to the SEGUE results in 2011, were restricted to the Solar neighbourhood (within about a 500 pc radius), except for those with relatively few stars in their samples. On the other hand, photometric surveys such as the SDSS (York et al. 2000) explored a much larger volume, but suffered from greater uncertainties in the derived parameters. This fact motivated, from 2005 to 2007, two

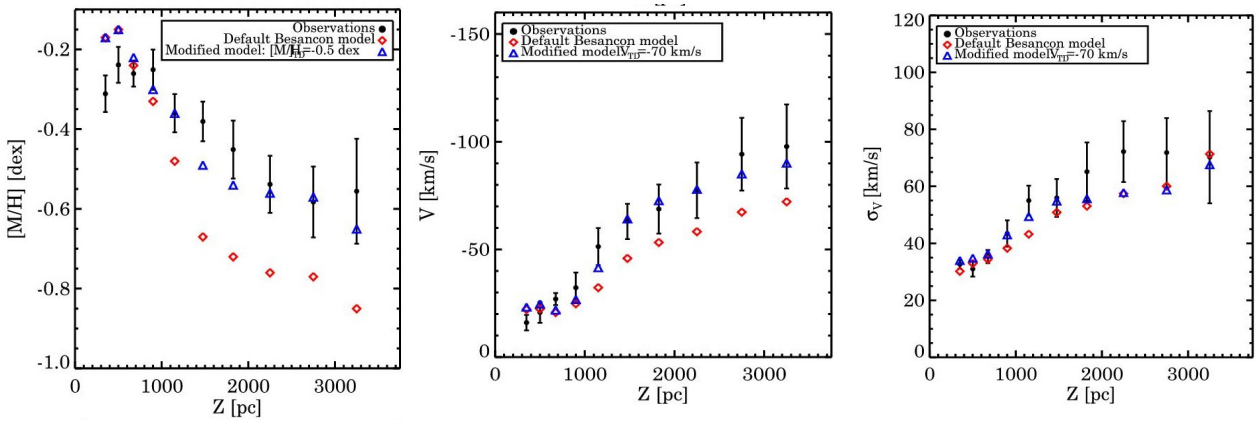


***Figure** 7: Median metallicities and V-velocities at different height bins above the Galactic plane from Kordopatis, Recio-Blanco et al. (2011b). Red diamonds represent the predictions of the raw Besançon model, whereas the blue triangles represent a modified model with metal-richer thick disc and halo, and a thick disc that lags behind the LSR by km/s.*

VLT/FLAMES programmes (075.B-0610-A & 077.B-0.382, P.I. A. Recio-Blanco) that were at the base of the articles Kordopatis, Recio-Blanco et al. (2011a) and (2011b). They were also the core of the PhD thesis of G. Kordopatis, who was from 2008 to 2011 member of our group at OCA. These data allowed us to spectroscopically explore the disc far from the Solar neighbourhood with a high enough statistics, towards (l ∼ 277◦ , b ∼ 47◦). Around 700 stars were observed with VLT/FLAMES feeding the GIRAFFE spectrograph with the LR8 grating (8206-9400 Å, R ∼6500). The spectra were complemented with the proper motions and U, B, V colours from Ojha (1994).

We adopted the pipeline presented in Kordopatis, Recio-Blanco et al. (2011a) that used simultaneously two different algorithms, MATISSE (Recio-Blanco et al. 2006) and DEGAS (Bijaoui et al. 2010), in order to iteratively renormalise the spectra and derive the atmospheric parameters of the observed targets. The method returns, for an intermediate metallicity dwarf star at S/N ∼ 50 (which was the mean S/N of our spectra), accuracies of ∼ 150 K, 0.3 dex and 0.2 dex for Teff, log g and [M/H], respectively. The derived effective temperatures, surface gravities and overall metallicities were then combined with stellar evolution isochrones, radial velocities and proper motions to derive the distances, kinematics and orbital parameters of the sample stars. Given the Ojha et al. proper motions and our radial velocities we were able to derive the distances and the positions for 479 stars of our sample and the 3D motions and the orbital eccentricities for 452 of them. The targets belonging to each Galactic component (thin disc, thick disc, halo) were selected either on their kinematics or according to their position above the Galactic plane, and the vertical gradients were also estimated.

We found a thick disc with a mean rotational velocity Vφ ∼ −167 km s^{-1} , a value slightly higher than the commonly adopted lag of less than 50 km s^{-1}. Nevertheless, it has to be emphasised that our sample of stars probed distances above 1 kpc from the plane, so this difference may imply a correlation between lag velocity and vertical velocity rather than a simple inconsistency with local data. This correlation was latter verified thanks to GES data (Recio-Blanco et al. 2014).

The mean measured metallicity of the thick disc in our sample is −0.45 dex. Its metal-poor tails extends to −1.8 dex, whereas its metal-rich tail goes up to solar and super-solar values. Depending on how the thick disc stars are selected (Z positions or velocities), these values may vary a little, but generally agree well between them.

The derived vertical velocity gradient, $\partial V\varphi / \partial Z$ = 19±8 km s^{-1} kpc^{-1}, and metallicity gradient ∂[M/H]/∂Z = −0.14±0.05 dex kpc^{-1} (see Fig. 7) for the regions where the thick disc is the dominant population (1 < Z < 4 kpc) seem to agree well with a smooth transition between the Galactic components, and are compatible with the values previously found by Chiba & Beers (2001); Allende Prieto et al. (2006); Girard et al. (2006); Lee et al. (2011) and Ruchti et al. (2011), whose values range from 16 ± 4 to 30 ± 3 km s^{-1} kpc^{-1} and from −0.07 ± 0.01 to −0.09 ± 0.05 dex kpc^{-1}. A correlation between the metallicity and the rotational velocity of $\partial V\varphi / \partial$[M/H] = 43 ± 11 km s^{-1} dex^{-1} is also found, in agreement with Spagna et al. (2010) and Lee et al. (2011).

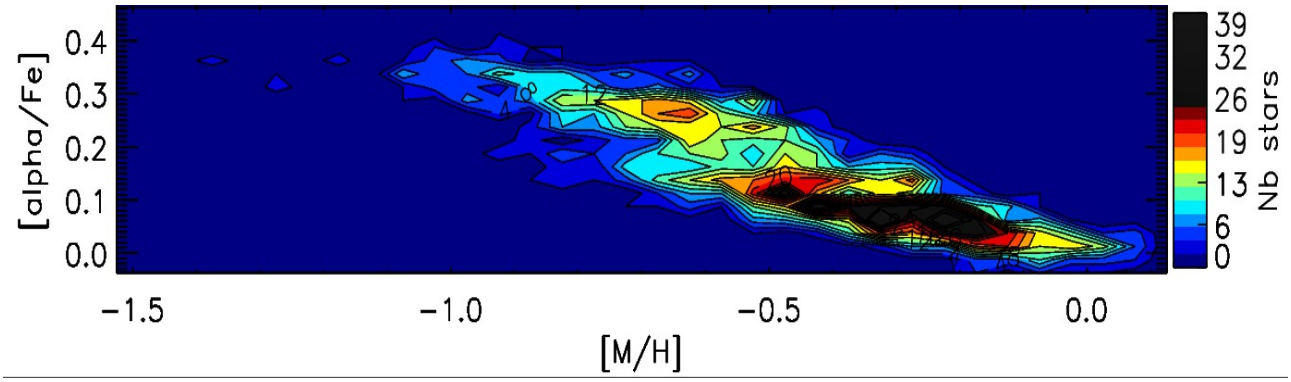


***Figure 8**: The thin and thick disc chemical separation from the GES iDR1 (Recio-Blanco et al. 2014a). Image selected for the A&A cover page of July 2014.*

In addition, we estimated the radial scale length and scale height of the thick disc to be $h_R \sim 3.4 \pm 0.7$ kpc and $h_Z \sim 694 \pm 45$ pc, respectively. This result agrees well with the SDSS estimations of Juric et al. (2008). No clear metallicity dependences were detected for h_R or for h_Z, pointing towards a thick disc that is mainly composed by only one population.

Finally, we found a broad peak of the eccentricity distribution for the thick disc around ~ 0.3 which, according to the works of Sales et al. (2009) and Di Matteo et al. (2011) seem to rule out a pure accretion scenario. These results agree with those previously obtained by Wilson et al. (2011) and Dierickx et al. (2010), who measured the eccentricity distributions for a sample of RAVE and SEGUE stars.

3.3 Chemical characterisation of the thin and thick discs.

The Galactic gas metal content increases with time, as it is progressively enriched by successive generations of stars. Indeed, the nuclear processes giving rise to the wealth of elements filling the periodic table are varied (fusions, n-captures, p-captures,…), so are their production sites, that are mostly related to the stellar mass. Therefore, the ratios of some element abundances with respect to others can be used to characterise or even define a given stellar population. The most famous example is that of the so-called α-elements (O, Mg, Si, S, Ca, Ti) versus iron. The former are predominantly synthesized in high-mass, very short-lived stars, and are ejected by type II supernova explosions (SNII). Iron is produced by both SNII and type I supernovae (SNIa), whose binary progenitors are believed to have a longer pre-explosion lifetime of typically one billion years (1 Gyr). Comparing the relative abundances of the α-elements and iron provides a measure of the SNIa/SNII ratio, and in turn a clock, with a resolution somewhat better than 1 Gyr. Each evolving system (galaxy, building block…) therefore bears the marks of its own star formation history and conditions encoded in the detailed chemical composition of its stars. Using this chemical record of individual stars to identify sub-populations and trace them back to possible remains of accretion events is often referred to as chemical tagging (Freeman & Bland-Hawthorn, 2002). Moreover, as discussed in Bovy et al. (2012b), defining stellar populations by abundances patterns is a better approach than the traditional kinematical criteria, as chemical abundances can correlate with disc structure, but are formally independent of it. The identification of possible chemical evolutionary paths and/or gaps in the abundance ratios distributions is crucial to disentangle the otherwise overlapping populations in the kinematical space. In particular, the high resolving power of GES spectra (compared to low resolution surveys like SDSS/SEGUE and RAVE) is a crucial asset of the project, that allows to take advantage of the chemical element information.

3.3.1 Thin-thick discs chemical separation

Using detailed chemical abundances in stellar samples in the solar vicinity to probe the Galactic disc(s) evolution is not a new topic, nowadays reaching exquisite accuracies on statistically significant samples (see for example the recent works by Fuhrmann, 2011; Adibekyan et al., 2012; Bensby et al., 2014, using samples of several hundreds to almost a thousand stars each). From these works, a particularly striking result is the clear distinction of thick and thin disc stars, that have been either identified kinematically (eg. Bensby et al., 2005, who identifies thin and thick disc stars in a Toomre diagram) and then shown to be chemically distinct, or identified chemically and then shown to present different kinematical properties (eg. Adibekyan et al., 2012). Up to 2013, most high-resolution spectroscopic studies of the Galactic disc(s) were confined to

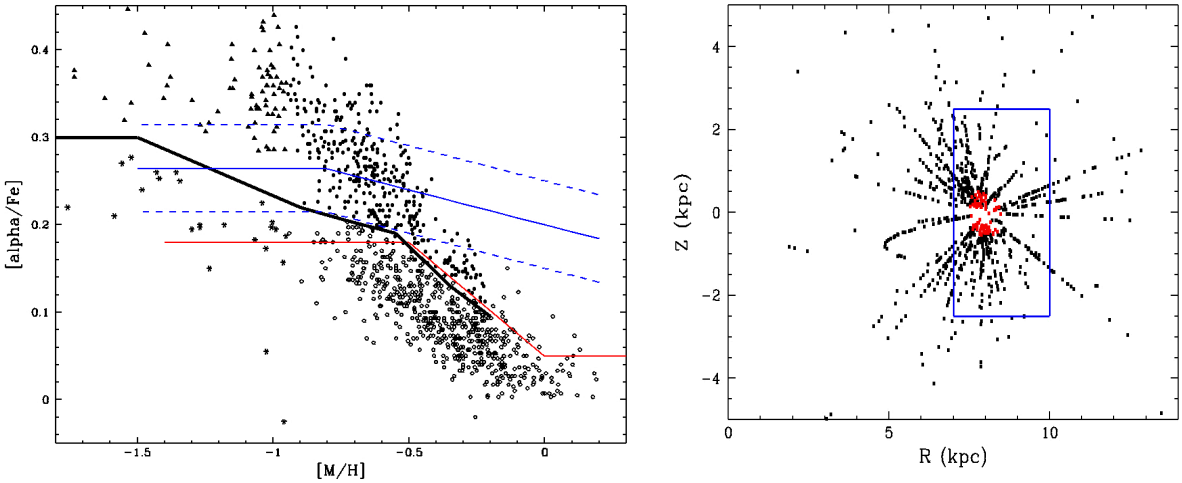


***Figure 9**. Left panel: α-elements over iron abundance as a function of metallicity from Recio-Blanco et al. (2014a). Filled dots are thick disc sequence stars, open circles are thin disc sequence objects. The black line shows the proposed division between the thin and thick disc sequences. The red line shows the separation proposed by the high resolution analysis of Adibekyan et al. (2012) for the Solar neighbourhood. The blue solid line is the separation proposed by Lee et al. (2011b) from low resolution SEGUE data. Right panel: Target's location in vertical distance to the Galactic plane (Z) and radial cylindrical Galactic coordinate (R). Red points indicate the stars with a distance value smaller than 600 pc from the Sun (10% of the sample). The blue rectangle shows the maximum R and Z values of the Lee et al. (2011b) SEGUE analysis.*

objects in the Solar vicinity. The Gaia-ESO survey is thus a new step in large spectroscopic data, obtaining high-resolution spectra of field and open cluster stars across the Galaxy.

In Recio-Blanco et al. (2014a), focussing on a subsample of 1016 GES DR1 spectra with high quality parameters, we have identified a thin to thick disc separation in the [α/Fe] v.s. [M/H] plane, thanks to the presence of a low-density region in the number density distribution (see Fig. 8). The covered spatial volume was within $|Z| < 4.5$ kpc and R in the range 2-13 kpc. Two sequences separated by a low density region can be identified: the thick disc one in the high-α regime and the thin disc one in the low-α regime (see below for the selection criteria). Both sequences overlap in metallicity from about -0.8 dex to -0.3 dex. We have studied the position of the low density region along the [α/Fe] vs. [M/H] plane, thanks to the analysis of the [α/Fe] distribution in four intervals of metallicity. The identified position of the gap in the [α/Fe] vs. [M/H] plane was used as the separation criterion between the thick and thin disc populations for further analysis.

The above gap is in agreement with the separation seen in the Adibekyan et al. (2012) high-resolution in the Solar neighbourhood. Indeed, Fig. 9 (left panel) shows the Adibekyan et al. (2012) division, as a red line with three segments, that can be compared to our proposed separation, in black. Both lines are compatible, with very small differences probably due to possible offsets in the abundance measurements between the GES analysis and the Adibekyan et al. (2012) one, or to a possible adjustment between the [M/H] and the [Fe/H] abundances. On the other hand, the Lee et al. (2011b) analysis proposes a division line with a shallower slope as illustrated by the blue solid line in Fig.9. The two dashed lines indicate their dividing points for the thin and the thick disc stars to avoid the misclassification of stars. We see that the lower dashed line allows to select thin disc stars in fair agreement with both our selection and the Adibekyan et al. (2012) one. However, the upper dashed line excludes an important part of the thick disc sequence with intermediate and low [α/Fe] values, even if a bias between our [α/Fe] measurements and the Lee et al. (2011b) ones could exist. This could come mainly from the identification of the metal-rich part of thick disc, that would be more difficult to separate from the thin disc from low resolution data, due to the small differences in the [α/Fe] values.

Furthermore, the difference of slope observed in our sample between the thin and the thick disc sequences seems in agreement with the Haywood et al. (2013) analysis of Adibekyan et al. (2012) data, that already points out an iron enrichment of the thin disc lower than the thick disc one.

Similar chemical separations between the thin and the thick disc in the [α/Fe] vs. [Fe/H] plane are found in

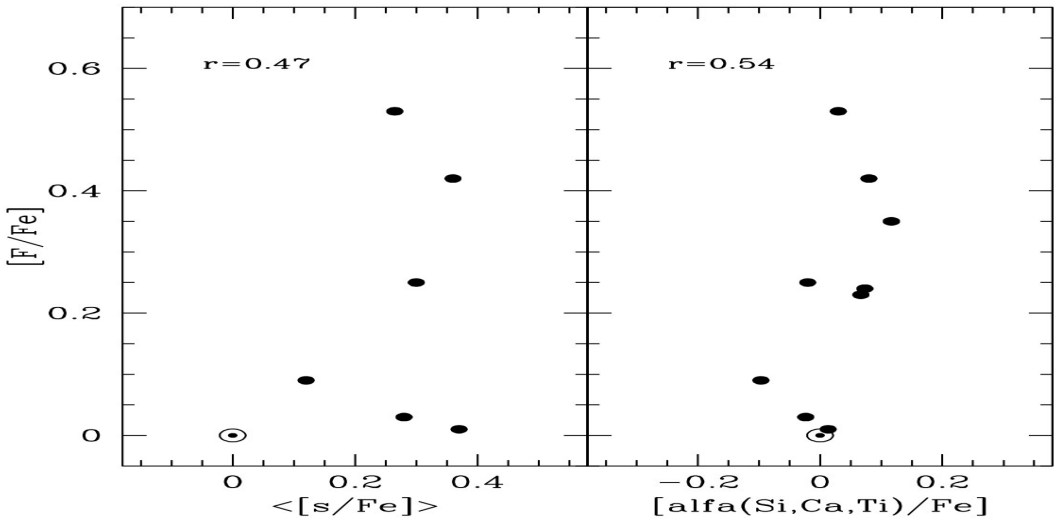


***Figure 10**: Fluorine abundances for thin disc stars from Recio-Blanco et al. (2011). The F abundance with respect to iron is shown as a function of the mean s-element content (derived from yttrium and zirconium lines; left panel) and the mean [α/Fe] (derived from Si, Ca, and Ti measurements by Gilli et al. 2006; right panel).The corresponding value for the Sun is shown as a reference.*

the most recent GES internal data releases to which we have highly contributed (Guiglion, Recio-Blanco et al. 2014; Rojas-Arriagada, Recio-Blanco et al. 2014b), and in the APOGEE data (Anders et al. 2014, Niedeber et al. 2014).

Finally, in Mikolaitis et al. (2014) we have also studied the chemical distinction between the thin and the thick disc using eight different individual element abundances from GES data. The general behaviour of element-to-iron ratios is very similar to those described, in the Solar neighbourhood, by other authors (Neves et al. 2009; Adibekyan et al. 2012; Ishigaki et al. 2013 etc.). The distribution is bimodal in most α-elements (Mg, Si, Ti and Ca), showing the most prominent separation in [Mg I/M], that we used to define chemically two populations attributed to the thin and thick discs. Calcium does show the least clear separation, as can be expected keeping in mind that it has a stronger contribution from SN-Ia than other α-elements. Also, we note, that dispersions for most of elements are compatible with the measurement errors and the intrinsic scatter is low or even non-detectable. On the other hand, the aluminium-to-iron ratio is similar to those found for α-elements. The thin and thick disc populations overlap, but the distributions are clearly distinct, with the thick disc above the thin disc. For iron-peak elements, the trends for chromium and nickel are well defined and come close to the Solar value with [Cr I/M]=−0.06 (rms 0.13 dex) and [Ni I/M]=−0.05 (rms 0.11 dex), with no separation between the thin and the thick discs. Finally, the only s-process element measured abundance, [Y II/M], shows scattered values around the Solar one and the thin and thick disc stars overlap completely.

3.2.2 Fluorine abundances in the thin disc.

As explained above, chemical abundances and their interpretation in the framework of a stellar population chemical evolution, are powerful tools for Galactic archaeology studies. For this reason, part of my work has also been dedicated to a better understanding of the nucleosynthesis of some key elements like fluorine, trying to improve our interpretation of their stellar abundances.

In spite of many observational efforts to characterise the chemical evolution of our Galactic disc, not much is known about the origin of fluorine (F). Models suggest that the F found in the Galaxy might have been produced mainly in three different ways, namely, Type II supernovae, Asymptotic Giant Branch nucleosynthesis, or in the core of Wolf-Rayet stars. Only a few observational measurements of F abundances are available in the literature and mostly for objects whose characteristics might hamper an accurate determination of fluorine abundance (e.g., complex mixing and nucleosynthesis processes, external/internal contamination). In particular, fluorine is associated to the Galactic globular clusters chemical anomalies, associated to the unexpected presence of multiple stellar populations.

In Recio-Blanco et al. (2011), we derived the F abundances of nine cool main-sequence thin disc stars in the solar neighbourhood, based on an unblended line of the HF molecule at 2.3 microns, thanks to high quality VLT/CRIRES spectra. In addition, we studied the α-elements and the s-process elements of five of these stars.

As shown in Fig. 10, several of the analysed stars seem to be slightly fluorine enhanced with respect to the Sun, although no correlation was found between the F abundance and the iron content. In addition, the most fluorine enriched stars are also yttrium and zirconium enriched, which suggests that Asymptotic Giant Branch fluorine nucleosynthesis could be the dominant source of fluorine production for the observed stars. Nevertheless, the correlation between [F/Fe] and the s-elements is rather weak and possibly masked by the uncertainties in the F abundance measurements. Finally, we compared our derived F abundances to previous measurements of α-element and iron-peak element abundances of the same stars. Type II core collapse supernovae do not appear to be the main site of F production for our targets, as no correlation seems to exist between the [F/Fe] and the [α/Fe] ratios.

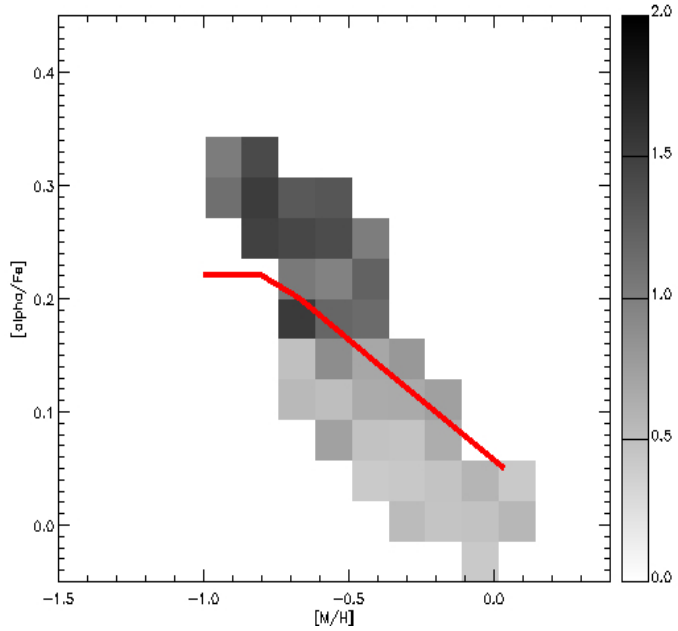


***Figure 11**: Distribution of the distances to the Galactic plane in [α/Fe] vs. [M/H] from Recio-Blanco et al. (2014a). The red line shows the separation between the thick and the thin discs sequences*

3.4 Spatial distributions of disc stellar populations

In addition to the chemical element abundance information, the structural properties of the Milky Way disc offer crucial constraints that can be examined in the light of different disc formation models. In particular, the observed radial and vertical stellar abundance distributions are interesting tools to study the chemical enrichment history of the Galactic disc, as they are sensitive to its formation process: inside out disc formation leaves a radial gradient that may be partially erased by radial mixing; vertical gradients can be created by several secular processes such as the heating of discs, intrinsic or violent mergers, radial migration can turn a radial gradient into a vertical one, etc. The GES data, sounding a large volume of the disc, are ideal for this kind of observational constraints. We have already used the GES iDR1 data for this analysis.

3.4.1 Distance to the Galactic plane

As already mentioned in Sect. 3.1, the thin and the thick discs are characterised by different scale heights. In order to explore the transition between these two populations, we have analysed in Recio-Blanco et al. (2014a) the distribution of the derived distances to the Galactic plane (from the absolute values of the Galactic Z coordinate) for the GES internal data release stars.

Fig. 11 shows a grey scale-coded two-dimensional plot of the distribution of Z values in the [α/Fe] vs. [M/H] plane. The red line shows the separation between the thick and the thin discs sequences.

Regarding the thick disc population, the mean distances to the Galactic plane seem to decrease along the sequence, from the metal-poor end to the metal-rich one:

– Z∼1.5 kpc at [M/H]∼-0.9 dex and 0.28<[α/Fe]<0.40 dex

– Z∼1.2 kpc at [M/H]∼-0.5 dex and 0.21<[α/Fe]<0.30 dex

– Z∼0.8 kpc at [M/H]∼-0.3 dex and 0.12<[α/Fe]<0.25 dex.

Therefore, as the metallicity increases, the thick disc seems to lay in thinner and thinner layers. On the other hand, the distribution of vertical distances to the plane with respect to the Galactocentric radial distance is

not perfectly homogeneous (c.f. Fig 9). More particularly, the sample is dominated by stars further away from the Galactic plane in the inner parts of the disc with respect to the typical heights probed in regions outside of the solar radius. Thus, different Z heights can be representative of different ranges in R, and, if there were significant metallicity variations with respect to R, this would manifest as a variation in metallicity with height. However, the data show a flat distribution of [M/H] and [α/Fe] with Galactocentric radius for the thick disc. Therefore, the gradient of Z that appears along the thick disc sequence in the [M/H] v.s. [α/Fe] plane, for increasing [M/H] values should be a real effect, not caused by sampling.

This finding could be in agreement with the Haywood et al. (2013) proposal of a thick disc forming stars in thinner and thinner layers for 4-5 Gyrs, also predicted by the dissipational settling formation scenario of Burkert et al. (1992). Similarly, Bovy et al. (2012c) already pointed out the scenario of an evolution in gradually thinner layers (as suggested by the dependence of their scale height distribution on [α/Fe]), although no clear separation between the thin and the thick disc sequences appears in their data. In addition, the recent hydrodynamic simulations of Bird et al. (2013) and Stinson et al. (2013) also show discs in which the younger stars have progressively shorter vertical scale heights.

On the other hand, the thin disc sequence shows a quite constant value of the mean distances of its stars to the Galactic plane of Z~0.5 kpc, from the metal-poor side ([M/H] ~-0.8 dex) to the metal-rich one ([M/H] ~0.3 dex). Again, this conclusion should not be influenced by the spatial coverage of the studied sample, despite the fact that the thin disc has a metallicity gradient with respect to R. This is because the thin disc Z range is fairly homogeneously covered at the full range of Galactocentric radius, and, in particular, the mean Z value of the stars in the thin disc sequence does not present any clear trend with R.

As a consequence of the above conclusions, the transition from the thick disc sequence to the thin disc one, in the [α/Fe] vs. [M/H] plane, implies a steeper change in the mean Z distances at [M/H] around -0.8 dex than around -0.3 dex. This coincides with the fact that the chemical separation between both sequences (by a gap or a lower density region) seems clearer in the metal-poor regime than in the metal-rich one.

3.4.2 Radial and vertical gradients

Attempts to study radial and vertical chemical gradients of the thick and thin discs separately are not numerous. The recent works of CosçkunoğLu et al. (2012), Bilir et al. (2012), Boeche et al. (2013) and Cheng et al. (2012a) provide metallicity gradients from large samples, although from low-resolution data. Many open questions remain as the precise value of the metallicity and the α-elements radial gradients in the thin disc. Vertical gradients are even poorly constrained (Ruchti et al. 2011, Boeche et al. 2013). In this context, we have analysed in Recio-Blanco et al. (2014a) and Mikolaitis et al. (2014) the radial and vertical gradients in the disc using GES iDR1 data.

Regarding the thin disc, a radial metallicity gradient is present, with a similar slope to the younger tracers such as Cepheids (Lemasle et al. 2008; Pedicelli et al. 2009), but also to the gradient measured by other large surveys such as SEGUE or RAVE for field stars close to the Galactic plane (Cheng et al. 2012b; Boeche et al. 2013); this gradient is confirmed in our own iron measurements. Positive radial individual α-over-iron (Mg/Fe, Si/Fe, Ca/Fe) gradients are also observed in the thin disc from the GES iDR1 data, matching the gradients observed in cepheids by some authors (Luck & Lambert 2011) and open clusters (Magrini et al. 2009; Pancino et al. 2010; Yong et al. 2012), but at variance from the gradients observed by Boeche et al. (2013) in RAVE. The thin disc also hosts a negative vertical metallicity gradient in the solar cylinder when studied with GES iDR1 data (similar to Bilir et al. 2012, from a kinematically selected thin disc sample in RAVE), accompanied by positive [α/Fe] and [Al/Fe] gradients, compatible with a thin disc where older stars (where [α/Fe] is taken as a proxy for age) are kinematically hotter than younger thin disc stars.

The thick disc on the other hand presents no radial metallicity gradient, in agreement with SEGUE (Cheng et al. 2012b) or RAVE (Boeche et al. 2013) samples selected far from the midplane, and a shallower (negative) vertical metallicity gradient than the thin disc. The thick disc displays shallow α-elements radial gradients detected at the ~ 2σ level, in the opposite sense than in the thin disc (decreasing [α/Fe] towards large R_{GC}), and a positive vertical [α/Fe] and [Al/Fe] gradients slightly stronger than those of the thin disc.

3.5 Chemo-kinematical and chemo-dynamical correlations

The analysis of the possible correlations between chemical abundances and the kinematical and dynamical properties of disc stars can be a strong constraint to the models. Known examples of this are the correlations

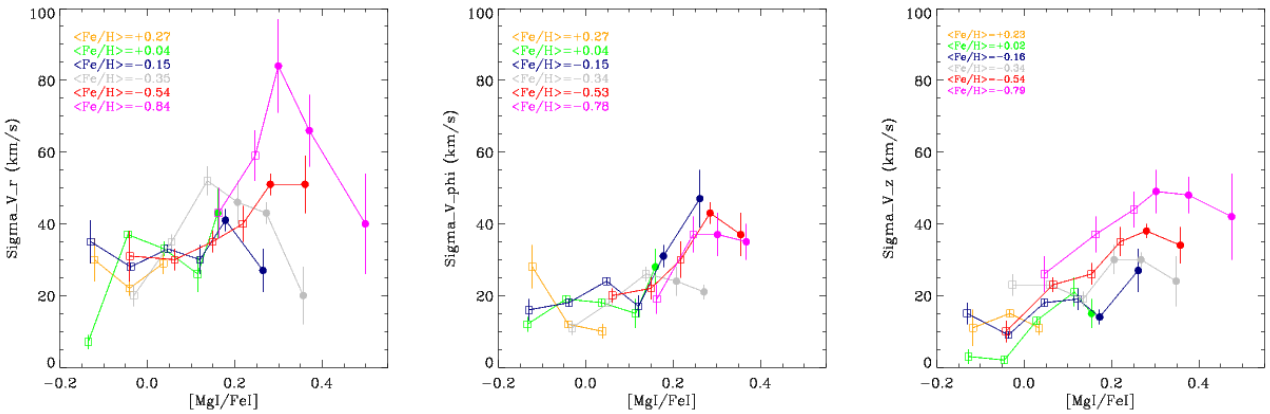


***Figure 12**: Radial, azimuthal and vertical velocity dispersions as a function of the [Mg/Fe] ratio for GES iDR2 data from Guiglion, Recio-Blanco et al. (2014).*

between the rotational velocity and the metallicity, the [α/Fe]-velocity dispersion relation or the dependences of the orbits eccentricity distribution on metallicity and [α/Fe].

In particular, the precise estimation of the correlation between rotational velocity and metallicity can constrain the degree of radial migration in the disc (ex. Spagna et al. 2010). In fact, in the presence of strong radial migration processes, no or only a very small correlation is expected in the transition region between the thin and the thick disc, because the older stars that compose the thick disc should have been radially well mixed.

On the other hand, the [α/Fe]-velocity dispersion relation can help to explore the time evolution (using [α/Fe] as an age proxy) of the stars velocity dispersions, linking them to the chemical substructure of the disc (Minchev et al. 2014). This implies to invoke physical processes intimately related to the galaxies evolution, like resonances with the Galactic bar (Quillen et al. 2003), (minor) mergers of dwarf galaxies (Toth & Ostriker 1992), radial migration, gravitational scatter by giant molecular clouds (Spitzer & Schwarzschild 1951),... In addition, general questions like the role of internal versus external heating or the possibility of distinguishing the effects of radial migration induced by satellite infall (Bird et al. 2012) can be addressed.

Finally, it is today widely accepted that the shape of the eccentricity distribution of the stellar orbits can provide important constraints on the formation mechanisms of the Galactic disc (Sales et al., 2009, Di Matteo et al. 2011). In general, stars formed in situ are expected to have low-eccentricity orbits, while accreted stars from satellites always dominate the high-eccentricity tails of the distributions. Therefore, changes in the relative proportion of *in situ* versus accreted stars drive the differences seen in the predicted histograms of each thick disc formation scenario. In other words, the analysis of the stellar eccentricities off the plane helps to unravel whether the bulk of stars was formed locally in the main progenitor (heating, migration, merger) or, on the contrary, was accreted from in falling satellites (accretion).

Once again, we have already addressed these questions thanks to high quality data from the GES iDR1 and iDR2.

3.5.1 Chemo-kinematical signatures

Taking advantage of the GES high resolution spectra and large spatial coverage, we have analysed in Recio-Blanco et al. (2014), the behaviour in Galactocentric rotational velocity of the thin and thick disc populations. The mean rotational velocities found for the thick and the thin disc sequences are in agreement with the canonical ones (VΦ =176±16 km/s and VΦ =208±6 km/s). In addition, the mean Galactic rotation also seems to increase progressively along the thick disc sequence, as the metallicity increases. Our data also confirm the already observed correlations between VΦ and [M/H] for the two discs.

In the case of the thick disc sequence, the mean value of the ΔVΦ /Δ[M/H] is 43±13 km s^{-1} dex^{-1} , is in agreement with the previous findings of Lee et al. (2011b), Kordopatis et al. (2011) and Spagna et al. (2010). This would confirm the disagreement with the SDSS result of Ivezic et al. (2008), based on photometric metallicities. Moreover, we have explored the possible influence of contaminating stars from the thin disc in the analysis of the correlation. If only the stars with the higher [α/Fe] values at each metallicity bin are considered, the derived ΔVΦ /Δ[M/H] is 64±9 km s^{-1} dex^{-1} . As a consequence, this steeper value of the gradient, cleaned from the influence of possible thin disc contaminants could be more characteristic of the real correlation for the thick disc. For the thin disc, a negative gradient of ΔVΦ /Δ[M/H]=-17±6 km s^{-1} dex^{-1}

is found. Consequently, the difference in the characteristic rotational velocities between the thin and the thick disc are again accentuated in the low metallicity regime, as for the mean distances to the Galactic plane.

Finally, thanks to the GES iDR2 data, containing a sensitively increased number of stars with respect to iDR1, we have studied in Guiglion, Recio-Blanco et al. (2014) the dependence of the velocity dispersion on the metallicity and the [α/Fe] abundance for the the thin and the thick disc. Our results, shown in Fig. 12, are quite compatible with those of Minchev et al. (2014), although the spatial coverage of GES is larger than that of the RAVE survey, from which the Minchev et al. results are derived. For the thin disc, a flat behaviour is observed for [α/Fe] < 0.1 dex, independently of the metallicity. For higher [α/Fe] enrichments, corresponding to the metal-poor tail of the thin disc sequence, the velocity dispersion increases in all the three cylindrical components, with similar values to those of the metal-rich part of the thick disc sequence. On the other hand, for the thick disc, the velocity dispersion seems to increase as [Fe/H] decreases and, specially, as the [α/Fe] content increases. In addition, and in agreement with Minchev et al. (2014), a decrease in the dispersion is observed for the higher [α/Fe] bins at each metallicity interval. However, while with the RAVE data Minchev et al. (2014) observed this decreasing behaviour only for [Mg/Fe] > +0.4 dex, our data show this tendency already for [Fe/H] < −0.35 dex and [Mg/Fe] > +0.20 dex. In fact, our bin with < [Fe/H] >= −0.35 dex (grey curve in Fig. 12) shows a decrease whatever the Galactic component, while with RAVE, it is visible only for the radial component at < [Fe/H] >= −0.45dex.

By comparison with a chemo–dynamical model, Minchev et al. (2014) explained this decrease in the velocity dispersion of the older thick disc stars as the effect of mergers on the outer parts of discs and the subsequent radial migration of older stellar populations with cooler kinematics born in the inner disc. In the light of our new results, the existence of kinematically cool thick disc stars also for [Fe/H] ~ −0.35 dex and [Mg/Fe] > +0.20 dex would imply a different (and eventually longer) time interval of the merger events. Comparisons with the Minchev et al. chemo–dynamical simulations for the GES data are in course.

Moreover, the Villalobos & Helmi (2008) scenario of thick disc formation via minor mergers heating a pre-existing disc (not invoking radial migration), would also allow for a remnant cooler disc, mainly located below |Z| = 1 kpc, as it is the case of our observed stars.

Finally, we have found a decrease in the radial and azimuthal velocity dispersion of the thick disc stars with Galactocentric radius, similar to the one reported in Sharma et al. (2014) for RAVE data. The dispersion values in the external parts of the disc are compatible with those attained by the cool thick disc stars in the higher [Mg/Fe] bins, suggesting a possible connection between this cooler thick disc kinematics and the external regions of the disc. This fact could leave room for scenarios invoking an initial high level of turbulence in the disc (that would in principle be in conflict with our results) if the highly turbulent regions are confined to the inner disc (c.f Bournaud et al. 2009; Haywood et al. 2013). For instance, the recent chemical evolution model of Snaith et al. (2014) proposes an independent evolution of the the outer disc in which metals coming from the inner disc may have been diluted by more pristine gas coming from the halo. This would allow them to keep a high-alpha enrichment in the outer parts without increasing the star formation efficiency. In any case, a more detailed comparison with model predictions combining chemical and kinematical data needs to be performed.

3.5.2 Chemo-dynamical signatures

The Recio-Blanco et al. (2014a) work also allowed us the study of the orbital eccentricities of the stars in identified thin and thick disc sequences. As expected, the thin disc distribution is strongly peaked at a low eccentricity value of ~ 0.15. On the other hand, the thick disc is significantly broader and its median eccentricity is around 0.3. Compared to previous determinations, such as those of Wilson et al. (2011), Lee et al. (2011b) and Kordopatis et al. (2011), the shape is flatter and does not decline as fast at high eccentricities, although because of the small number of stars, the significance of this may be questionable.

In addition, the thin disc sequence presents a very similar eccentricity distribution through its whole metallicity range, with a majority of low eccentric orbits. In addition, when only thin disc stars with a distance to the plane lower than 400 pc are considered, most of the thin disc stars with higher eccentric orbits disappear. Moreover, this high eccentricity tail of the thin disc suffers from very low statistics in the GES iDR1 data and relatively large errors in the derived eccentricities. On the other hand, the thick disc sequence seems to present highly eccentric orbits mainly in the metal-poor regime ([M/H]< −0.6 dex). Additionally, the metal-rich part of the thick disc sequence shows very similar eccentricities to the thin disc one. A similar

behaviour of the mean eccentricity distribution with metallicity has also been observed by Adibekyan et al. (2013) in the Solar neighbourhood.

Finally, the derived slopes of the eccentricity dependence on metallicity, $\Delta e/\Delta[M/H]$, are -0.158±0.081 dex^{-1} for the thick disc and -0.027±0.045 dex^{-1} for the thin disc. These values are also in agreement with those determined by Adibekyan et al. (2013) for the solar neighbourhood (-0.184±0.078 dex^{-1} and - 0.023±0.015 dex^{-1} for the thick and the thin disc, respectively).

3.6 General conclusions about the Galactic disc.

The general picture emerging from the above described analysis is that of a thick disc that lays in progressively thinner and thinner layers as the metallicity increases and the [α/Fe] decreases with time (until about [M/H] = −0.25 dex and [α/Fe] = 0.1 dex).

During this settling process, the thick disc rotation increases progressively and, possibly, the azimuthal velocity dispersion decreases. No measurable metallicity or [α/Fe] gradients with Galactocentric distance seem to remain for the thick disc. At about [M/H] = −0.25 dex, the mean characteristics of the thick disc in [α/Fe], vertical distance to the plane, rotation and rotational dispersion are in agreement with (or just slightly different than) that of the thin disc stars of the same metallicity, suggesting a possible connection between the two populations at a certain epoch of the disc evolution. This is in agreement with the Haywood et al. (2013) scenario, in which the inner thin disk (R<10kpc) inherited from the chemical conditions left at the end of the thick disk phase (the observed metal-rich end of the thick disc sequence in the [α/Fe] vs. [M/H] plane), some 8 Gyr ago. In their view, there may be an age gap in the star formation possibly causing the gap in [α/Fe] enrichment, after which, star formation proceeds in a thin disk.

For the thin disc, no clear gradient of the mean vertical distance to the plane with the stellar metallicity is observed. On the contrary, the stars in the metal-poor thin disc sequence tail seem to have a mean Galactic rotation velocity higher than those in the metal-rich part. Moreover, the existence of a small positive gradient in [α/Fe] with R leads to a thin disc that would be slightly more metal-poor and [α/Fe]-rich in the outer parts. These two characteristics, similar to those of the metal-poor end of the thin disc sequence in the [α/Fe] v.s. [M/H] plane, would favour the picture, suggested by Haywood et al. (2013) and Haywood (2006), of this metal-poor thin disc being formed in the outer parts.

Contrary to the similarities between the thin and the thick discs around [M/H] ∼ −0.3dex, the stars in the metal-poor regime are more clearly separated in their mean physical properties (chemistry, kinematics, possibly orbital eccentricities). This separation seems to be confirmed by the gap (or low-density region) in the [α/Fe] vs. [M/H].

On the other hand, the tight bimodal distribution of [α/Fe] at every value of [M/H] poses severe constraints to models predictions. Recent attempts to define an age-metallicity relation for stars currently in the Solar neighbourhood (e.g. Haywood et al., 2013; Mishenina et al., 2013) hint at an evolutionary path in which a very wide range of ages corresponds to a single [M/H] value. Haywood et al. (2013) results (c.f. their Fig. 8) show that at a value of about [M/H]=-0.5 dex stars have an age range of around 10 Gyr. On the other hand, the present work and other studies focussed in the Solar neighbourhood (e.g. Adibekyan et al., 2013) show that the distribution of [α/Fe] at [M/H]=-0.5 dex appears narrowly bimodal, with two essentially unresolved but quite discrete values of [α/Fe] being found. As a consequence, although stars with [M/H]≈-0.5 dex formed over 10Gyr, they seem to be formed with only two values of [α/Fe]. This is a quite remarkably severe constraint that can be analysed in the light of Galactic models in which radial migration (e.g. Sellwood & Binney, 2002; Schönrich & Binney, 2009c,b; Roskar et al., 2008), and churning, is a major factor.

Schönrich & Binney (2009b) claim that a bimodal, although continuous, distribution of [α/Fe] can naturally come out as a consequence of the standard assumptions about star formation rates and metal enrichment, with no need to invoke breaks in the Galaxy's star formation history or accretion events. However, the tightness of the well populated observed thick and thin disc sequences in the [α/Fe] vs. [M/H] plane, with possibly only two values of [α/Fe] for a given metallicity, poses severe constraints.

If radial migration occurs, one can suppose an evolutionary path in which enrichment in the high-α branch happened rapidly, up to metallicities close to [M/H]= −0.25 dex. This should occur across a large enough radial range of the proto-galactic disk.

In fact, to preserve the tightness of the high-α sequence, the stars should had formed in a narrow time interval from radially well mixed interstellar medium (ISM) gas, through all the galactocentric radii which generated stars that are today at a given R (ex. in the Solar neighbourhod). Then, to explain the low-α sequence, one can postulate a significant gas accretion, reducing the disc ISM metallicity to, for instance, -0.6 dex. This should be followed by disc evolution in which large scale gas flows (as in fountains, c.f. Fraternali et al., 2013, and references therein) retain a tight [α/Fe]-[M/H] correlation, over the radial region which today populates the solar neighbourhood. In addition, this scenario should, somehow, also conciliate the higher rotation values observed in the metal-poor thin disc regime. Otherwise, other possibility to explain the observed [α/Fe] vs. [M/H] distributions, is to suppose that strong radial migration in the sense of churning did not occur (see also the discussion in Haywood et al., 2013).

More recently, the APOGEE results of Nidever et al. (2014) suggest that the two α-element sequences in the inner Galaxy could be explained by a single chemical evolutionary track, while this cannot hold in the outer Galaxy, requiring instead a mix of two or more populations with distinct enrichment histories. Similarly, Snaith et al. (2014) have very recently presented a chemical evolution model of the disc, in which the inner (thick +thin) discs and the outer disc are two systems that can be mostly considered to be the result of two distinct chemical evolution paths. The results of our recent chemo-kinematical study of GES iDR2 disc data can help to further constrain this proposal, as well as the importance and time-scale of minor mergers in the disc (Minchev et al. 2014).

Many pieces of the Milky Way disc puzzle remain to be found, but all the previous results already show the importance of precise chemical abundance measurements to disentangle the Galactic disc history. The stellar chemical patterns can guide the definition of useful stellar sub-samples to unveil the evolutionary paths in the disc formation history and to give clearer constraints to the models.

Chapter 4

ARCHAEOLOGY OF THE GALACTIC BULGE

The bulge is a major component of our Galaxy, comprising approximately a quarter of its total stellar mass ($M_{bulge} \sim 1.8 \times 10^{10}$ $M_{\odot}$, Sofue et al. 2009). Bulges are very common structures in galaxies, which in cosmological scales harbour approximately 70% of the stellar mass (Fukugita et al. 1998). Because they consist of most of the oldest stars in a galaxy, studying bulges represents a valuable opportunity of understanding the chemo-dynamical processes involved in the general formation of the host galaxy. Furthermore, because of its proximity, the Galactic bulge presents an ideal opportunity of performing detailed observations for hypothesis-testing on a star-by-star basis, an advantage that is not available for external bulges, except for M31.

The bulge complex internal structure and kinematic and chemical patterns have inspired several studies in the community during the past decade that aimed at explaining its formation and evolution. The three main formation scenarios currently invoked are (i) in situ formation via dissipative collapse of a protogalactic gas cloud in a free-fall time scale (Eggen et al. 1962), (ii) accretion of substructures, disk clumps or external building blocks in a ΛCDM context (e.g. Immeli et al. 2004; Scannapieco & Tissera 2003; Bournaud et al. 2007a,b), and (iii) secular formation from disk material through bar formation, vertical instability, buckling, and fattening, which produces a structure commonly called pseudo-bulge (e.g. Combes et al. 1990; Pfenniger & Norman 1990; Kormendy & Kennicutt 2004, Martínez Valpuesta & Gerhard 2013; Di Matteo et al. 2014). Moreover, bulges can also be formed in clumpy discs and/or via bar resonances in the frame of Modified Newtonian Dynamics (MOND) models (Combes 2014).

Finally, the possible Galactic disc-bulge connection is a crucial ingredient of the Milky Way history general picture, as well as a benchmark for the relative importance of the internal secular process with respect to external ones in the Galaxy evolution. This fact has also motivated the work presented here below, performed in collaboration with one of the PhD students I am presently supervising (A. Rojas-Arriagada), and based on GES iDR1 data. It will be soon extended with iDR4 data (which contains about 2300 bulge stars).

4.1 Observational framework and formation scenarios.

In the past years, Milky Way bulge studies have been the object of intense debate, when it became evident that it was impossible to consider it as a single stellar population (Babusiaux et al. 2010; Hill et al. 2011; Bensby et al. 2011; Ness et al. 2013a). Its complex internal structure and kinematic and chemical patterns have inspired several studies in the community during the past decade that aimed at explaining its formation and evolution. The increasing amount of observational evidence supports different formation scenarios in an apparently contradictory way.

The shape and kinematics of the Milky Way bulge both support the existence of a bar. The bulge presents a boxy/peanut appearance as displayed in 2MASS star counts (López-Corredoira et al. 2005) and COBE-DIRBE near-infrared light distribution (Dwek et al. 1995). Star counts using red clump (RC) stars characterize the bar as a triaxial structure of ∼ 3.5 kpc in length that points at the first quadrant at ∼ 25◦ with respect to the Sun-Galactic center line of sight (Rattenbury et al. 2007). Several models have subsequently interpreted this boxy structure as an edge-on buckled bar (Zhao 1996; Fux 1999; Shen et al. 2010). Boxy bulges present a characteristic cylindrical rotation, namely, a nearly constant stellar rotation speed with height above the Galactic plane. Classical bulges rotate more slowly at increasing height (Falcón-Barroso et al. 2004). After studies of various probes (K giants, globular clusters, PNe), the first and recent large data set of systematically collected radial velocities in the Galactic bulge was assembled by the BRAVA project (Rich et al. 2007b), and showed indistinguishable rotation curves in strips at b = −4◦ , b = −6◦ , and b = −8◦ (l ± 10). BRAVA velocities are fitted nicely by the model of Shen et al. (2010), which is able to reproduce a boxy/peanut bulge just from accreted stars from the disk and constrains any possible classical component to be less than 8% of the disk mass. This could challenge some attempts to detect it, even in large data samples.

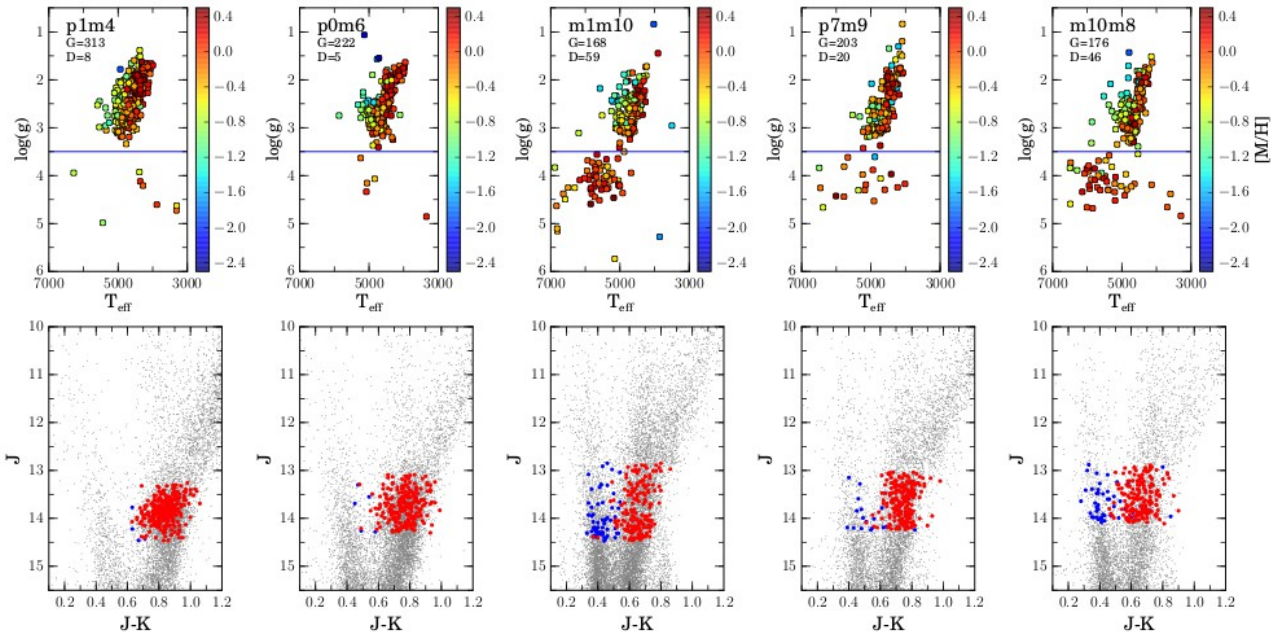


***Figure 13**: Upper panels: HR diagrams for the five bulge fields constructed from the stellar parameters obtained as described in the text, and colour-coded according to the metallicity [M/H]. Our adopted limit for giants (log g = 3.5 dex) is marked by a horizontal blue solid line in each panel. Lower panels: J vs. (J-Ks) colour-magnitude diagrams constructed from VVV VISTA photometry, completed with 2MASS for stars brighter than Ks = 12 mag, where VVV magnitudes start to saturate. The different selected samples are apparent from the distribution of observations in the bulge RC and MS regions in each field, colour-coded according to the stellar gravity as dwarfs (blue) and giants (red).*

Furthermore, the Galactic bulge has been shown to display an X-shape. In an extensive analysis using star counts of RC members in a large area, McWilliam & Zoccali (2010) using 2MASS, and Nataf et al. (2010) using OGLE-III, have revealed the existence of a bimodality in the RC magnitude at $|b| > 5.5^{\circ}$. The distance between the two magnitude peaks appears to be nearly constant with longitude and decreases toward the Galactic plane. This is interpreted as evidence for an X-shaped Galactic bar. Saito et al. (2011) and Wegg & Gerhard (2013) have confirmed these findings by tracing the bulge structure along the line of sight in several slices in l and b using density maps. The underlying X shaped structure is seen as boxy/peanut from the Sun position because of the almost edge-on perspective. In this way, the double red clump arises from the intersection of the line of sight with the two overdensities that correspond to the X shape. In addition, as found by Ness et al. (2012), the double red clump feature is verified only for stars with [Fe/H]>- 0.5 dex. Some dynamical models predict X-shaped bulges as extreme cases of boxy/peanut bulges (e.g, Athanassoula 2005; Martinez-Valpuesta et al. 2006; Debattista et al. 2006). This type of structure has also been observed in external galaxies (Bureau et al. 2006).

Radial velocity measurements by Rangwala et al. (2009) in the region dominated by the bar have revealed stellar streaming motions at (l, b) = (±5, −4). Babusiaux et al. (2014) who used RC stars in four fields with b = 0, found streaming motions induced by the bar at l ± 6 that were more evident for stars with [Fe/H] ≥ −0.2 dex. Dedicated investigations that probed radial velocity in bulge fields displaying the double RC feature have reached different conclusions: i) De Propris et al. (2011) found no radial velocity difference between the two RC overdensities at (l, b) = (0, −8), ii) Vásquez et al. (2013) detected two streams by comparing the bright and faint RC at (l, b) = (0, −6), for which they used both radial velocities and transverse motions, and iii) Uttenthaler et al. (2012) found no statistically significant difference between the two RCs in the field at (l, b) = (0, −10) in the bulge outskirts. These results compare well with predictions extracted from evolutionary N-body models (Athanassoula 2003; Ness et al. 2012; Vásquez et al. 2013) and highlight the complex orbital structure of the bar component.

Finally, a very important piece of evidence, still largely unexplored, is the true shape of the metallicity distribution function (MDF) across the whole bulge region and its relation with the different structural and kinematical observed features. Most of the early work was mainly restricted to Baade's Window, thus

preventing the detection of any variation of the MDF with (l,b). Zoccali et al. (2008) presented the first complete MDF determination based on high-resolution spectra for three fields in the bulge minor axis. Their sample revealed a metallicity gradient that was interpreted as evidence in favour of an early collapse formation scenario. Such a gradient would be absent at latitudes lower than b = −4◦ (Rich et al. 2007a, 2012). Using the same data, Babusiaux et al. (2010) suggested that two chemically and kinematically distinguishable populations might coexist in these fields. Babusiaux et al. (2010) and Hill et al. (2011) specifically showed that the most metal-rich, alpha-poor population in Baade's Window presents a vertex deviation that is compatible with bar-like kinematics, while the metal-poor, alpha-rich population did not, as expected for a spheroid, for example. More recently, from a large sample of 28,000 low to medium-resolution spectra in 28 fields, Ness et al. (2013a) presented a detailed MDF study that suggests there might be up to five underlying component populations. This new characterization agree with the observation reported by Zoccali et al. (2008) that the metallicity gradient is produced by a change of MDF shape and not by a solid shift with latitude. It also agrees with the results of Babusiaux et al. (2010) and Hill et al. (2011) that suggested two chemically and kinematically distinguishable populations. These findings reveal the bulge as a very complex structure, consisting of several populations with different characteristics, origins, and possible formation mechanisms.

4.2 The Gaia-ESO Survey bulge observations.

In Rojas-Arriagada, Recio-Blanco et al. (2014) we analysed the metallicity and kinematic trends of the Milky Way bulge thanks to GES data from the first internal data relase (iDR1). The analysed sample consists of spectra for ∼ 200 stars per field that were obtained in five lines of sight toward the bulge. In total, 1220 stars were observed with the ESO/VLT/FLAMES facility in the MEDUSA mode of the GIRAFFE multi-object spectrograph, using the HR21 setting. Spectral coverage spans from 8484 to 9001 Å with a resolving power of R ∼ 16200. Individual signal-to-noise ratio values and other general information are presented in Table 1. In this table and in the following, fields are referred to by their names, which are assembled from their Galactic longitude (l) and latitude (b), with the p/m letter coding the +/− sign: for example, the field in Baade's Window at l = +1 and b = −4 deg is named p1m4.

Radial velocities were determined for each star through a dedicated pipeline by cross-correlation against real and synthetic templates, as described in Koposov et al. (2014, in prep.). Typical internal errors are on the order of 0.2 km s^{-1} . The recommended parameters Teff , log g , and global metallicity [M/H] for bulge data in the internal Data Release 1 (hereafter iDR1) are those determined with the MATISSE algorithm (Recio-Blanco et al. 2006) by the GES work package in charge of the GIRAFFE spectrum analysis for FGK-type stars. No other methods were applied to these data for iDR1, therefore the MATISSE parameters were those recommended by the GES consortium and were adopted for our analysis. The corresponding nominal errors adopted for these corrected quantities are ΔTeff = 100 K, Δlog(g) = 0.2 dex, and Δ[M/H] = 0.2 dex .

According to the initial photometric selection criteria for the target stars, the observed samples are expected to consist mainly of: i) bulge red clump (RC) and first-ascent giant stars, ii) a small contribution from foreground inner-disk RC stars, and iii), a field-to-field variable amount of contaminants from the dwarf main-sequence. The dwarf sample is clearly separated in the Teff vs. log g plane after the atmospheric parameters are determined for the full sample (see Fig. 13). The last column of Table 1 shows the remaining percentages of giant stars in each field after removing the dwarf foreground stars by adopting a threshold value of log g ~3.5 dex. The upper panels of Fig. 13 show the Hertzsprung-Russell diagram of each field. The metallicity based colour-code enables verifying the consistency of the parameters, with an apparent metallicity gradient with Teff , expected from isochrones for red giants. The separation between dwarfs and giants is also clear in each field, consistent with our threshold value of log g = 3.5, as shown by the blue horizontal lines. It is also

Field name	*l*	*b*	SN	E(J-K)	N_{stars}	%Giants
p1m4	1	-4	90	0.21	321	98
p0m6	0	-6	82	0.14	227	98
m1m10	-1	-10	101	0.06	227	74
p7m9	7	-9	81	0.11	223	91
m10m8	-10	-8	98	0.06	222	79

***Table1**: Characterization of the GES iDR1 bulge fields from Rojas-Arriagada, Recio-Blanco et al. (2014).*

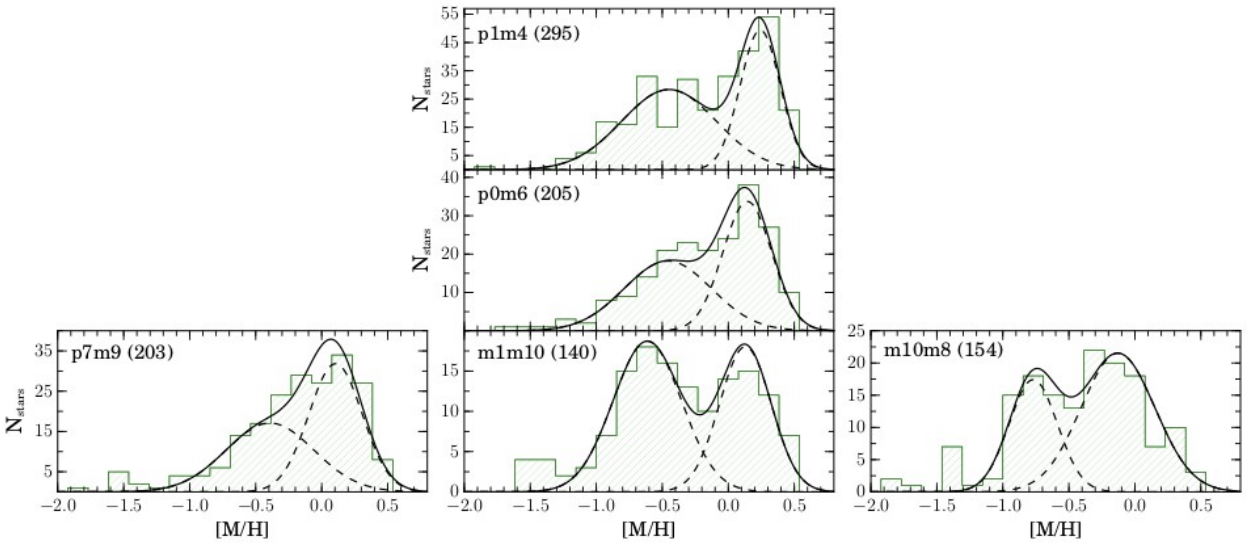


***Figure 14**: Metallicity distribution functions for the five bulge fields studied in Rojas-Arriagada, Recio-Blanco et al. (2014).*

consistent with the amount of stars located in the disk main sequence (MS) region (bluer than the RC location) of the corresponding colour-magnitude diagrams (CMD) in the lower panels. These dwarf stars have, on average, a metallicity close to solar, and a lower radial velocity dispersion than the giants in each field. These properties characterize them as disk stars distributed along the line of sight.

4.3 Metallicity distribution functions

The analysis of the metallicity distribution functions and their (l,b) dependence is a powerful tool for unveiling the complex bulge structure and possible stellar population mix. To this purpose, we selected a sample of stars centred on the red clump, including an unavoidable amount of RGB disk contaminants.

Figure 14 shows the MDF for the observed fields. The MDFs show some substructure, which suggests a complex nature. We decomposed them using a number of Gaussian profiles. To do this, we adopted a Gaussian-mixture models (GMM) formalism. We tried fits with 1 up to 4 components, using the expectation-maximization algorithm. To decide which was the best model fit with the number of components supported by the data and their relative weights, we used the Akaike information criterion (AIC). Figure 14 displays the components identified in each field as dashed Gaussian functions, with the sum as a solid line. The MDF is decomposed into two metallicity groups, whose relative proportion accounts for the mean metallicity variations in the bulge region. The metal-rich component (i) is a narrow distribution with a nearly constant mean metallicity in our fields, except for m10m8, where it is at subsolar metallicity. The metal-poor component (ii) is wider and on average more metal-poor with increasing (l,b), with the exception of p7m9, where the component is less metal- poor than expected for its location. Table 2 summarizes the characteristics of the fitted models and lists the mean metallicity, dispersion, and relative weights of each component.

The relatively limited statistics of our individual field samples has to be kept in mind. The number of stars currently observed in each field is indeed not large enough to explore a more detailed decomposition with a higher number of components, as in the analysis of Ness et al. (2013a). However, our analysis has the advantage of comparing specific individual fields, while Ness et al. (2013a) merged stars in very wide strips in Galactic longitude l, which may have blurred some intrinsic gradient in their components.

Moreover, we have compared our set of MDFs with those determined by Ness et al. (2013a) for the ARGOS survey. To this purpose, we selected the three closest ARGOS strips (b = -5° , -7.5° or -10°) to our GES individual fields. In general, the agreement is not very good, except maybe for m1m10 and m10m8. Our distributions follow the same vertical trend as ARGOS, changing the relative proportion of metallicity components with b, but only roughly resembling the exact shapes given by the ARGOS fields. We note that if we were to shift the ARGOS metallicity scale upwards by $\sim$ 0.2 dex, the differences would be strongly alleviated: components A+B of ARGOS would fit our component (i) nicely, while ARGOS component C

would fit our (ii). Furthermore, Ness et al. (2012) showed that stars with [Fe/H]≥ −0.5 dex display the X-shape, while we find this limit to be closer to −0.2 (see Sec. 4.4), which again indicates a more metal-poor metallicity scale for ARGOS.

4.3.1 Vertical gradient and positional variations

By comparing fields on the minor axis, Zoccali et al. (2008) found a metallicity gradient of about −0.075 dex/deg, while Gonzalez et al. (2013) measured a gradient twice smaller of ∼ −0.04 dex/deg from their photometric metallicity map. From the p1m4, p0m6, and m1m10 fields, we explored the presence and properties of such average metallicity variations on the bulge minor axis. This change in mean metallicity is caused by the variation in the relative weight of components (i) and (ii), with a larger proportion of metal-rich stars confined to the central regions of the bulge. The main effect of moving outward on the bulge minor axis is the decrease of the contribution of component (i) to the global MDF.

Name (distance deg)	Mean [M/H]	σ	weight
p1m4 (4.12)	−0.16 ± 0.03	–	–
(i)	0.24	0.15	0.42
(ii)	-0.45	0.36	0.58
p0m6 (6.0)	−0.17 ± 0.03	–	–
(i)	0.14	0.19	0.51
(ii)	-0.46	0.33	0.49
m1m10 (10.05)	−0.37 ± 0.04	–	–
(i)	0.13	0.20	0.42
(ii)	-0.61	0.26	0.58
p7m9 (11.35)	−0.18 ± 0.03	–	–
(i)	0.11	0.20	0.53
(ii)	-0.39	0.33	0.47
m10m8 (12.73)	−0.41 ± 0.04	–	–
(i)	-0.13	0.28	0.65
(ii)	-0.77	0.18	0.35

***Table 2**: Characteristics of the different MDF components in each field. The average radial projected distance in degrees from (l, b) = (0, 0) for each field is quoted in brackets.*

Finally, the mean position of component (i) presents small variations along the minor axis (Table 2), but still well inside the generic parameter error of 0.2 dex. On the other hand, the mean position of component (ii) is similar for the two internal fields p1m4 and p0m6, but different from that of the m1m10 field. The difference in the mean metallicity of component (ii) between the two inner and the outer field is ∼ 0.2dex, this time similar to or larger than the uncertainties. This may be a hint that component (ii) hosts a real metallicity gradient with |b|.

4.3.2 Off-axis fields

Two of the five observed fields are located away from the minor axis, at similar latitudes of b ∼ −9 ± 1 deg, and opposite longitudes. Interestingly, the p7m9 field lies in a highly metal-rich region in the map of Gonzalez et al. (2013), unlike the symmetric fields at negative longitudes, which at these latitudes far from the Galactic midplane are rather metal-poor. In fact, the MDF has a prominent peak at [M/H] ∼ 0.10 dex and a relatively sharp tail decreasing to lower metallicity.

On the other hand, the bulk of stars in m10m8 have low metallicity, in agreement with what is expected for a field far for the midplane and from the minor axis. Its mean metallicity of -0.41 dex, in agreement with Gonzalez et al. (2013), confirms this general picture. Both components of the m10m8 MDF are more metal-poor than the respective component in other fields.

The contrasting properties of p7m9 and m10m8 MDFs are consistent with the

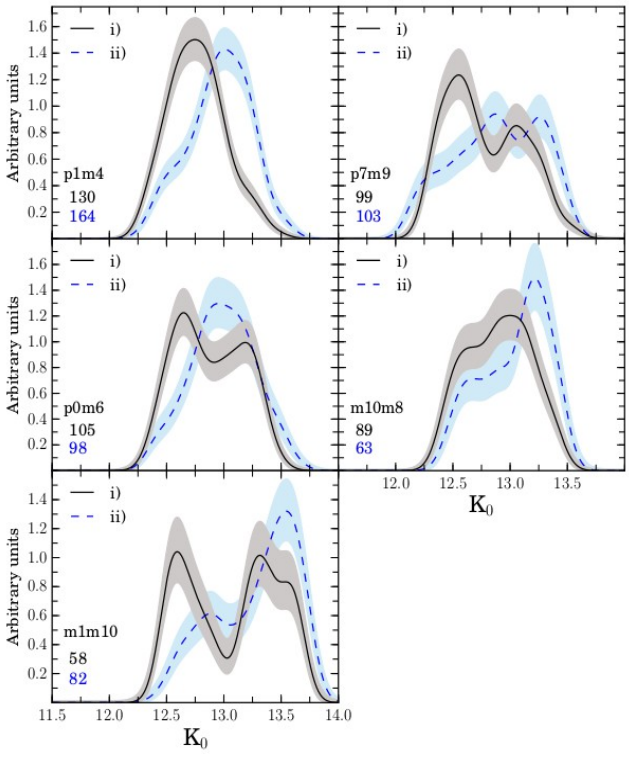


***Figure 15**: K-magnitude distributions for the metallicity components. Black (blue) solid (dashed) lines stand for the metal-rich (poor) MDF component.*

observed asymmetry in the map of Gonzalez et al. (2013) with respect to the minor axis. The asymmetry was attributed in Gonzalez et al. (2013) to a perspective effect. Since at positive (resp. negative) longitude, the line of sight intersects the near (resp. far) sides of the bar, the stars at positive longitudes are, on average, closer to the observer and hence to the plane than those at negative longitudes and same b. This fact, together with an intrinsic bulge vertical metallicity gradient, could explain the observed metallicity asymmetries.

On the other hand, we have shown in the previous section that the gradient through the minor axis can be explained from a variable mix ratio of metal-poor and metal-rich stars with b and not a solid shift-type of metallicity gradient. In this context, the MDFs of the off axis fields can be interpreted in a slightly different way, where the metallicity components (i) and (ii) would correspond to separated structures with different spatial distributions, allowing to reproduce the map asymmetry from their particular geometrical properties.

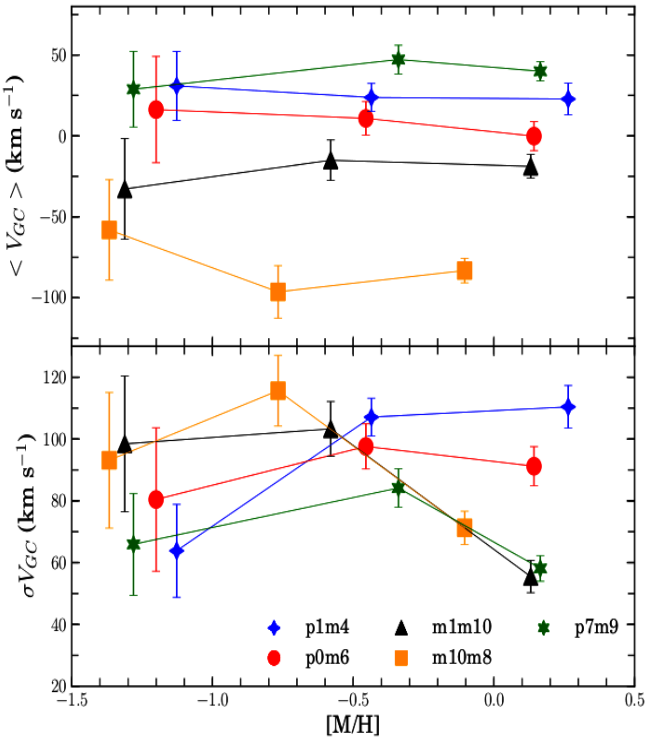


***Figure 16**: Mean and dispersion velocity versus metallicity. There are three points per field, corresponding to components (i), (ii), and the metal-poor tail of stars with [M/H] < −1.0 dex.*

4.4 Double red clump characterisation

Figure 15 shows the magnitude distributions of our clump stars in different metallicity ranges, corresponding to the components found in Sect. 4.3. In every field where the general red clump luminosity function displays more than one structure (i.e. where the line of sight crosses more than one structure in the maps of Wegg & Gerhard (2013)), the metal-rich component (i) also displays a bimodal K magnitude distribution. This occurs on the minor axis for $|b| \leq 5$, so in our p0m6, and m1m10 fields. The p1m4 field is too close to the plane for double red clump structures to appear because the arms of the X-shaped bulge, seen almost as an edge-on structure, merge in a central density of stars. Accordingly, the magnitude distribution of the metal-rich component (i) shows a single-peak.

To summarize, our metal-rich component (i) traces a gradual increase in the magnitude separation between the bright and faint peaks of the red clump luminosity histogram, corresponding to the arms of the X-shaped secular bulge structure.

4.5 Kinematical features

We characterize the substructures sampled by our RC-based metallicity components thanks to a detailed examination of the sample kinematics. For this purpose, we estimated the Galactocentric velocity V_{GC} by correcting the radial heliocentric velocities for the solar motion with respect to the Galactic centre.

Figure 16 provides a detailed view of the kinematics as a function of metallicity. The three points per field in each panel represent the two MDF components plus the metal-poor tail with [M/H] < −1.0 dex. It is clear that the two metallicity populations identified in our fields display different kinematic signatures. The metal-poor spatially extended component (ii) appears to be systematically hot throughout the area sampled by our fields. And, in contrast, the kinematic properties of metal-rich component (i) are highly dependent on the specific position of the field, are generally hotter close to the plane and cooler with increasing (l,b). This depicts an inhomogeneous and more complex spatial orbital distribution for the structure traced by these

metal-rich stars.

We can understand the observed kinematical properties of component (i) stars in terms of the orbital structure of the X-shaped bar that is traced by our metal-rich stars: an instability-driven mechanism that forms X-shaped structures starts from a disk instability and takes stars from the internal disk(s) to form a bar. As a transient structure, the bar undergoes vertical instabilities, buckling and bending the stellar distribution, and resulting in a rearranged dynamical system consisting of many types of stellar orbit families. The global structure of this mix of orbits is complex (cf. Figs. 3 and 8 of Martinez-Valpuesta et al. 2006). One of the possible stable orbit families, sometimes named banana-like orbits, has profiles that are up-bended or down-bended if seen edge-on, participating in an X-shaped structure. In this context, the observed variation in velocity dispersion for component (i) with Galactic latitude might arise from the different mixture of orbit families on the line of sight. In the central parts of the bulge, the different families of orbits intersect, which builds a large velocity dispersion in these fields. In contrast, the line of sights intersect the arms of the X in external regions, where in general there are streams of dynamically similar stable banana orbits, which leads to lower velocity dispersions.

4.6 General conclusions about the Galactic bulge

In a more general context, population (i) can be interpreted as a pseudobulge structure formed over a long time-scale through secular disk evolution. The initial instability drives a reorganization of the stars, producing a stable orbital structure with some of the family orbits forming an X-shaped structure. A metallicity gradient is predicted in some models for this structure, in which the mixing during the bar and buckling instabilities is incomplete. Therefore, any preexisting radial gradient in the initial disk is trans ferred to some degree to the newly formed structure as a vertical gradient (Martinez-Valpuesta & Gerhard 2013).

The second, metal-poor component (ii), with subsolar metallicity, presents a clear negative metallicity gradient with increasing (l,b). The σV_{GC} values present small variations from field to field, indicating a uniform kinematically hot structure. The respective field magnitude distributions are flat or single peaked, without statistically strong signatures of double RC. We interpreted this component as an extended structure, possibly a classical spheroid, formed on a rapid time-scale. It coexists with the bar, surrounding it in the bulge region. From a sample of 7663 RR-Lyrae stars that sampled the old metal-poor population, Dékány et al. (2013) found that their distribution in the bulge shows no X-shape and not even a bar, but has a more spheroidal centrally concentrated distribution. As a dissipatively collapsed structure, this component would be expected to present a radial metallicity gradient (Larson 1974), with the more metal-poor stars in the outskirts, similarly to what is observed.

In this scenario, a line of sight at a given (l,b) crosses a fraction of stars that belong to the metal-rich boxy bar (if visible) plus a group of spheroid stars that become more metal-poor with increasing distances from the bulge center. This scenario is in conflict with the N-body Galaxy model of Shen et al. (2010), who constrained any classical bulge contribution to be lower than 8% of the disk mass. The model of Shen et al. (2010) fits the BRAVA data nicely when a pure disk galaxy is modelled. But the BRAVA data have no metallicity information. Because the BRAVA data are for M giants, they might even be biased toward metal-rich stars. We showed that the kinematics behaves differently for the metal-rich and metal-poor MDF components, which means that the characteristics of the global distribution depend on the proportion of stars of each component in a given field. In the same line, Babusiaux et al. (2010) found a variation of kinematics with metallicity on the minor axis, with the σV_r behaviour of metal-rich and metal-poor stars being reproduced by the disk and spheroid populations of the model of Fux (1999).

Furthermore, the coexistence of classically and seculary evolved pseudobulge structures has been observed in external galaxies (Peletier et al. 2007; Erwin 2008) and is also predicted by N-body simulations (Athanassoula 2005). It is interesting to note that while the two metallicity components have different σV_{GC} profiles, they behave similarly in terms of mean rotational velocity. This is not necessarily expected if only component (i) participates in the X-shaped bar/bulge, but it might be explained as a dynamical influence of this structure on the spheroid kinematics (Saha et al. 2012; Bekki & Tsujimoto 2011).

Finally, it is interesting to note that the proportion of the metal-poor (ii) component in all of our fields is significant. This might be interpreted, with the caveat of our limited statistics and spatial coverage, as an

indication for a structure that probably has a similar mass-content as the bar structure. We also note that the relationship of this spheroid population with the very inner parts of the Galactic thick disk is only poorly established (chemical parenthood of the two populations, see, for example, Meléndez et al. 2008, Hill et al. 2011, Gonzalez et al. 2011a, Bensby et al. 2013), which leaves the possibility open that part of this rotating spheroidal structure might be part of the inner thick disc.

This scenario has recently been examined by Di Matteo et al. (2014), who argued that the characteristics (kinematics, chemistry) of the metal-poor bulge component agree better with a thick-disk nature than with a spheroid. In particular, they argued that a classical bulge spheroid with the mean metallicity of ARGOS C cannot be larger than 10^8 $M_\odot$ (Gallazzi et al. 2005), which is incompatible with the number of stars in that component. If we assume a thick-disk origin for the metal-poor component, the similar Vrot of the (i) and (ii) components can be understood because both discs are affected by the bar potential (Bekki & Tsujimoto 2011). However, our component (ii) is slightly more metal-rich than component C of ARGOS and would allow for a 5×10^9 $M_\odot$, or even up to 10^{10} $M_\odot$, this time compatible with a metal-poor component accounting for $\sim$ 50% of the total bulge mass. Furthermore, our metal-poor component displays a vertical gradient of its own, and although current models are not really designed to address this particular question, if the initial thick disk had no radial gradient (Recio-Blanco et al. 2014b; Mikolaitis et al. 2014), no vertical gradient in the final inner thick disk is expected (Bekki & Tsujimoto 2011).

Chapter 5

STELLAR PARAMETERISATION OF GAIA SPECTROSCOPIC DATA

The European Space Agency Gaia mission has been successfully launched on December 19, 2013 from the French Guiana Space centre in Kourou. It consists in an ambitious astrometric, photometric and spectroscopic survey of a large part of the Milky Way: about 1% of the Galactic stellar content down to the 20th magnitude will be observed several tens of times. Gaia will thus revolutionize our view of the Galaxy together with our understanding of its formation and evolution histories. Apart from the astrometric instrument, Gaia is equipped with two low resolution prism spectrophotometers, which together provide the spectral energy distribution of all targets from 330 to 1050 nm. Data from these spectrophotometers (named BP and RP for "blue photometer" and "red photometer") will be used to classify sources and to determine their astrophysical parameters (APs), such as stellar metallicities, line-of-sight extinctions, and the redshifts of quasars. The spectrophotometry is also required to correct the astrometry for colour-dependent shifts of the image centroids. In addition, spectra from the higher resolution radial velocity spectrograph (RVS, 847–871 nm) on board will provide further information for estimating APs as well as some individual abundances for the brighter stars. Recent summaries of these instrument characteristics, their main goals, and expected scientific impact can be found in de Bruijne (2012); Bailer-Jones et al. (2013).

Gaia scans the sky continuously, building up data on sources over the course of its five year mission. Its scanning strategy, plus the need for a sophisticated self-calibration of the astrometry, demands an elaborate data processing procedure. It involves numerous interdependent operations on the data, including photometric processing, epoch cross-matching, spectral reconstruction, CCD calibration, attitude modelling, astrometric parameter determination, flux calibration, astrophysical parameter estimation, and variability analysis, to name just a few. These tasks are the responsibility of a large academic consortium, the Data Processing and Analysis Consortium (DPAC), comprising over 400 members in 20 countries. The DPAC comprises nine coordination units (CUs), each dealing with a different aspect of the data processing.

One of these CUs, CU8 "Astrophysical Parameters" (see Bailer-Jones et al., 2013), is responsible for classifying and estimating the astrophysical parameters of the Gaia sources. The data processing system developed to achieve this goal, called Apsis, comprises a number of modules dedicated to : i) a probabilistic classification into classes (DSC), ii) stellar parameters estimation for the BP/RP spectra (GSP-Phot) and the RVS spectra (GSP-Spec), iii) extended stellar parametrization (ESP) which operates on specific types of stars, iv) unresolved stellar binaries parametrisation (MSC), v) quasar (QSOC) and unresolved galaxies (UGC) parametrisation, vi) outlier analysis (OA) and clustering analysis (OCA) and, vii) an estimator of the stellar luminosity, mass and age (FLAME).

Since the DPAC formation, I am responsible of the CU8 top-level work package in charge of developing and maintaining the Apsis GSP-Spec module (Generalised Stellar Parametrizer – Spectroscopy), together with the scientific validation of its results. In this chapter, I describe my activities, devoted to the automated stellar parametrisation of Gaia RVS spectra.

5.1 Stellar parameters from the Gaia RVS : Generalized Stellar Parametrizer – Spectroscopy (GSP-Spec)

The RVS is a high-resolution integral-field spectrograph that will survey the whole sky. It will collect spectra with large enough signal-to-noise ratio (S/N) in order to derive their radial velocity for stars brighter than GRVS < 16 (i.e. about 150 millions stars, G_{RVS} being the Gaia magnitude of the targets through the RVS filter). The RVS will provide spectra in the CaII IR triplet region (from 847 to 871 nm) at a spectral resolution of ~11 240 (Prusti, 2012, private communication). On the other hand, the binning in the CCDs readout can be increased by a factor three for stars fainter than G_{RVS} = 10 in order to improve their spectra S/N although decreasing their effective spectral resolution to around 7 000. This possibility is nevertheless being reconsidered after the results of the Gaia commissioning phase.

In the RVS spectral range, one encounters in late-type star spectra weak lines of Si I, Ti I, Fe I, etc, together

with the CaII strong lines. In hotter (A-F types) star spectra appear weak lines of N I, S I, and Si I around the Ca II lines and the strong Paschen hydrogen lines. Even hotter (Teff > 15 000 K) stellar spectra contain lines of N I, Al II, Ne I, and Fe II whereas the Ca II lines start to decrease, and some He I lines appear.

The RVS will allow to measure the radial velocity of the stars in order to get their full 3D space motions when combined with the Gaia proper motions. In addition, the RVS data will be also very useful to parametrize the brightest stars observed by Gaia in complement to the parametrization performed independently from the two more sensitive low-resolution spectrophotometers (see Liu et al., 2012, for an estimate of the expected parametrisation performances with BP/RP data).

GSP-Spec estimates Teff, log g, global metallicity [M/H], alpha-element abundance [α/Fe], and some individual chemical abundances for single stars using continuum-normalized RVS spectra (i.e. each spectrum is divided by an estimate of its continuum). Source selection is based on the DSC single star probability, and GSP-Spec can optionally use the measured rotational velocities (v sin i) from CU6, as well as the the stellar parameters from GSP-Phot. As the estimation of the atmospheric parameters and individual abundances is sensitive to the pseudo-continuum normalization, GSP-spec renormalizes the RVS spectra through an iterative procedure coupled with the stellar parameters (Kordopatis et al. 2011a).

Presently, three algorithms are integrated in the GSP-Spec module: MATISSE (Recio-Blanco et al. 2006), DEGAS (Kordopatis, Recio-Blanco et al. 2011a; Bijaoui, Recio-Blanco et al. 2012), and GAUGUIN (Bijaoui, Recio-Blanco et al. 2012). As described in Chapter 2, the three methods cover three very different parametrization approaches. MATISSE is a local multi-linear regression method that determines the stellar parameters through the projection of the input spectrum on a set of vectors, calculated during a training phase. The DEGAS method is based on an oblique k-d decision tree. GAUGUIN is a local optimization method implementing a Gauss–Newton algorithm, initialized by parameters determined by GSP-Phot, DEGAS or MATISSE. In addition to these three methods, the performances of two other algorithms, FERRE (Allende-Prieto et al. 2006) and an Artificial Neural Network (Mateiga et al. 2010), have been extensively compared to those of the integrated methods. The results are presented in Recio-Blanco et al. (2014).

The algorithms perform differently in different parts of the AP and SNR space. Which results will be provided by which algorithm will be decided once we have experience with the real Gaia data, and following the first analysis (operations rehearsal #5 and cycle 0 analysis) in 2015.

5.2 Comparison of different algorithm performances for GSPspec parameterisation.

In Recio-Blanco et al. (2014), and in the framework of the GSPspec DPAC workpackage, we have analysed the performances of different parametrization algorithms that have been specifically developed or adapted for RVS spectra. We have studied their expected performances in the recovered stellar atmospheric parameters (effective temperature, surface gravity, overall metallicity) for B- to K- type stars. The performances for the determinations of the [α/Fe] ratio were also analysed for cool stars. All the results shown here correspond to the expected performances before launch. We are currently evaluating the impact of the scattered light issue detected during the commissioning, that will affect the signal-to-noise ratio at a given magnitude. Nevertheless, all the results concerning the brightest sources (around $G_{RVS} < 13$) will most probably remain unaffected.

The tested algorithms are based on optimization (FERRE, Allende-Prieto et al. 2006) and (GAUGUIN, Bijaoui et al. 2012), projection (MATISSE, Recio-Blanco et al. 2006) or pattern recognition methods (Artificial Neural Networks, Manteiga et al. 2010). The MATISSE method was coupled with the GAUGUIN algorithm for this analysis (this coupled method will be refeered as MATISSE_G hereafter). The different algorithms have been homogeneously tested with a large grid of RVS simulated synthetic spectra of BAFGK-spectral types (dwarfs and giants) with metallicities varying from $10^{-2.5}$ to $10^{+0.5}$ the Solar metallicity, and considering variations of ±0.4 dex in the composition of the α-chemical species. The tests have been performed for S/N ratios corresponding to stars having RVS filter magnitudes from about 7 to 15.

For the robustness evaluation of the tested algorithms, and to understand their optimal applicability domains, we have analysed their performances as a function of the signal to noise, stellar metallicity and surface gravity. In summary, the properties of each algorithm in its application to the RVS parameterisation are:

-The FERRE parametrization is always very satisfactory with good results for any parameters of any type of stars. Its performances are most of the time better than what is found with the other methods in the magnitude range $10<G_{RVS}<14$. However, for the faintest spectra, the performances degrade strongly leading to rather badly classified cool metal-poor dwarfs whereas the classification of late-type metal-rich giants is still acceptable.

– The $MATISSE_G$ method performs rather similarly to FERRE with satisfactory parametrisation for every situation. $MATISSE_G$ actually produces slightly better results for good quality spectra when GRVS < 10-11 but slightly worse for smaller S/N ratios. In addition, $MATISSE_G$ can sometimes produce the best estimates when the physical parameters information is low, although still not completely degraded at $G_{RVS} = 15$ (as for metal-rich cool giants and early-type stars). It clearly seems that the present version of $MATISSE_G$ (in which we assume a white Gaussian-like dominated noise) is very sensitive to the RVS noise simulated in this work, which can have strong pixel-correlations. When the noise amplitude starts to dominate the strength of the spectral signatures, the $MATISSE_G$ performances degrades very rapidly (FERRE also seems to be as sensitive). This will be improved in the near future with the development of an optimized version of $MATISSE_G$ when real RVS spectra will be available together with a precise knowledge of their noise properties.

– The ANN algorithm always provides the best results for late-type stars when $G_{RVS}=15$ with respect to those of FERRE and $MATISSE_G$. We remind that such stars will represent the largest sample collected by Gaia RVS. This capability of the ANN algorithm with respect to the other two is additionally possible to identify in the residual distributions of GK-type metal-poor dwarfs stars, at $G_{RVS} =15$. A small bias in log(g) appears in the ANN analysis, but without affecting that much the Q68 quantiles. We point out that, however, for early-type stars, $MATISSE_G$ sometimes performed better. The ANN is a bit less efficient at larger S/N ratios for every stellar parameter and type of stars.

5.3 Expected parametrization performances for Gaia RVS end-of-mission data

From the previous examination of the different parametrisation algorithms, we have derived the final (end-of-mission) GSP- Spec expected results by choosing the optimal method for each applicability domain .

– For $G_{RVS} < 14$, the mean of the FERRE and the $MATISSE_G$ solutions has been adopted as the final GSP-Spec performances. No significant differences appear between both methods.

– For $G_{RVS} \geq 14$ and FGK stars, the mean solution of FERRE, $MATISSE_G$ or ANN is chosen. No significant differences appear for metal-rich stars, while the ANN method is favoured for late-type metal-poor spectra.

– $G_{RVS} \geq 14$ and hot stars, $MATISSE_G$ solutions have been selected.

The final expected perfornances of GSPspec for dwarfs and giants of different stellar types are summarized in Table 3 and discussed below.

5.3.1 Performances for late-type stars

FGK-spectral type stars will represent the majority of the Gaia RVS targets and therefore, special attention has to be given to the GSP-Spec parametrisation capabilities of their spectra. Figures 17 and 18 illustrate the expected errors (defined as the 68% quantile of the $\Delta\theta$ distributions) for G-type dwarfs and K-type giants, respectively.

For stars with $G_{RVS} <13$, the FGK stars parametrisation is accurate enough to precisely characterize the stellar properties (typical errors are smaller than 0.1 dex in [M/H] and [α/Fe]) and, therefore, to conduct Galactic population studies as already performed from ground-based Galactic archaeology surveys (see Recio-Blanco et al., 2014a, for instance). Such accuracy in the stellar atmospheric parameters will allow, in a second step, quite accurate determinations of individual chemical abundances (see, for instance, Guiglion et al., 2014). For the faintest stars at $G_{RVS} \geq 14$, where the noise amplitude becomes too strong with respect to the available stellar spectroscopic signatures, the accuracy in the parameters estimation degrades (with metallicity errors found in the range 0.2 to 0.5 dex, for instance).

On the other hand, the dependency of the parameters accuracy on the stellar metallicity is illustrated by the clear separation of the continuous (metal-rich), dashed (metal-intermediate) and dotted (metal-poor) curves. As expected, metal-rich stars are more easily parametrized than the cool metal-poor ones whatever the S/N

Table 3: *Expected end-of-mission performances for GSPspec quantified by the 68% quantile.*

	$T_{\rm eff}$ (K)						log(g) (dex)						[M/H] (dex)						[α/Fe] (dex)					
$G_{\rm RVS}$(mag)	7	9	11	13	14	15	7	9	11	13	14	15	7	9	11	13	14	15	7	9	11	13	14	15
DWARFS																								
B metal-rich	35	89	219	606	758	1181	0.01	0.01	0.01	0.04	0.08	0.21	0.01	0.03	0.08	0.21	0.52	0.82						
B interm. met.	36	105	229	667	778	1282	0.01	0.01	0.01	0.04	0.09	0.22	0.02	0.05	0.12	0.31	0.61	0.93						
B metal-poor	42	108	236	681	792	1245	0.01	0.01	0.02	0.04	0.10	0.23	0.02	0.06	0.16	0.44	0.73	1.05						
A metal-rich	8	21	49	161	334	514	0.01	0.01	0.02	0.06	0.13	0.23	0.01	0.01	0.04	0.12	0.23	0.29						
A interm. met.	8	21	55	165	358	560	0.01	0.01	0.02	0.06	0.13	0.24	0.01	0.02	0.05	0.18	0.42	0.55						
A metal-poor	9	24	55	166	369	624	0.01	0.01	0.02	0.07	0.13	0.28	0.01	0.03	0.08	0.27	0.54	0.73						
F metal-rich	7	19	53	155	285	534	0.01	0.03	0.08	0.20	0.30	0.51	0.01	0.02	0.04	0.13	0.20	0.33	0.01	0.01	0.03	0.09	0.19	0.36
F interm. met.	10	23	63	212	315	625	0.01	0.03	0.10	0.24	0.32	0.53	0.01	0.03	0.09	0.22	0.32	0.63	0.01	0.02	0.07	0.19	0.34	0.37
F metal-poor	13	30	81	213	316	675	0.02	0.05	0.11	0.28	0.35	0.59	0.02	0.05	0.13	0.34	0.37	0.70	0.02	0.05	0.12	0.30	0.35	0.40
G metal-rich	7	19	41	157	264	611	0.02	0.05	0.12	0.33	0.42	0.53	0.01	0.01	0.04	0.13	0.21	0.32	0.01	0.01	0.03	0.10	0.21	0.31
G interm. met.	14	33	99	283	469	730	0.03	0.08	0.23	0.36	0.50	0.59	0.01	0.03	0.09	0.26	0.40	0.51	0.01	0.02	0.05	0.14	0.28	0.37
G metal-poor	23	69	167	318	517	773	0.05	0.13	0.30	0.43	0.55	0.64	0.02	0.06	0.18	0.35	0.50	0.61	0.01	0.04	0.09	0.20	0.25	0.35
K metal-rich	4	7	35	70	227	404	0.01	0.04	0.11	0.23	0.43	0.55	0.01	0.01	0.03	0.09	0.18	0.32	0.01	0.01	0.03	0.05	0.21	0.26
K interm. met.	8	16	43	118	348	485	0.02	0.05	0.12	0.26	0.50	0.61	0.01	0.02	0.04	0.10	0.23	0.45	0.01	0.01	0.04	0.09	0.22	0.26
K metal-poor	19	47	127	292	398	670	0.04	0.15	0.29	0.39	0.55	0.65	0.02	0.05	0.13	0.28	0.44	0.58	0.01	0.03	0.06	0.21	0.26	0.30
GIANTS																								
B metal-rich	11	31	62	170	579	714	0.01	0.01	0.02	0.07	0.12	0.23	0.01	0.02	0.05	0.19	0.45	0.62						
B interm. met.	13	32	72	220	620	751	0.01	0.01	0.02	0.07	0.12	0.23	0.01	0.03	0.10	0.31	0.65	0.73						
B metal-poor	16	33	82	308	652	782	0.01	0.01	0.02	0.07	0.12	0.23	0.02	0.05	0.14	0.44	0.69	0.77						
A metal-rich	7	27	52	154	332	585	0.01	0.01	0.02	0.07	0.13	0.21	0.01	0.02	0.04	0.11	0.21	0.27						
A interm. met.	9	27	54	163	363	607	0.01	0.01	0.02	0.07	0.14	0.27	0.01	0.02	0.06	0.19	0.36	0.49						
A metal-poor	11	27	57	175	373	639	0.01	0.01	0.02	0.08	0.15	0.27	0.01	0.04	0.07	0.27	0.50	0.70						
F metal-rich	5	10	29	100	212	401	0.01	0.02	0.05	0.15	0.31	0.44	0.01	0.01	0.03	0.10	0.21	0.25	0.01	0.01	0.03	0.10	0.19	0.35
F interm. met.	6	16	35	111	234	421	0.01	0.03	0.06	0.21	0.34	0.44	0.01	0.03	0.06	0.17	0.28	0.35	0.01	0.02	0.06	0.16	0.30	0.38
F metal-poor	6	17	39	113	235	446	0.01	0.04	0.07	0.21	0.36	0.64	0.02	0.05	0.15	0.34	0.32	0.38	0.02	0.05	0.14	0.29	0.39	0.36
G metal-rich	5	12	36	147	282	557	0.01	0.03	0.07	0.29	0.44	0.71	0.01	0.01	0.04	0.13	0.22	0.26	0.01	0.01	0.03	0.09	0.18	0.32
G interm. met.	10	26	75	264	404	593	0.02	0.06	0.19	0.41	0.60	0.88	0.01	0.03	0.08	0.25	0.37	0.41	0.01	0.02	0.05	0.16	0.26	0.34
G metal-poor	15	43	86	271	422	608	0.04	0.11	0.21	0.48	0.67	0.88	0.02	0.06	0.12	0.29	0.43	0.50	0.01	0.04	0.09	0.23	0.29	0.36
K metal-rich	5	11	34	102	234	377	0.02	0.04	0.12	0.33	0.58	0.86	0.01	0.01	0.04	0.10	0.19	0.27	0.01	0.01	0.02	0.06	0.14	0.28
K interm. met.	6	18	47	146	335	529	0.02	0.06	0.15	0.42	0.66	1.00	0.01	0.02	0.05	0.17	0.31	0.45	0.01	0.01	0.04	0.12	0.23	0.34
K metal-poor	13	39	104	319	459	706	0.04	0.10	0.25	0.55	0.77	1.03	0.02	0.05	0.12	0.30	0.40	0.50	0.01	0.04	0.07	0.20	0.26	0.36

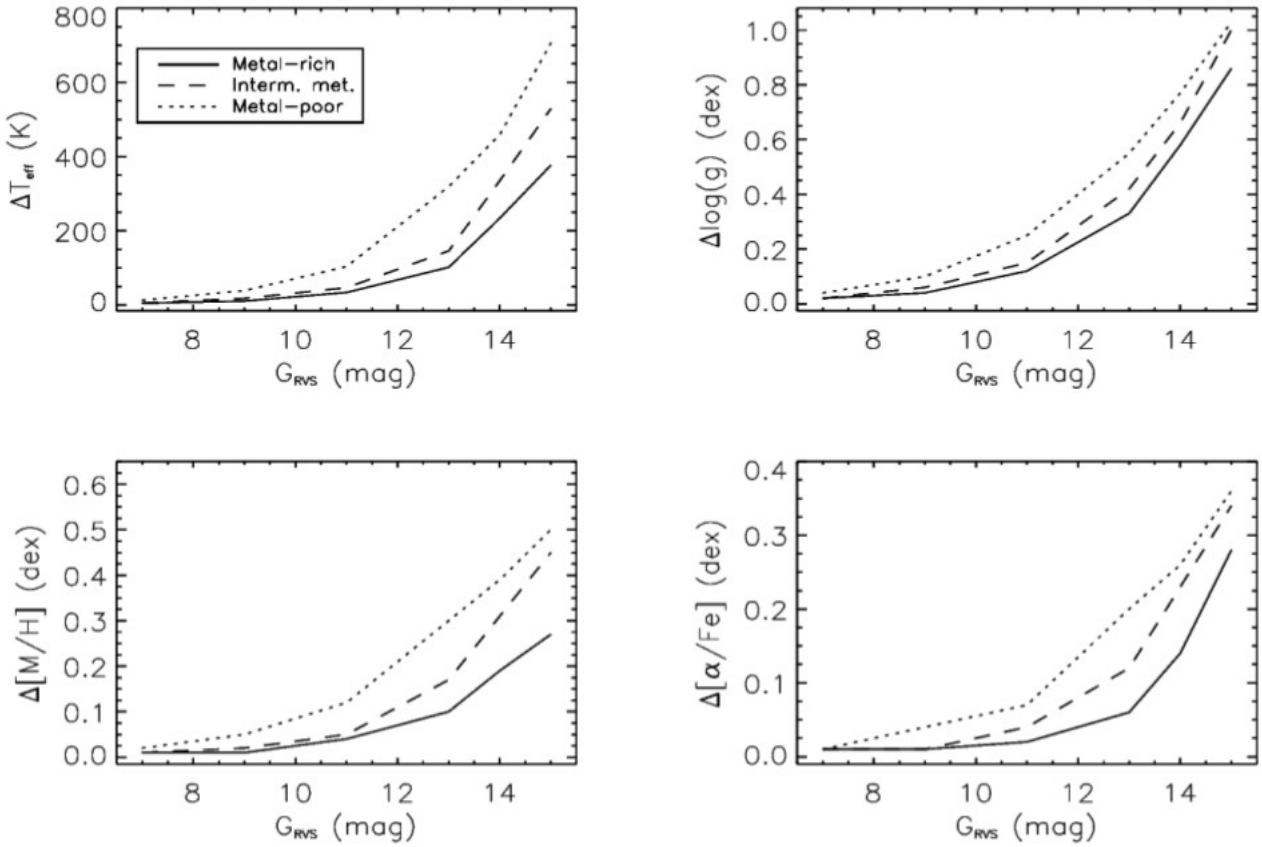


***Figure 17**: Variation of the end-of-mission GSP-Spec performances (quantified by the 68% quantile of the residuals) as a function of increasing magnitudes for the K-giant stars.*

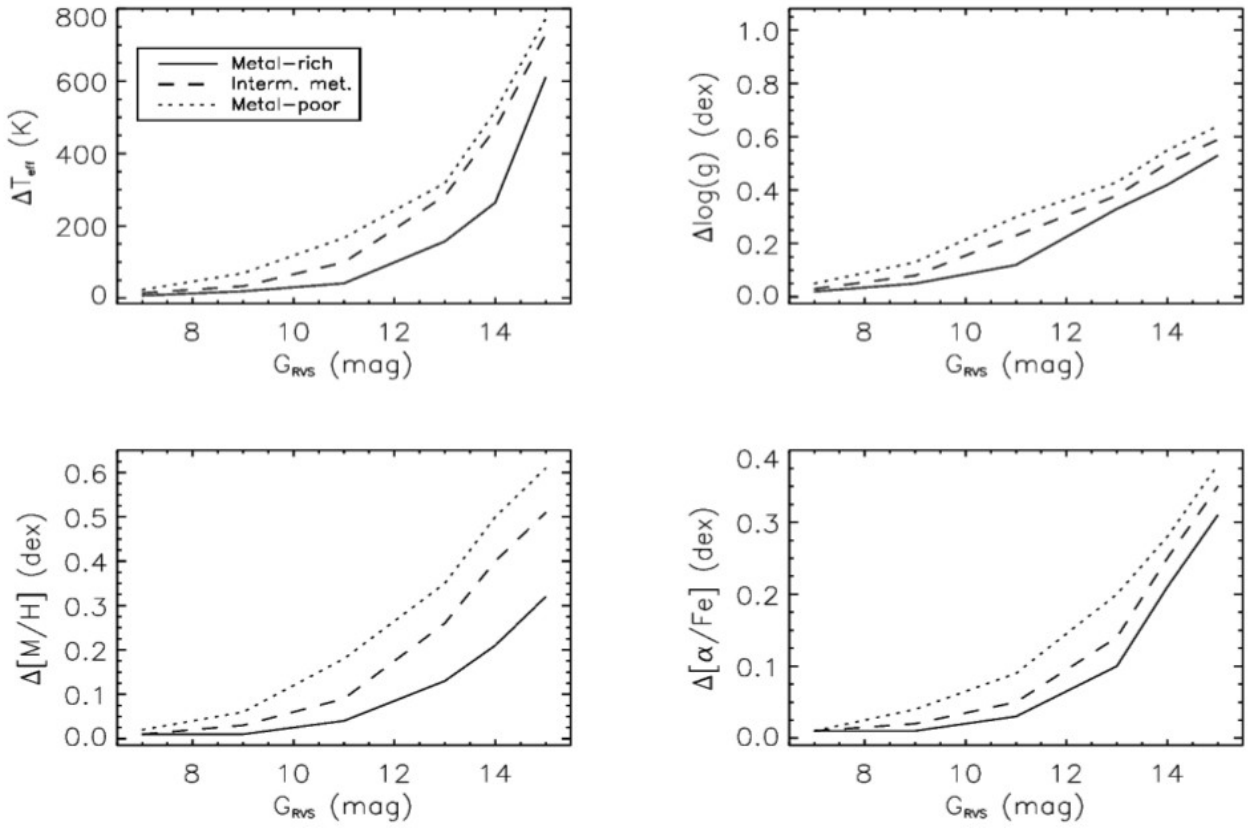


***Figure 18**: Same as Figure 17, but for G-dwarf stars*

ratios are. This is evidently caused by the number of spectroscopic signatures (lines sensitive to the atmospheric parameters and abundances) available to perform the spectral analysis, that dramatically decreases below [M/H]<-0.5 dex.

Another important physical parameter influencing the parametrization performances is the effective temperature. In the range concerning FGK-type stars (Teff approximately between 4 000 and 7 000 K), the behaviour of errors in Teff , log(g) and [M/H] shows a maximum around ~5 500 K. From that point, the errors decrease in both directions, that is for lower and higher Teff . In the first case (for cooler stars), molecular signatures start to be visible in the spectra, being more abundant as the temperature decreases. Those molecular signatures are sentitive to both Teff and log(g), as molecules formation is favoured for lower temperatures and higher gas pressure (and therefore log(g)). In the second case (for stars with Teff higher than about 6 000 K), the appearance of the hydrogen Pachen lines and their rapid change with Teff brings a precious gravity indicator that reduces the errors in log(g) and brakes the Teff-log(g) degeneracy. As a consequence, the derivation of Teff and [M/H] are also improved for those hot stars.

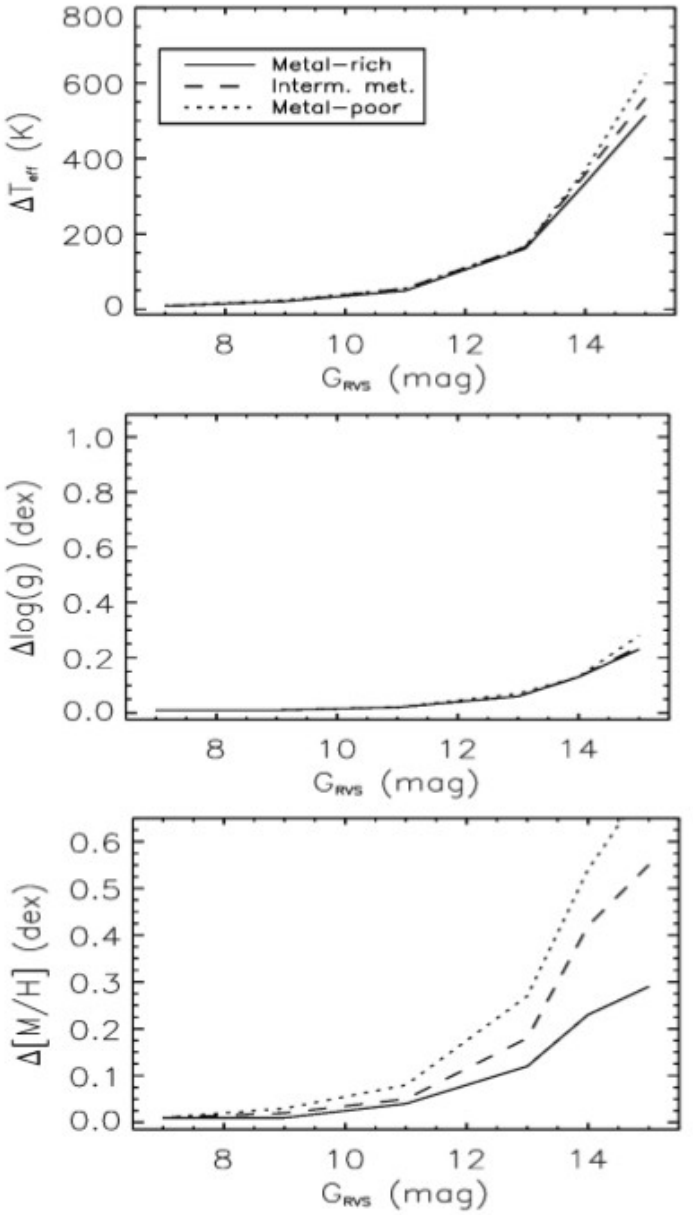


***Figure 19**: GSPspec performances for A-dwarf stars*

In summary, the Gaia RVS data of FGK-type stars will allow accurate studies of the Galactic disc and halo populations. In particular, for stars with metallicity higher than around −0.5 dex, that will be the majority of the RVS survey, the metallicity and α-enrichment estimates will be very accurate, with typical errors smaller than 0.1 dex in [α/Fe] down to G_{RVS} ~13.5 (a few tens of million of stars). In addition, K-giants will allow to perform Galactic studies up to distances of ~5 kpc (for G_{RVS} =12, and low extinction regions), or even ~13 kpc (for G_{RVS} =14).

5.3.2 Performances for early-type stars

Figure 19 shows the expected errors (defined again as the 68% quantile of the Δθ distributions) for A-type stars. As for FGK stars, three different curves are reported for each stellar parameter, illustrating the behaviour for metal-rich, metal-intermediate and metal-poor stars.

First of all, we can conclude that the parametrisation of hot stars with G_{RVS} <13, is expected to be very good (and actually excellent for the stellar surface gravity). As an example, the typical error in [M/H] for hot metal-rich stars will be smaller than 0.1 dex down to that magnitude. In fact, this results from the pressure sensitivity of the Paschen lines that is a classical luminosity indicator for early-type stars, specially for Teff >9 000 K. This comes from the pressure dependence of the Stark effect. As a consequence, thanks to this important gravity indicator, hot stars show no dependence of the gravity estimation accuracy with any atmospheric parameter. Only a small degradation with the S/N is detected. On the contrary, both the estimation of the effective temperature and the metallicity are very sensitive to Teff. In fact, the number of metallic lines drastically decreases for hot stars spectra.

Finally, even for faintest stars, the parameter accuracy is high enough to allow their classification into the main stellar classes (spectral subtypes, dwarf/subgiant/giant luminosity classes, with errors in log(g) lower than approximately 0.2 dex). The stellar metallicity is expected to be recovered with an error smaller than 0.8 dex for the faintest early-type stars (being smaller than 0.3 dex for A-type metal-rich stars). We recall that A-type dwarfs are bright stars that will allow to extend the RVS sounded volume up to distances of 5 Kpc from the Sun (for G_{RVS} =14).

5.4 Comparison with expected performances from Gaia BP/RP data.

Liu et al. (2012) reported the expected performances of stellar parameterisation from Gaia BP/RP spectrophotometry. Liu et al. (2012) analysed the results of different tested methods within the context of the DPAC/Working Group: Global Stellar Parametrizer - Photometry (GSP-Phot). Some of the end-of-mission GSP-Phot expected performances have then been recently updated in Bailer-Jones et al. (2013, see their Tab. 4). The present section discusses the comparison between the expected end-of-mission parametrisation performances between RVS (GSP-Spec) and BP/RP (GSP-Phot) data for stars brighter than $G_{RVS} < 15$. We recall that stars fainter than $G_{RVS} \sim 15$ will have only BP/RP based parameters. Although the tested random samples, the adopted statistical criteria and the detailed performances for different types of stars and magnitudes are not exactly the same in our study and in the Liu et al. (2012) or the Bailer-Jones et al. (2013) ones, a rough quantification of the expected differences can still be performed. We point out that, in the following (as in the core of all these papers), the reported uncertainties in the recovered stellar atmospheric parameters refer to internal errors only, i.e. relative star-to-star uncertainties.

For the purpose of this GSP-Phot and GSP-Spec comparison, we adopted the relationship between the G-band (Gaia white light) and G_{RVS} magnitudes provided by Jordi et al. (2010) together with the photometric colours – Teff transformations of Ramírez & Meléndez (2005). It is then found that the G_{RVS} magitude is brighter than the G-band one of about 0.5 mag for A- type stars, of 0.6 to 0.7 mag for F-type stars (with the magnitude range reporting the metallicity effect from metal-poor to metal-rich stars), of 0.8 to 1.0 mag for G-type stars and of 1.2 to 1.4 mag for the K spectral type. The variation between cool giants and cool dwarf stars is weak and has been neglected.

First, the study of Liu et al. (2012) reveals that the GSP-Phot stellar parametrisation is performed with almost the same efficiency as long as G < 15 and starts to degrade for fainter stars, only. This is also confirmed by the Tab.4 of Bailer-Jones et al. (2013) in which the performances at G=9 and G=15 are almost identical. On the contrary, the GSP-Spec parametrization degrades earlier, for G_{RVS} fainter than ~11 or 12 mag, depending on the metallicity.

By comparing our Tab. 3 and the Tab.4 of Bailer-Jones et al. (2013), the following performance differences can be deduced:

– Bright dwarf and giant A-type stars ($G_{RVS} < 13$) should be always better parametrized in Teff , log(g) and [M/H] from their RVS spectra. We recall that very good surface gravities and global metallicities (with an accuracy better than 0.1 dex) will be available for such type of stars from their GSP-Spec parametrisation. For A-stars fainter than $G_{RVS} \sim 13$, although log(g) and [M/H] are still better estimated from their RVS spectra, the effective temperature derived from BP/RP data should be more accurate.

– The GSP-Spec effective temperature of F-type stars should be favoured for $G_{RVS} < 13$ (dwarfs) and 14 (giants). Their GSP-Spec surface gravity and global metallicity should also be adopted as long as $G_{RVS} < 14$. Their accuracy should be better than 0.1 dex when $G_{RVS} < 12$.

– GSP-Spec stellar parameters of GK-spectral type stars should be adopted as long as $G_{RVS} < 12$-13.

– The global [α/Fe] chemical index will be estimated from the GSP-Spec pipeline only for FGK-spectral type stars. Uncertainties of the order of 0.1 dex (or even smaller) are expected as long as $G_{RVS} < 13$.

In summary, it can be concluded that, for all the considered stellar types, the stars brighter than $G_{RVS} \sim 13$ will be very efficiently parametrized by the GSP-Spec pipeline, including good estimations of the [α/Fe] chemical index. From these stellar atmospheric parameters, individual chemical abundances (such as Fe, Ca, Ti, Si,...) will be derived with an expected uncertainty smaller than 0.1 dex for most of the RVS sample with about GRVS < 12, i.e. for a few millions of targets. For faintest stars that are better parametrised from their BP/RP photometry, a Teff input from GSP-Phot as an initial condition for GSP-Spec will allow the

improvement of its final log(g), [M/H] and [α/Fe] estimates. Such a GSP-Phot/GSP-Spec link is already implemented in the Apsis processing system developed by the CU8 and combined performance tests are being implemented.

Finally, it can also be stressed that the spectral parametrisation for extincted stars should be easier with the GSP-Spec pipeline since a Teff-extinction degeneracy appears in the parametrisation of BP/RP low-resolution spectra with too large line-of-sight interstellar extinction (assuming that their brightness in the RVS band is not too faint to collect high enough S/N spectra). In those cases, a feedback from GSP-Spec to GSP-Phot, in a second iteration of the analysis cycle, will also improve the final parameters estimations.

5.5 Expected scientific impact of the Gaia GSPspec parameterisation results

The errors in the recovered stellar atmospheric parameters reported here permit to clearly identify, and quantify in detail, the enormous variety of science cases that will be obtained from the interpretation of pure *Gaia* data (without any need of references to external catalogues). We stress, on the other hand, that the above reported uncertainties refer to internal errors only, i.e. relative star-to-star uncertainties, and pre-launch RVS properties. Total errors will be, in many cases, dominated by external ones (partly caused by the possible synthetic spectra mismatches with respect to real observed ones) and they will be estimated from the analysis of real Gaia RVS spectra of benchmark reference stars, during a results validation phase. In addition, the *GSP-Spec* pipeline will be optimised in the light of the first analysed real RVS spectra over the next two years (we recall for instance the possibility of keeping the same nominal resolution of ~11200 for all the RVS targeted magnitude range, that could slightly change our performance predictions).

The final version of the Apsis *GSP-Spec* module is expected to be delivered for operations around mid-2016. It will be running in operations cycle 4 in 2017, with a possible contribution to the third *Gaia* data release. The current *GSP-Spec* version, integrated in the general Apsis chain, already meets the tight requirements in processing speed (17 Mflops per source), needed to repeatedly treat tens of million of spectra.

The contribution of the RVS based stellar parameters will be unique for stars with G_{RVS} <13 (a few tens of millions of stars). On the one hand, the GSP-Spec parameters will be more accurate than the majority of the parameters derived from the spectrophotometry in that magnitude range. This will allow, thanks to the use of the Gaia parallaxes, a better estimation of the stellar evolution phase and, as a consequence, of the isochrone based age estimations (for which the effective temperature accuracy is a dominant source of error). Accurate stellar ages will be one of the revolutions in Milky Way astrophysics that the Gaia mission will accomplish, and the RVS data will strongly contribute to it, sharpening our view of the Galactic history in a volume of very precise measurements (up to ~8 kpc from the Sun for K-giants and ~1 kpc for G-dwarfs).

On the other hand, accurate metallicity and chemical abundance measurements as the [α/Fe] content are today recognised as crucial information for the understanding of the highly complex evolution of Galactic stellar populations. As an example, the classical kinematically-based definitions of the thin and the thick disc populations blurred our comprehension of the Galactic disc substructure (c.f. Bovy et al., 2012; Recio-Blanco et al., 2014). The RVS chemical abundance estimations, with accuracies better than 0.1 dex, will therefore be a unique and precious sample of several millions of stars for which many pieces of the Milky Way history puzzle will be available, with unprecedented precision and statistical relevance.

Chapter 6

CONCLUSIONS AND PERSPECTIVES

The study of the Galactic stellar populations, started by W. Baade in 1944, is now at the dawn of a revolution. Although remarkable progresses have been achieved in the last 70 years, many crucial questions, intimately linked to our comprehension of the formation and evolution of disc galaxies remain still opened. Moreover, the Milky Way has today to be understood in coherence with its cosmological framework, including the expansion and large scale distribution of galaxies, the evidences motivating dark matter and dark energy, etc... As a consequence, Galactic archaeology studies are now also addressing general questions like our comprehension of the galaxies characteristics in a ΛCDM paradigm, what determines that a galaxy has a given type (e.g. a barred disc-type with a central bulge), or what are the dominant physical processes (external vs. internal; fast vs. secular) in a galaxy formation and evolution. More particularly, these questions are linked to precise unveiled points of the Milky Way populations (Rix & Bovy 2013) like: what processes set the exponential radial and vertical profiles seen in the stellar distributions of the Galactic disc? Was some fraction of disc stars formed from very turbulent gas early on forming a primordial thick disk? How much did in-falling satellites impulsively heat the disc? What is the contribution of the Galaxy secular evolution to the disc (e.g. by radial migration) and bulge formation (e.g. vertical resonances with the bar), etc... In addition, to address the above mentioned points that *we would like to understand*, we still need to unveil several physical properties of the Milky Way that *we would like to know*.

The work presented in this report carries the imprint, at my modest scale, of the state and evolution of the Galactic archaeology observational context over the last years, with its progresses and its still opened questions. It describes my main contributions to the development of new automated spectrum analysis techniques (chapter 2), to the scientific results about the chemo-dynamical properties of the disc (chapter 3) and the bulge (chapter 4) and their implications for their formation scenarios, and finally, to the Gaia mission activities on spectroscopic stellar parametrisation (chapter 5).

Nevertheless, the constraints at our disposal are still insufficient. Three-dimensional distributions and 3D stellar velocities are only available for relatively small samples, mostly in the Solar neighbourhood. In addition, stellar ages are, in practice, impossible to derive for most of the survey targets, due to imprecise distance estimations. As a consequence, the temporal dimension, so crucial to the understanding of the Milky Way history and for comparison with model predictions, is not available.

But fortunately the situation is evolving quickly. As a way of example, Table 4 shows the evolution of the estimated errors in distances, ages (when available), effective temperature (if used for age estimation) and α-element abundances with respect to to iron, for two characteristic magnitude ranges around V~13.5 (10 million stars) and V~16.5 (150 million stars) with Gaia data. The availability of only GES data, Gaia data only and a combination of Gaia and GES data is considered.

	Now-2016			**2016-2018**								
	GES			**Gaia only**					**Gaia+GES**			
Vmag	σdistance	σage	σ[α/Fe]	σdistance	σteff (RVS)	σteff (BPRP)	σage	σ[α/Fe]	σdistance (Gaia)	σteff (GES)	σage	σ[α/Fe] (GES)
13-14	~20%	-	0.05dex	1%	100 K	150 K	~5%	0.10dex	1%	50 K	~3%	0.05dex
16-17	~35%	-	0.05dex	10%	-	250 K	~25%	-	10%	50 K	~15%	0.05dex

Table 4. *Estimated errors in distances, ages, effective temperatures and α-element abundances with respect to iron for two characteristic magnitude ranges.*

The impact of precise Gaia astrometric distances is evident from Table 4, allowing among other things, the

possibility of age estimations. In addition, the combination with a high resolution spectroscopic survey like GES permits (i) to have high precision chemical abundances for faint stars and (ii) to enhance the precision in the age estimation for those stars thanks to more accurate effective temperature estimations.

We are thus entering now a new era of Galactic investigation that will revolutionise our knowledge of the galaxy in which we live. This Gaia era is the context in which my research activities will be developed in the next years.

6.1 The ARCHEOGAL project: The Milky Way disc formation in the Gaia era

My planned activities for the near future are included in the ANR ARCHEOGAL project that I have defined. Thanks to the complementary scientific exploitation of GES and Gaia, I aim to contribute to the building up of an extensive and homogeneous time evolving chemo-dynamical picture of the Milky Way disc. To this purpose, my project activities, organised following the GES and Gaia data releases, will analyse the disc physical properties, linking them to the processes that led the Milky Way to form and evolve as a disc-type galaxy, in the more general context of galaxy evolution. In particular, the main points of the project work program are centred on:

1) The GES stellar spectra parameterisation and the scientific validation of the Gaia/RVS stellar parameters.
2) From GES and Gaia chemical element abundances, the analysis of the disc chemical substructures.
3) From GES spectro-photometric distances, followed by Gaia astrometric data, the study of the structural properties of chemically defined disc populations.
4) Thanks to GES+Gaia radial velocities and Gaia proper motions, the analysis of existent chemo-kinematical and chemo-dynamical correlations.
5) From combined Gaia+GES data, the estimation of precise stellar ages and the reconstruction of chemo-dynamical temporal gradients, to be compared with present scenarios of disc formation.

Several points will be particularly treated to achieve the above mentioned goals:

Accounting for survey selection functions

The analysis and conclusions of the chemo-dynamical and structural properties of Galactic stellar populations strongly depend on the careful characterisation of the selection functions. Various selection cuts (e.g. in colours, magnitudes, or even Teff and log g) reduce the relative number of observed stars with certain properties. In order to quantify in detail the selection effects, specific analysis tools have to be developed (e.g. Bergemann et al. 2014). Moreover, the selection cuts can be directly applied to stellar population synthesis models such as the Besançon model (Robin et al. 2003) or the Trilegal model (Girardi et al. 2005). These models aim to reproduce, for each line of sight, the observed properties such as stellar parameters, colours, magnitudes, radial velocities, etc. for each Galactic component, assuming their initial mass functions, star formation rates, metallicity distributions, density laws, etc.. These hypothesis can be also constrained, in turn, thanks to GES and Gaia.

Therefore, in the near future the work concerning the selection functions characterisation will be one of the main points that I plan to develop.

Stellar ages

Dating the processes that led the Milky Way to form and evolve as we see it today is certainly one of the major goals of Galactic archaeology. At present, the majority of the stellar ages derived for relatively large samples of field stars rely on the isochrone fitting method. This is of course very sensitive to the stellar distance estimations that dominate the error. As a consequence, precise stellar ages (with the exception of particular cases as globular and open clusters, eclipsing binaries,...) are today mostly confined to the Solar Neighbourhood. They are limited to either stars with Hipparcos parallaxes (Haywood et al. 2013) or small samples with very high resolution data (as the GES UVES spectra up to 1-2 kpc from the Sun, with errors smaller than 30%, Bergemann et al. 2014). In the majority of the cases, the temporal gradients are studied through parameters that act as a proxy of age, like the [α/Fe] abundance (Minchev et al. 2014, Recio-Blanco et al. 2014a). The possibility of determining precise stellar ages for very important samples of stars (about

10-15 millions of stars) will be a strong qualitative and quantitative change.

The "sphere" of very precise ages will contain about 10 millions of stars, down to magnitude V=14-15 (c.f. Haywood et al. 2009). In this volume of stars with Gaia distances to 1%, the errors in the ages will be of the order of 250 million years for a G-type subgiant star (~5% for a thin disc star and ~2% for a thick disc one). This sphere of precise ages will reach a distance of around 1.5-2 kpc from the Sun. The Gaia atmospheric parameters should be precise enough in this volume, with eventually improvements from very high resolution spectroscopy, as the GES UVES data (10 000 stars).

In a more extended sphere, with distances to 10% there will be around 150 millions of stars down to V=16-17. For these stars, and relying on Gaia data alone, the errors on the ages will be of around 1 Gyr for a G-type subgiant star (that means ~20% for a thin disc star, and ~30% for a thick disc one). The corresponding sounded distances will reach 3 kpc from the Sun (Galactocentric radii from ~5 to 11 kpc). In addition, as described above, the age precision will be improved thanks to the ground-based GES spectroscopic parameters for around 10^5 stars, as the degradation in the error is dominated by the precision in the effective temperature.

In the following years, I aim to i) develope the necessary tools for the derivation of stellar ages and ii) analyse the time-evolution of the chemo-dynamical characteristics of the Milky Way populations in the light of their formation scenarios.

The Galactic Bulge

The new GES data releases include many new observations of the Galactic bulge. Following the work of Rojas-Arriagada et al. (2014), we will continue the exploration of the bulge stellar population properties, including individual abundances. In addition, the evolutionary link between the bulge stellar populations and the disc and/or the halo ones will be also carefully studied, thanks to a robust homogeneus treatment of the GES data.

Comparison with model predictions

Different aspects of the observational analysis included in the ARCHEOGAL project will be carefully compared to model predictions. In particular, the interaction with research groups dedicated to disc formation models, chemical evolution models and chemo-dynamical models and simulations will be essential.

Comparison with disc formation and chemical evolution models.

On one hand, the identified substructures in the observed chemical patterns will be examined in the light of predictions from chemical evolution models (eg. Chiappini et al. 1997, 2003; Romano et al. 2010). From these comparisons, insight can be gained both on the timescales of disc(s) formation as well as detailed constraints on the astrophysical sites responsible for the synthesis of elements (eg. North et al. 2012). On the other hand, the presence of chemical substructures in the disc is a key diagnostic to identify environmental evolutionary processes like accretion of stars or gas. In particular, accreted stars from satellite galaxies would have different ratios of chemical element abundances than those of the Milky Way stars formed in situ (Tolstoy, Hill & Tosi, 2009) as they come from populations with different chemical enrichment histories. Their identification is therefore crucial for our understanding of the role of mergers in the building up of the disc.

In addition, the study of thin disc gradients, scale-lengths and heights can provide strong evidences to the mechanisms of Galaxy formation (e.g. Chiappini et al. 1997; Alibés et al. 2001; Cescutti et al. 2007). In particular, the inside-out disc formation (c.f. Matteucci & François, 1989) or the outside-in disc evolution (Haywood et al. 2013) can be tested. Moreover, the dynamical heating of a primary disc by a violent merger (eg. Kazantzidis et al., 2008; Villalobos & Helmi, 2008; Qu et al., 2011) of a smaller satellite can heat the stars into thick disc like scale-heights. If vertical chemical gradients were present in the primary disc, they would be preserved (Bekki & Tsujimoto, 2011). Furthermore, radial migration processes studied by Schönrich & Binney (2009a,b) examine the continuous radial and vertical re-arragement (radial mixing via blurring and churning) by triggered spiral-arms and molecular clouds. The metal-poorer and older stars are more affected by heating and achieve higher $|Z|$, thus producing negative metallicity and small positive α-enrichment gradients. Moreover, numerical simuations (Qu et al. 2011) have revealed that the increase of the

scale-height in the outer regions of the Galactic thick disk could inform us about the total accreted mass by minor mergers. As a consequence, the absence of such variations would be in agreement with the model of Bournaud et al. (2009) in which the thick disk would have been formed by the star and gas dispersions caused by the inhomogeneities of the initial thin disc.

Comparison with chemo-dynamical models

The arrival of Gaia data will allow an important improvement of the kinematical and dynamical constraints to the models, that are hampered today by important distance errors, cumulated and propagated in all the derived physical parameters needed for the stellar orbits estimations.

In particular, the precise estimation of the correlation between rotational velocity and metallicity can constrain the degree of radial migration in the disc. In fact, in the presence of strong radial migration processes, no or only a very small correlation is expected in the transition region between the thin and the thick disc, because the older stars that compose the thick disc should have been radially well mixed.

In addition, it is today widely accepted that the shape of the eccentricity distribution of the stellar orbits can provide important constraints on the formation mechanisms of the Galactic disc (Sales et al., 2009, Di Matteo et al. 2011). In general, stars formed in situ are expected to have low-eccentricity orbits, while accreted stars from satellites always dominate the high-eccentricity tails of the distributions. Therefore, changes in the relative proportion of in situ versus accreted stars drive the differences seen in the predicted histograms of each thick disc formation scenario. In other words, the analysis of the stellar eccentricities off the plane helps to unravel whether the bulk of stars was formed locally in the main progenitor (heating, migration, merger) or, on the contrary, was accreted from infalling satellites (accretion).

Finally, constraints on stellar ages are precious information for disc formation and evolution models. Stellar ages are naturally an output of disc models and chemo-dynamical simulations, but we are lacking today of robust and extensive observational data for comparison. Some classical examples can be mentioned here. The age-metallicity relation will pose constraints on the degree of accreted gas, triggering new star formation, and/or accreted stars. In addition, its combined study with the presence of radial and vertical chemical abundance gradients will also constrain the models of inside-out formation of the disc, or, eventually, outside-in formation scenarios. In addition, the age-velocity dispersion relation can constrain the processes which change the velocities of initially slow-moving young stars into ‘hotter’, higher dispersion orbits. In particular, what was the role of internal heating? Is the radial migration induced by satellite infall (Bird et al. 2012) distinguishable from pure internal processes? Minchev et al. (2013b) interpreted the [Mg/Fe]-velocity dispersion relation found in the RAVE data as perturbations from massive mergers in the early universe, which have affected the outer parts of the disc more strongly, and the subsequent radial migration of stars with cooler kinematics from the inner disc. The Minchev et al. results also suggest that the Milky Way disc merger history can be recovered by relating the observed time evolution of the chemo–kinematical relations to the properties of past merger events. In addition, one of the strong predictions of the Minchev et al. (2013a) model that could be tested is that the chemical abundance gradients of mono-age populations are independent of the distance to the Galactic plane. Finally, the observed variations in the abundance patterns as a function of age can be reproduced with a chemical evolution model to infer the Galactic star formation history (Snaith et al. 2014, and Fig. 13).

6.2 The Gaia GSPspec activities

In Recio-Blanco et al. (2014b), after having analysed the results of different independent methods, we have estimated the end-of-mission expected parametrization performances of the Gaia DPAC pipeline (GSP-Spec) in charge of the RVS stellar spectra atmospheric parameters and chemical abundances derivation. The reported uncertainties in the recovered stellar atmospheric parameters refer to internal errors only, i.e. relative star- to-star uncertainties. The GSP-Spec pipeline will be optimised in the light of the first analysed real RVS spectra over the next two years. In particular, the different parameterization algorithms are very sensitive to the noise nature. The existence of a highly correlated noise would imply the partial modification of the mathematical basis of some algorithms.

Once GSPspec will be optimised for real RVS data, the final version of the Apsis GSP-Spec module is expected to be delivered for operations around mid-2016. It will be running in operations cycle 4 in 2017,

with a possible contribution to the third Gaia data release.

Finally, we have already started to organise the scientific validation of the GSPspec outputs. As described in Kordopatis, Recio-Blanco & Ordenovic (2014), an internal and a external validation phases are foreseen. In addition, a cross-validation considering the coherence with the spectrophotometric parameters will also be implemented. Our experience with the scientific validation of GES data will help in the implementation of validation and calibration procedures for the Gaia data.

6.3 Long term perspectives

Several projects and instruments like WHT/WEAVE, VISTA/4MOST, VLT/MOONS, ELT+HIRES/MOSAIC and MSE will complement the Gaia data either in the faint magnitudes (where radial velocities will not be available) or in the detailed individual chemical abundances. In particular, I am already involved in two of these future projects: WEAVE and MSE.

WEAVE will have a 2º-diameter-wide field, 1000-fibre multi-object spectroscopy (MOS) mode and two spectral resolution modes, R=5000 for the radial velocity survey and R=20000 for the chemical composition survey. WEAVE will concentrate on surveys to elucidate the formation and evolution processes of the outer halo and disk(s), best observed from the Northern Hemisphere. Located in the Southern Hemisphere, 4MOST will pursue studies of the inner halo and disk and the bulge-disk transition. The Galactic halo is large and diffuse, and therefore a wide-field survey is required to fully characterize its chemo-dynamical properties that record crucial information on the early history of our Galaxy.

On the other hand, the "next generation CFHT" – now named the Maunakea Spectroscopic Explorer (MSE) – will upgrade the current 3.6 m telescope to a 10 m dedicated wide field spectroscopic telescope. With a field of view of ~1.5 degrees in which up to ~3200 separate objects could be observed simultaneously at spectral resolutions ranging from ~2,000 – 20,000. One of the three working groups composing the MSE Science Team is dedicated to the Milky Way and resolved stellar populations and I am already one of its members.

Finally, with the start of operations planned for the next decade, the E-ELT will have an enormous impact on many different areas of research, among which Galactic Archaeology. In particular, a multi-object spectrograph, E-ELT-MOS, will allow spectroscopic studies of resolved stellar populations from the dense regions of the Bulge (reaching main sequence stars) until the galaxies of the Local Group. At the era of the final Gaia catalogue and results, the roads and challenges of Galactic Archaeology will have to be redefined.

Bibliography

Abadi et al., 2003, ApJ 591, 499
Abia, Recio-Blanco et al. 2009, A&A, 694, 971
Adibekyan et al., 2012, A&A, 545, A32
Adibekyan et al., 2013, A&A, 554, A44
Alibés et al. 2001, A&A, 370, 1103
Alibés, A., Labay, J., & Canal, R. 2001a, arXiv:0107016
Alvarez & Plez, 1998, A&A, 330, 1109
Allende Prieto, C., Beers, T. C., Wilhelm, R., et al. 2006, ApJ, 636, 804
Anders, F., Chiappini, C., Santiago, B. X., et al. 2013, arXiv:1311.4549
Andreuzzi, G., Bragaglia, A., Tosi, M., & Marconi, G. 2011, MNRAS, 412, 1265
Andrievsky, S. M., Kovtyukh, V. V., Luck, R. E., et al. 2002, A&A, 381, 32
Andrievsky, S. M., Spite, M., Korotin, S. A., et al. 2008, A&A, 481, 481
Athanassoula, E. 2003, MNRAS, 341, 1179
Athanassoula, E. 2005, MNRAS, 358, 1477
Baade, W., 1944, ApJ 100, 137
Babusiaux, C., Gómez, A., Hill, V., et al. 2010, A&A, 519, A77
Babusiaux, C., Katz, D., Hill, V., et al. 2014, ArXiv e-prints
Bailer-Jones et al, 2013, A&A 559, 74
Baumueller, D. & Gehren, T. 1997, A&A, 325, 1088
Bekki & Tsujimoto, 2011, ApJ, 738, 4
Bensby et al., 2005, A&A, 433, 185
Bensby et al., 2007, ApJ, 663, L13
Bensby & Feltzing, 2010, in IAU Symp., 265, 300
Bensby, T., Adén, D., Meléndez, J., et al. 2011, A&A, 533, A134
Bensby, T., Yee, J. C., Feltzing, S., et al. 2013, A&A, 549, A147
Bensby et al., 2014, A&A, 562, A71
Bergemann, M. 2011, MNRAS, 413, 2184
Bergemann, M., Kudritzki, R.-P., Wu ̈rl, M., et al. 2013, ApJ, 764, 115
Bergemann et al., 2014, A&A, 565, 89
Bijaoui et al., 2012, Statistical Methodology, vol. 9, p.55
Bijaoui et al., 2013, EAS Pub. Ser., 59, 265
Bilir et al., 2012, MNRAS, 421, 3362
Binney, 2010, MNRAS, 401, 2318
Binney, 2012, MNRAS, 426, 1328
Binney & McMillan, 2013, MNRAS 413, 1889
Bird et al. 2013, ApJ, 773, 43
Blanco-Cuaresma et al. 2014, A&A 566, 98
Blanco-Cuaresma et al. 2014, A&A, 569, 111
Boeche, C., Siebert, A., Williams, M. et al. 2011, AJ, 142, 193
Boeche et al., 2013, A&A, 553, A19
Bonifacio, P., Caffau, E. 2003, A&A, 399, 1183
Bournaud et al., 2009, ApJ 707, L1
Bovy et al. 2012a, ApJ 751, 131
Bovy et al. 2012b, ApJ 755, 148
Bovy et al. 2012c, ApJ 759, 131
Brook et al. 2004, ApJ, 612, 894
Brook et al. 2007, ApJ, 658, 60
Bureau, M., Aronica, G., Athanassoula, E., et al. 2006, MNRAS, 370, 753
Cabrera-Lavers, A., Garzo ́n, F., & Hammersley, P. L. 2005, A&A, 433, 173
Carretta, Recio-Blanco et al. 2007, ApJ, 671, 125
Carretta et al. 2010, A&A, 516, 55
Carretta, E., Gratton, R. G., Bragaglia, A., D'Orazi, V., & Lucatello, S. 2013, A&A, 550, A34
Carollo et al. 2010, ApJ, 712, 692
Casagrande et al. 2011, A&A 530, 138
Casetti-Dinescu et al., 2011, ApJ, 728, 7
Cescutti et al. 2007, A&A, 462, 943
Cheng et al., 2012, ApJ, 752, 51
Chiappini et al. 1997, ApJ, 477, 765
Chiappini et al., 2001, ApJ 554, 1044
Chiappini et al., 2003, A&A 410, 257
Combes, F., 2009, ASPC 419, 31

Combes, F., 2014, A&A, 571, 82
CosçkunoğLu et al., 2012, MNRAS, 419, 2844
de Bruijne, J. H. J. 2012, Ap&SS, 341, 31
de Laverny et al. 2012, A&A, 544, A126
de Laverny et al. 2013, The Messenger 153, 18
de Laverny & Recio-Blanco, 2013a, A&A, 555, 121
de Laverny & Recio-Blanco, 2013b, A&A 560, 74
De Pascale et al., A&A, 570, 68
Di Matteo et al., 2011, A&A, 525, L3
Di Matteo et al., 2013, A&A, 553, 102
Di Matteo et al., 2014, A&A, 567, 122
Edvardson et al. 1993, A&A, 275, 101
Eggen, n, O. J., Lynden-Bell, D., & Sandage, A. R. 1962,ApJ, 136, 748
Eisenstein et al., 2011, AJ 142, 72
Falcón-Barroso, J., Bacon, R., Bureau, M., et al. 2004, Astronomische Nachrichten, 325, 92
Feltzing et al., 2001, A&A, 377, 911
Fraternali & Binney, 2008, MNRAS 386, 935
Freeman & Bland-Hawthorn, 2002, ARA&A, 40, 487
Frinchaboy, P. M., Thompson, B., Jackson, K. M., et al. 2013, ApJ, 777, L1
Fuhrmann, 1998, A&A, 338, 161
Fuhrmann, 2004, Astronomische Nachrichten, 325, 3
Fuhrmann, 2008, MNRAS, 384, 173
Fuhrmann, 2011, MNRAS, 414, 2893
Fukugita, M., Hogan, C. J., & Peebles, P. J. E. 1998, ApJ, 503, 518
Fux, R. 1999, A&A, 345, 787
Gazzano et al., 2010, A&A 523, 91
Gazzano, J.-C., Kordopatis, G., Deleuil, M. et al. 2013, A&A, 550, A125
Gehren,T.,Liang,Y.C.,Shi,J.R.,Zhang,H.W.,&Zhao,G.2004,A&A,413, 1045
Gehren, T., Shi, J. R., Zhang, H. W., Zhao, G., & Korn, A. J. 2006, A&A, 451, 1065
Guédé et al. 2012, Sf2A-2012 Conf. Proceedins, p.195
Gilmore & Reid, 1983, MNRAS, 202, 1025
Gilmore et al., 2012, The Messenger 147, 25
Girardi et al., 2005, A&A, 436, 895
Guiglion, G., Recio-Blanco, A., & de Laverny, P. 2014, in IAU Symposium, Vol. 298, IAU Symposium, ed. S. Feltzing, G. Zhao, N. A. Walton, & P. Whitelock, 408–408
Guiglion et al. 2014, A&A, to be sumitted
Gonzalez, O. A., Rejkuba, M., Zoccali, M., et al. 2011a, A&A, 530, A54
Gonzalez, O. A., Rejkuba, M., Zoccali, M., et al. 2013, A&A, 552, A110
Gonzalez, O. A., Rejkuba, M., Zoccali, M., Valenti, E., & Minniti, D. 2011b, A&A, 534, A3
Gustafsson et al., 2008, A&A, 486, 951
Harris, W. E. 1996, AJ, 112, 1487
Hayden et al. 2014, AJ, 147, 116
Haywood et al. 2008, MNRAS, 388, 1175
Haywood et al. 2009, ApJ, 698, L1
Haywood et al., 2013,A&A, 560, A109
Heiter, U., Soubiran, C., Netopil, M., & Paunzen, E. 2014, A&A, 561, A93
Helmi et al., 2011, ApJ 733, L7
Hill, V., Lecureur, A., Gómez, A., et al. 2011, A&A, 534, A80
Howard, C. D., Rich, R. M., Reitzel, D. B., et al. 2008, ApJ, 688, 1060
Immeli, A., Samland, M., Gerhard, O., & Westera, P. 2004, A&A, 413, 547
Ishigaki, M. N., Aoki, W., & Chiba, M. 2013, ApJ, 771, 67
Ivezic', Z˘.,Sesar, B.,Juric´, M.,et al.2008,ApJ,684,287
Jacobson, H. R., Friel, E. D., & Pilachowski, C. A. 2009, AJ, 137, 4753
Jordi, C., Gebran, M., Carrasco, J. M., et al. 2010, A&A, 523, A48
Jofre, P., Heiter, U., Soubiran, C., et al. 2013, ArXiv e-prints
Jones & Wyse, 1983, MNRAS, 205, 983
Juric et al. 2008, ApJ, 673, 864
Kazantzidis et al., 2008, ApJ, 688, 254
Koleva, M., Prugniel, P., Bouchard, A. et al. 2009, A&A, 501, 1269
Kordopatis et al. 2011a, A&A, 535, A107
Kordopatis et al. 2011b, A&A, 535, A107
Kordopatis et al., 2013, AJ, 146, 134
Kormendy & Kennicutt 2004, ARA&A, 42, 603
Larson, R. B. 1974, MNRAS, 166, 585

Lee et al., 2011a, AJ, 141, 90
Lee et al., 2011b, ApJ, 738, 187
Lemasle, B., Franc ̧ois, P., Genovali, K., et al. 2013, A&A, 558, A31
Lemasle, B., Franc ̧ois, P., Piersimoni, A., et al. 2008, A&A, 490, 613
Liu & van de Ven, 2012, MNRAS, 425, 2144
Liu, C., Bailer-Jones, C. A. L., Sordo, R., et al. 2012, MNRAS, 426, 2463
Loebman et al., 2011, ApJ, 737, L8
López-Corredoira, M., Cabrera-Lavers, A., & Gerhard, O. E. 2005, A&A, 439, 107
Luck, R. E. & Lambert, D. L. 2011, AJ, 142, 136
Magrini, L., Randich, S., Romano, D., et al. 2014, A&A, 563, A44
Magrini, L., Sestito, P., Randich, S., & Galli, D. 2009, A&A, 494, 95
Manteiga, M., Ordo ́n ̃ez, D., Dafonte, C., & Arcay, B. 2010, PASP, 122, 608
Martinez-Valpuesta, I. & Gerhard, O. 2013, ApJ, 766, L3
Martinez-Valpuesta, I., Shlosman, I., & Heller, C. 2006, ApJ, 637, 214
Mashonkina, L., Ryabtsev, A., & Frebel, A. 2012, A&A, 540, A98
Matteucci& Francois, 1989, MNRAS, 239, 885
McWilliam, A. & Zoccali, M. 2010, ApJ, 724, 1491
Meléndez, J., Asplund, M., Alves-Brito, A., et al. 2008, A&A, 484, L21
Mikolaitis et al., 2014, A&A, accepted, arxiv1408-6687
Minchev & Famaey, 2010, ApJ, 722, 112
Minchev I., Chiappini C., Martig M.,, 2013, A&A, 558, A9
Minchev et al., 2014, ApJ, 781, 20
Minniti, D., Lucas, P. W., Emerson, J. P., et al. 2010, New A, 15, 433
Mucciarelli, A., Pancino, A., Lovisi, L. et al. 2013, ApJ, 766, 78
Nataf, D. M., Udalski, A., Gould, A., Fouqué, P., & Stanek, K. Z. 2010, ApJ, 721, L28
Nelder, J. A. & Mead, R. 1965, Computer Journal, 7, 308
Neves, V., Santos, N. C., Sousa, S. G., Correia, A. C. M., & Israelian, G. 2009, A&A, 497, 563
Ness, M., Freeman, K., Athanassoula, E., et al. 2013a, MNRAS, 430, 836
Ness, M., Freeman, K., Athanassoula, E., et al. 2013b, MNRAS, 432, 2092
Ness, M., Freeman, K., Athanassoula, E., et al. 2012, ApJ, 756, 22
Nidever, D. L., Bovy, J., Bird, J. C., et al. 2014, ArXiv e-prints
Nissen & Schuster, 2010, A&A, 511, L10
Nordström et al. 2004, PASA, 21, 129
North et al. 2012, A&A 541, 45
Pace, Recio-Blanco et al. 2006, A&A 452, 875
Pedicelli, S., Bono, G., Lemasle, B., et al. 2009, A&A, 504, 81
Peletier, R. F., Falcón-Barroso, J., Bacon, R., et al. 2007, MNRAS, 379, 445
Pfenniger, D. & Norman, C. 1990, ApJ, 363, 391
Posbic, H., Katz, D., Caffau, E. et al. 2012, A&A, 544, 154
Prochaska et al., 2000, AJ, 120, 2513
Putman, M.E.; Peek, J. E. G. & Joung, M. R., ARA&A 50, 491
Qu et al., 2011, A&A, 530, A10
Quillen et al. 2003, AJ, 125, 2998
Quinn et al., 1993, ApJ, 403, 74
Ramírez, I. & Meléndez, J. 2005, ApJ, 626, 465
Ramírez et al., 2013, ApJ, 764, 78
Randich, S., Gilmore, G., & Gaia-ESO Consortium. 2013, The Messenger, 154, 47
Rangwala, N., Williams, T. B., & Stanek, K. Z. 2009, ApJ, 691, 1387
Rattenbury, N. J., Mao, S., Sumi, T., & Smith, M. C. 2007, MNRAS, 378, 1064
Re Fiorentin, P., Bailer-Jones, C. A. L., Lee, Y. S et al. 2007, A&A, 467, 1373
Recio-Blanco et al., 2006, MNRAS 370, 141
Recio-Blanco & de Laverny, 2007, A&A, 461, 13
Recio-Blanco et al. 2009, in *SF2A-2009,* p.75
Recio-Blanco et al. 2012, in *SF2A-2012,* p.107
Recio-Blanco et al., 2014a, A&A, 567, 5
Recio-Blanco et al., 2014b, A&A, submitted
Recio-Blanco et al., 2014c, A&A, GES WP10 analysis, to be submitted
Reddy et al. 2003, MNRAS, 340, 304
Reddy et al., 2006, MNRAS, 367, 1329
Rich, R. M., Origlia, L., & Valenti, E. 2007a, ApJ, 665, L119

Rich, R. M., Origlia, L., & Valenti, E. 2012, ApJ, 746, 59
Rich, R. M., Reitzel, D. B., Howard, C. D., & Zhao, H. 2007b, ApJ, 658, L29
Rix & Bovy, 2013, A&A Rev., 21, 61
Robin et al. 2003, A&A, 409, 523
Roeser et al., 2010, AJ, 139, 3440
Rojas-Arriagada et al., 2014, A&A, 569, 103
Romano et al., 2005, A&A, 430, 491
Romano et al., 2010, A&A, 522, 32
Roskar et al., 2013, MNRAS, 433, 976
Ruchti et al. 2011, ApJ, 737, 9
Saha, K., Martinez-Valpuesta, I., & Gerhard, O. 2012, MNRAS, 421, 333
Saito, R. K., Hempel, M., Minniti, D., et al. 2012, A&A, 537, A107
Saito, R. K., Zoccali, M., McWilliam, A., et al. 2011, AJ, 142, 76
Sales et al., 2009, MNRAS, 400, L61
Scannapieco, C. & Tissera, P. B. 2003, MNRAS, 338, 880
Scannapieco et al. 2012, MNRAS, 423, 1726
Schlegel, D. J., Finkbeiner, D. P., & Davis, M. 1998, ApJ, 500, 525
Schlesinger, K. J., Johnson, J. A., Rockosi, C. M., et al. 2012, ApJ, 761, 160
Schönrich & Binney 2009a, MNRAS, 396, 203
Schönrich & Binney 2009b, MNRAS, 399, 1145
Schultheis et al. 2014, GES 3D extinction analysis, A&A to be submitted
Seabroke & Gilmore (2007
Searle & Zinn, 1978, ApJ, 225, 357
Sellwood & Binney, 2002, MNRAS 336, 785
Semelin, B. & Combes, F., 2005, 441, 55
Serenelli et al., 2013, MNRAS, 429, 3645
Sharma, S., Bland-Hawthorn, J., Binney, J., et al. 2014, ApJ, 793, 51
Shen, J., Rich, R. M., Kormendy, J., et al. 2010, ApJ, 720, L72
Skrutskie et al., 2006, AJ, 131, 1163
Smolinski et al., 2011, AJ, 141, 89
Snaith et al., 2014, ApJ, 781, 31
Snaith et al., 2014, arxiv1410.3829
Soderblom, 2010, ARA&A, 48, 581
Sofue, Y., Honma, M., & Omodaka, T. 2009, PASJ, 61, 227
Sousa, S.G., Santos, N.C., Israelian, G. et al. 2007, A&A, 469, 783
Spagna et al. 2010, A&A, 510, L4
Spitzer & Schwarzschild, 1951, ApJ, 114, 385
Statler, 1988, ApJ, 331, 71
Steinmetz et al. 2006, AJ, 132, 1645
Stinson et al. 2013, MNRAS 436, 625
Tolstoy, Hill & Tosi, 2009, ARA&A, 47, 371
Toomre, 1977, ARA&A, 15, 437
Toth & Ostriker, 1992, ApJ, 389, 5
Twarog, 1980, ApJ, 242, 242
Uttenthaler, S., Schultheis, M., Nataf, D. M., et al. 2012, A&A, 546, A57
Vásquez, S., Zoccali, M., Hill, V., et al. 2013, A&A, 555, A91
Valenti, J. A. & Piskunov, N. 1996, A&AS, 118, 595
Van der Swaelmen, M., Hill, V., Primas, F., & Cole, A. A. 2013, A&A, 560, A44
Villalobos & Helmi, 2008, MNRAS 391, 1806
Yanny, B., Rockosi, C., Newberg, H. J., et al. 2009, AJ, 137, 4377
Yoachim, P. & Dalcanton, J. J. 2006, AJ, 131, 226
Yong, D., Carney, B. W., & Friel, E. D. 2012, AJ, 144, 95
Yong, D., Carney, B. W., & Teixera de Almeida, M. L. 2005, AJ, 130, 597
Wegg, C. & Gerhard, O. 2013, MNRAS, 435, 1874
Worley, C. C., de Laverny, P., Recio-Blanco, A., et al. 2012, A&A, 542, A48
Worley et al. 2014, A&A, to be submitted

Wyse & Gilmore, 1995, AJ, 110, 2771
Yanny et al., 2009, AJ, 137, 4377
Yoshii, 1982, PASJ, 34, 365
Zhao, H. 1996, MNRAS, 283, 149
Zoccali, M., Gonzalez, O. A., Vasquez, S., et al. 2014, A&A, 562, A66
Zoccali, M., Hill, V., Lecureur, A., et al. 2008, A&A, 486, 177
Zwitter, T., Siebert, A., Munari, U. et al. 2008, AJ, 136, 421